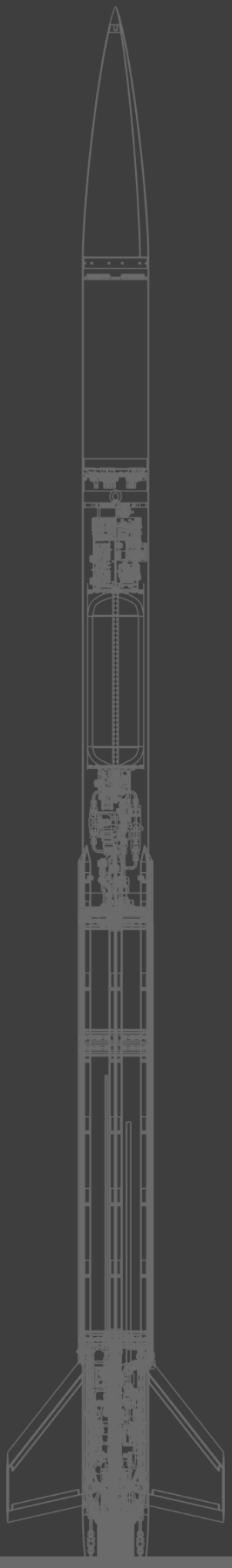

PLUTO
Technical Report

Team 18 Technical Report to the 2025 EuRoC

September 7, 2025

IMPERIAL COLLEGE
LONDON ROCKETRY

Abstract

This report aims to deliver a comprehensive overview of the design of ICLR's EuRoC 2025 entry, Pluto. Pluto has been designed and built by Imperial College London Rocketry to flight test the SRAD airframe, recovery, electronics and propulsion subsystems developed by the team thus far. Pluto is a 81 kg, 4.5 m long rocket, and is simulated to reach an apogee of approximately 4500 m using an SRAD regeneratively cooled N2O-IPA bi-propellant engine. The rocket features generatively designed airframe components, a 3U CubeSat payload developed in collaboration the Natural History Museum in London, and a custom-designed advanced open-source avionics ecosystem. Pluto is intended to launch in early October 2025, at Campo Militar de Santa Margarida at EuRoC '25.

PLUTO
Technical Report

Team 18 Technical Report to the 2025 EuRoC

September 7, 2025

By the members of Imperial College London Rocketry (ICLR)
Submitted to the European Rocketry Challenge 2025

Contact at: *icl.rocketry@gmail.com*

Supervised by Dr. Aaron Knoll
Department of Aeronautics, Imperial College London

Contents

List of Figures

List of Tables

1 Introduction

Imperial College London Rocketry (ICLR), founded in 2018, is a student-led rocketry team from Imperial College London. The team consists of approximately 150 students from various engineering departments. The primary goal for the team is to educate and engineering students in both the practical and theoretical aspects of rocketry and spacecraft engineering. However, from a more technical standpoint, the team's long-term ambition is to reach space with a fully student-researched and developed vehicle. This will be achieved through incremental developments of smaller rockets to mark key technical milestones towards this goal.

The team has competed at EuRoC for the past 4 years, setting increasingly challenging goals, pushing ourselves to become more technically proficient. EuRoC 21 saw our first launch of a large-scale commercial off-the-shelf (COTS) solid rocket, *Constant Impulse*. The following year at EuRoC 22, the team attempted to launch their first student researched and developed (SRAD) hybrid rocket, *Sporadic Impulse*, which unfortunately was not launched after encountering an electronics voltage instability. For EuRoC 23, the team decided to further upgrade and improve the design and manufacturing of its flight vehicles, culminating in *Nimbus*, our first ever liquid bi-propellant rocket. *Nimbus* was powered by THANOS A, our first liquid engine and the first of it's kind to be successfully fired in the UK amateur rocketry community. Unfortunately, *Nimbus* suffered a tank failure during a launch attempt due to incorrect assembly which ended the vehicle's launch campaign. Last year's entry, *Nimbus 24*, successfully launched, powered by our first regeneratively cooled bi-prop engine. Building on *Nimbus 24's* success, *Pluto*, the team's entry into EuRoC 25, is competing in the 9 km altitude category.

1.1 Team Structure

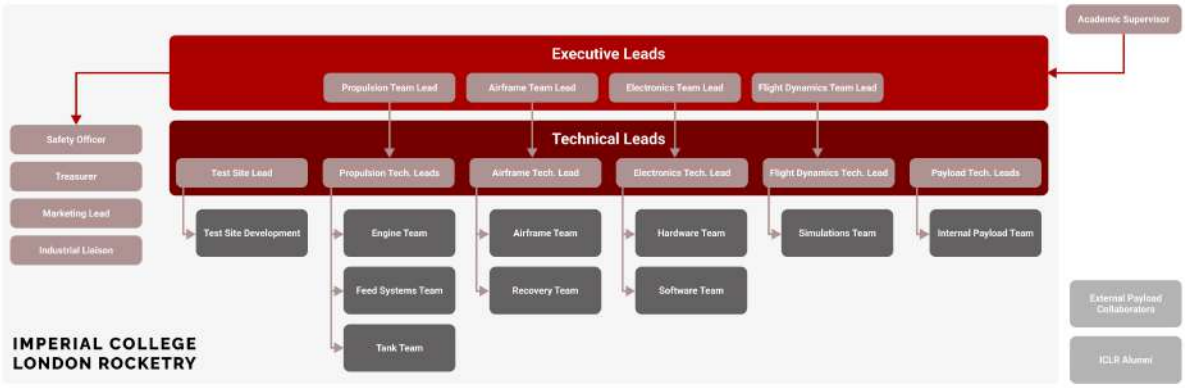

Figure 1: Organisational structure of ICLR, including external members

ICLR's organisational structure is detailed above in Figure 1. The team leads decide critical matters and set the overall direction for the team. The technical leads provide technical expertise for the rest of the team, whilst the safety officer and treasurer manage the team's safety procedures and finances respectively. The team is overseen by its academic supervisor, Dr Aaron Knoll.

The team is divided into sub-teams, each responsible for the development of a specific subsystem of the project. **Airframe** is responsible for structural, aerodynamic, and recovery components of the vehicle. **Propulsion** designs and tests the rocket's propulsion system, including the engine, feed system, tanks, and filling station. **Electronics** develops SRAD hardware and software for all systems. **Flight Dynamics** is responsible for sizing and simulating the flight vehicle. **Payload** collaborates with external partners to integrate scientific payloads.

1.2 Partners

Despite the hard work of ICLR's leads and members, as well as the contributions and support of the Imperial College London Departments of Aeronautics and Mechanical Engineering, significant outside support is needed to enable the team to survive and to build *Pluto*. Almost all contributions to ICLR come from local and international businesses, who can be divided into four categories: providing direct monetary support; providing critical components and materials; providing testing, logistical, or manufacturing capabilities; and providing discounts or software licenses. Some of our major suppliers and partners are detailed below, all of whom have been critical to the successful manufacture and test of *Pluto*.

Airborne Engineering Ltd

Airborne Engineering is a UK-based company that specialises in testing and developing propulsion devices for space propulsion companies worldwide. They kindly sponsored ICLR with multi-day access to their propulsion test facilities, allowing us to full-stack cold flow and hot-fire test our integrated propulsion and avionics subsystems for flight qualification.

Alloyed Ltd

Alloyed is a UK-based metal alloy development and manufacturing company that specialises in additive manufacturing. Alloyed provided ICLR with all of our regeneratively cooled engines and other in-development experimental components.

Space Logistics Network

Space Logistics Network is a specialist group of world leading companies dedicated to supporting the global aerospace industry. SLN's UK component, Davies Turner Air Cargo and the Aviation Logistics Network, are providing ICLR with logistics capabilities, including transportation of the *Pluto* flight vehicle and related equipment to EuRoC 25.

1.3 Project Goals

The goals for this year's project were set as:

- Optimise the design of our liquid bi-propellant engine
- Participate in the 9km flight category at EuRoC
- Build a robust recovery system, building on the shortcomings of *Nimbus 24*

1.4 Mission Objectives

Pluto is ICLR's third liquid bi-propellant rocket developed, building on the foundations laid by *Nimbus* in 2023 and *Nimbus 24*. This vehicle aims to use the lessons learned across both of these to ensure a smoother and more reliable experience from assembly to recovery - whilst pushing ourselves to compete in the higher category this year. The mission objectives for *Pluto* are:

- Reach an apogee of 9000 m using an SRAD airframe, propulsion, and avionics system
- Carry the rocket's payload to the target altitude and to demonstrate an integrated scientific experiments on board
- Complete a nominal flight from launch to full recovery of the vehicle
- Retrieve detailed subsystem telemetry, regardless of mission outcome.

2 Flight Vehicle Architecture

2.1 *Pluto* Overview

With the mission objective of reaching an apogee of 9000 m, the *Pluto* system design emphasises low mass, reduced complexity, and minimal structural sections. The rocket consisting of a propulsion system, an avionics system, a recovery system and a payload, can be physically split into 4 coupling sections.

The SRAD liquid propulsion system is divided into five subsystems, with a common bulkhead propellant tank separating the lower feed section and engine from the upper feed section and pressurant tank. The lower feed section is enclosed within a monocoque boat tail and fin-can, providing aerodynamic stability and drag reduction. The common bulkhead tank transfers engine loads into the single composite body tube, which houses the upper feed system, the pressurant tank, and both the main avionics bay and the smaller "mini" avionics bay. Power and communication from the upper sections to the lower sections is housed in through externally running raceways which also cover pressurant and fuel lines running along the rocket.

The recovery bay contains a single reefed main parachute, which initially acts as a drogue before fully inflating to slow the rocket for landing.

Finally, the payload subsystem is enclosed within the separable nose cone, this year carrying HORIZON (High-altitude Observation & Recovery for Investigating Zero-G on Oxygen & traNscriptome), a 3U CubeSat. HORIZON hosts the experiment module, CHIMERA – which studies the effects of launch loads on cyanobacteria through in-flight fluorescence monitoring and post-flight genetic analysis.

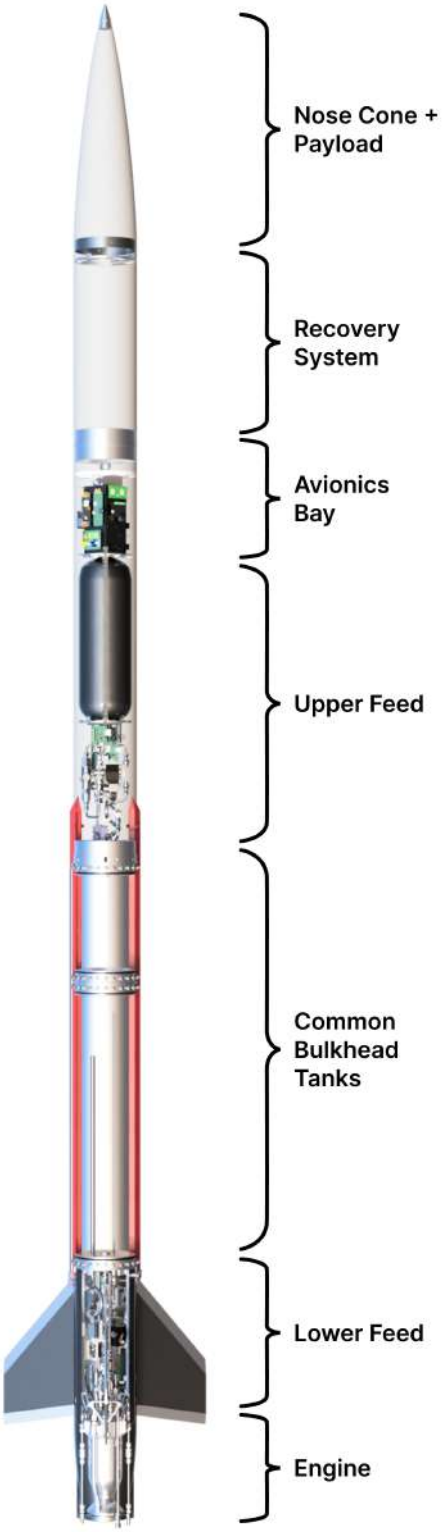

Figure 2: Overview of the *Pluto* flight vehicle and its subsystems

2.2 Propulsion Subsystem

2.2.1 Overview

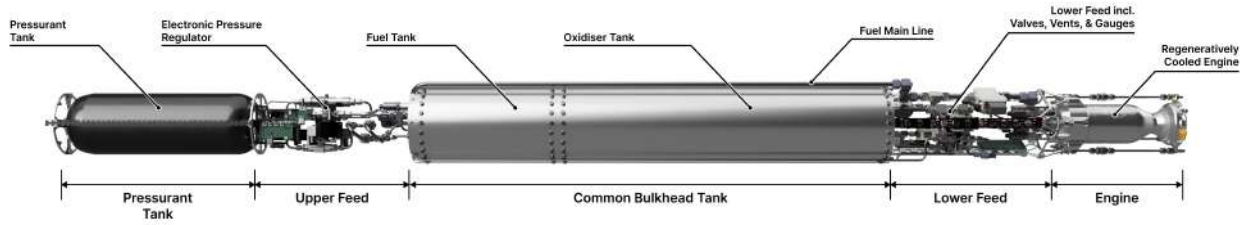

Figure 3: Propulsion subsystem sectional breakdown

Pluto aimed to build on the foundations of the previous year's liquid bi-propellant propulsion system to achieve a 9 km apogee. The rocket uses a pressure-fed system, utilising IPA as the fuel and nitrous oxide (N_2O) as the oxidiser, with Nitrogen gas (N_2) as the pressurant. As seen above in Figure 3, the propulsion feed system is divided into 3 main sections: Upper feed - containing pressurisation and fuel feed systems, Lower feed - containing engine and oxidiser feed systems, and tanks - containing structural tanks and raceways. This year's propulsion device is a regeneratively cooled engine chamber with an oxidiser-centered pintle injector. The engine design is a product of experience and lessons learned from multiple test campaigns at ICLR, including EuRoC 24. The ignition system remains pyro activated, using a C-class solid motor.

2.2.2 Propellant Feed System

N2 Tank & Upper Feed

Pluto's pressurant is Nitrogen (N_2), and pressure will be held inside a COTS 9L Composite Overwrapped Pressure Vessel (COPV), with a maximum expected operating pressure (MEOP) of 300 bar. The pressurant tank has been hydrostatically tested to 300 bar. A final hydrostatic test to 400 bar will be conducted by September 14th for the test reports. During operations, the COPV will see no more than 270 bar. A mechanical regulator set to 60 bar, with a normally open solenoid after, is attached to the high pressure lines. This is to ensure safe venting when power is off, whilst also keeping solenoid power usage low due to the lower pressures. This has the added benefit of reducing the chance the solenoid overheats and blows, increasing reliability of *Pluto's* de-pressurisation system.

Also connected to the high-pressure line is the E-REG, the feed system's electronic pressure regulator. Two check valves are connected in parallel, separating the fuel and oxidiser lines. Since the fuel tank is on the top, a reverse dip tube is used as the main fuel line, with the pressurant line entering from the top bulkhead. Fuel propellants are weighed precisely before being pumped into the tank, to ensure design ullage volume is maintained. In the event of an overpressure, the upper feed system has a COTS Pressure Relief Valve (PRV), calibrated to 60 bar, and a COTS Burst disk, which bursts at 70 bar $\pm$ 10% [1]. With a DN (Diamètre Nominal) of 8 mm [1] the burst disc is suitable for a 8mm pipe which has a much larger orifice size than the max orifice size of the 1/4" E-REG ball valve. Therefore, ensuring no risk of over pressurising the tank past it's yield point.

Raceway Interfaces

This feed system features 3 raceway pipes: A 1/2" fuel main line, as well as an 1/8" pipe for filling the N2 tank and a 3/8" pressurisation line to the oxidiser tank. A 1/2" fuel pipe was chosen to minimise total pressure loss through the pipe between the tank and engine. The 3/8" pressurisation line was also selected to minimise pressure loss, this time to the oxidiser tank to ensure the E-REG has sufficient control over tank pressure.

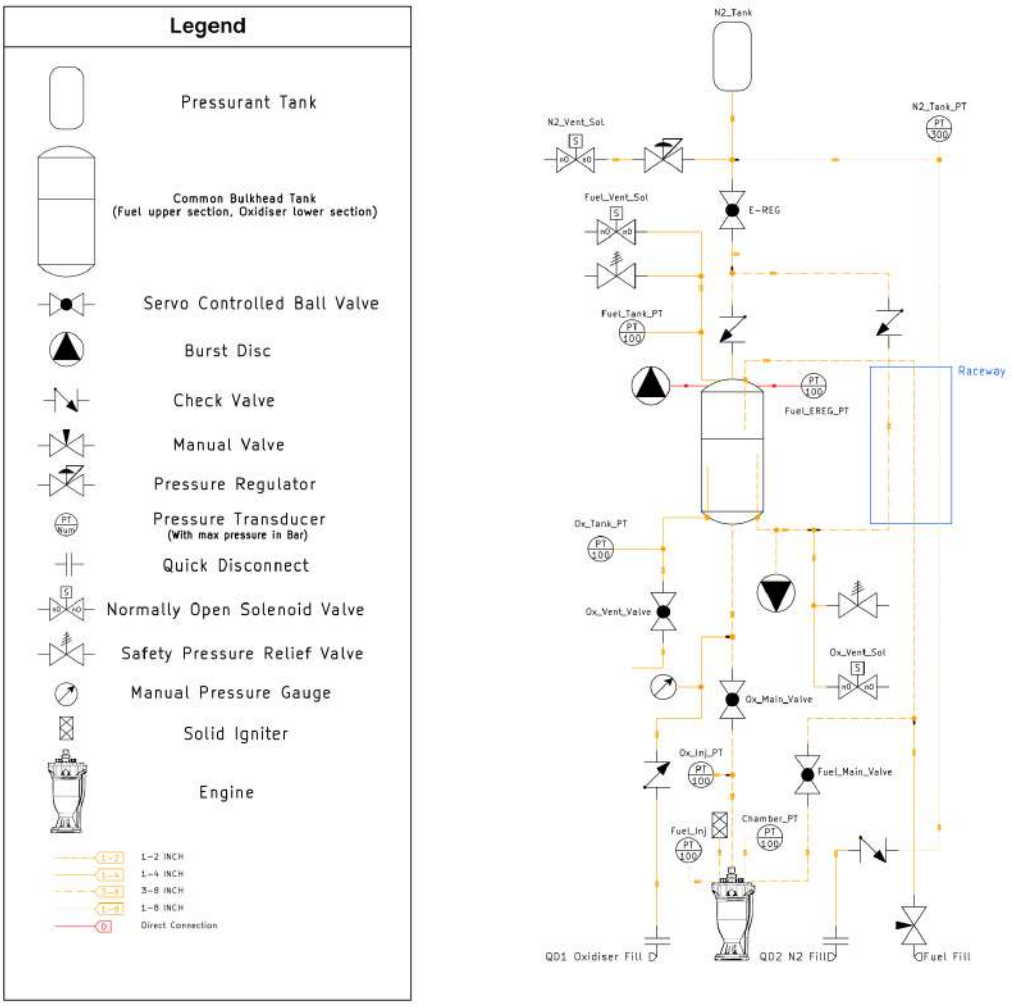

Figure 4: Flight vehicle propellant feed system

Common Bulkhead Tank

The Common Bulkhead Tank is an SRAD component, located between the upper and the lower feed systems. Tank assembly consists of two aluminium tubes connected via a in-house machined aluminium common bulkhead. Either side of the two tubes has an in-house machined aluminium bulkhead. This design reduces the need for an extra bulkhead, saving mass compared to a two-tank design. Due to the elimination of the mid-feed section and the airframe connection between the two tanks, more mass is saved in the overall system.

As shown in Figure 5, radial shoulder bolts are used for pressure containment and piston working O-rings are used to seal the tank. The analyses for the O-Ring seal are provided in Appendix G.1.9. This allows for the disassembly of the tank for inspection and cleaning. The shoulder bolts used,

have a fillet with diameter smaller than the shoulder diameter, right after the bolt head. Washers are used as spacers at the radial bolts, to ensure maximum interaction between the bolt shoulder and the tank. Bulkheads on the either end of the tank have flat faces to accommodate multiple fittings to be connected to the tank, with the additional benefit of directly threading the burst disc and pressure traducers to the tank bulkheads. BSPP fitting to Swagelok fitting adapters are threaded to the tank bulkheads using dowty washers for simple assembly and reusability.

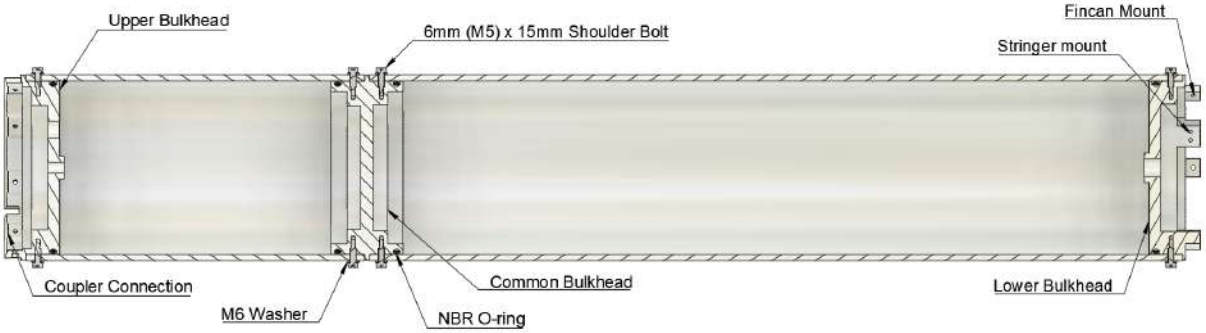

Figure 5: Cross-section view detailing the mechanical construction of the common bulkhead tank

The oxidiser (N_2O) is located in the lower tank tube and the fuel (IPA) is located in the upper tank tube. Both tank sections are designed to yield at a pressure above 120 bar with a maximum expected operating pressure (MEOP) of 60 bar. To simulate the worst case scenario, each tank section has been individually hydrostatically proof tested to 90 bar, 1.5x the MEOP. To ensure that the tank can handle the stated pressure, various failure modes have been analysed in Appendix G.1. The Common Bulkhead Tank has a total mass of 18.5 kg and a total length of 1213 mm. Specifications of the individual tank sections are listed in Tables 1 and 2.

Table 1: Oxidiser tank specifications

Capacity (L)	17.5
N_2O Capacity (kg)	15.7
Length (m)	797
Tube Diameter (mm)	190.7
Tube Thickness (mm)	6.4
MEOP (bar)	60
Minimum Burst Pressure (bar)	120

Table 2: Fuel tank specifications

Capacity (L)	6.7
IPA Capacity (kg)	5.3
Length (mm)	309.0
Tube Diameter (mm)	190.7
Tube Thickness (mm)	6.4
MEOP (bar)	60
Minimum Burst Pressure (bar)	120

The Common Bulkhead tank is designed to be a structural tank that transfers loads from the lower feed system to the upper feed system. The upper bulkhead incorporates an integrated coupler connection, shown in Figure 5 for efficient load transfer to the tank airframe coupler. The lower bulkhead features connection points, shown in Figure 5 for the stringers to transfer loads. The lower bulkhead also has fincan mounting points, shown in Figure 5. The longitudinal load capacity of the tank is analysed in Appendix G.1.8. This eliminates the need for stringers or body tube around the tank for load transfer. Due to the lack of machining capabilities, the outer diameter of the tank is the size of a 7.5 inch stock aluminium round tube, which is larger than the outer diameter of the rocket. The bulkheads at each end of the tank provide the transition between two different outer diameters. The tank architecture has changed from the *Pluto* concept report [2] as such: the location of the oxidiser and the fuel tanks have been swapped, and we have eliminated the need for internal pipe, inter-propellant seals and vent holes. These changes were made due to an unavailability of testing time.

Lower Feed

For main flow out of the oxidiser tank, a 1/2" pipe goes directly from the tank to the main oxidiser throttle valve. The nitrous filling line from the quick disconnects is connected to this line. There are two dip tubes into the oxidiser tank: One 1/2" dip tube is connected to the oxidiser tank burst disk, and the other is known as the filling dip tube. The burst disk dip tube is 1/2" to ensure the fastest possible venting in an overpressure event.

The N2 pressurant raceway connects directly to the burst disk dip tube. A key consideration is that the burst disk dip tube is 20mm longer than the oxidiser filling dip tube. This is operationally important because as N_2O fills the tank up through the main oxidiser line from the bottom, it will first reach the filling dip tube and come out of the servo ball valve venting system attached to that line. This means that the burst disk dip tube will always be pressurised pneumatically, ensuring that the burst disks can operate as expected. Similarly, an emergency ox-venting solenoid is attached to the burst disk dip tube line, to ensure the solenoid does not freeze from liquid nitrous oxide being in the line. Additionally, another COTS PRV calibrated to 60 bar is attached to this line. A manual pressure gauge is also connected to the oxidiser tank to inform the recovery team of tank pressure in the event of power loss on the rocket and to pressure transducers.

2.2.3 Electronic Tank Pressure Regulator (E-REG)

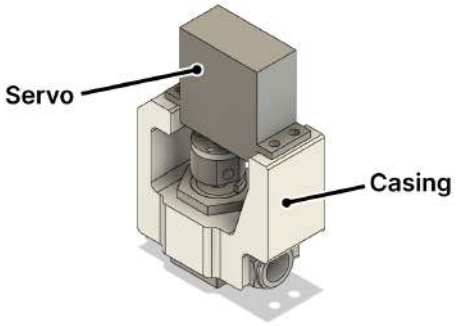

Figure 6: E-REG Valve

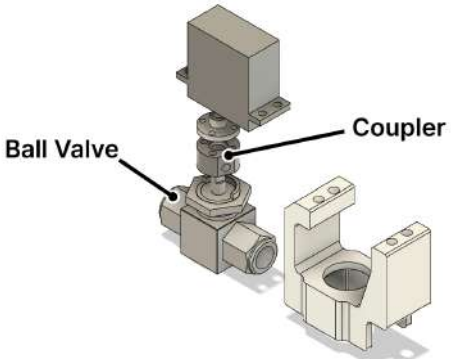

Figure 7: E-REG Valve (Exploded View)

Overview

To keep optimal tank pressures throughout the flight, Pluto uses a second-generation E-REG. Using this over a conventional COTS mechanical regulator is desired, since these regulators often do not achieve the desired flow rates. An affect of this is a large pressure loss experienced in the tank between static and flowing conditions, often called "droop". The solution is a servo-actuated ball valve with a simple proportional feed-forward controller that adjusts ball valve angle based off the difference in pressure between the high pressure N2 tank, and the fuel tank. The controller also takes into account the oxidiser tank pressures; however, it only uses this as a 'red-line', shutting the valve if it detects a sudden overpressure in the ox tank from events such as instant valve closure. Whilst feedback from the ox tank would be useful, constraints from the high pressure drop along the N2 raceway mean that E-REG will overcompensate its outlet pressure to achieve target ox tank pressure, which will over-pressurise the fuel tank.

Controller

The controller is a simple proportional controller, with feed forward and gain scheduling. This is done for saftey reasons, since including K_i and K_d could cause risk of undesired control response. K_i risks massive spikes on initial startup of flow due to control events such as windup. Including

an untuned K_d value risks causing too much rise time delay, meaning E-REG will be slow to react in situations where a smaller orifice is needed through the valve, risking overpressure. Subsequently, this requires lots of testing and tuning for minimal improvement and added risk, hence it was not included.

The overall logic of this control system, is that it adjusts the orifice size of the valve depending on the N2 and Fuel tank pressures. The controller uses the orifice equation to estimate the valve angle and required pressure drop for the setpoint, and error corrects based off the fuel tank pressures.

E-REG States and Safety

At the start of the burn, the N2 Tank pressure is at its highest, around $250 - 300$ bar, and the propellant tank ullage volume is at its lowest. This means that at this point, the tank pressures are the most sensitive to any small changes from E-REG. Therefore, K_p and the feed forward angle are at their lowest, to ensure the changes in valve angle are minimal.

After flowing, both the N2 tank pressure decreases and propellant tank ullage volume increases rapidly, meaning that over time the feed forward angle and K_p increase relationally. This makes E-REG more aggressive as sensitivity drops, keeping risks minimal. This is the flow state of the E-REG, and is automatically triggered when the Ox and Fuel main valves are actuated. As mentioned before, the E-REG will rapidly close if it detects an overpressure from either the oxidiser or fuel tanks.

The worst case scenario for E-REG is the valve being stuck open from either structural failure of the housing between servo and ball valve, or the servo burns out. In this situation, if the rocket is on launch pad, the tank will pressurise until it reaches the burst pressure of the two burst disks. Once the burst disks fail, the tank will safely vent, since the opening diameter of each burst disk is 8mm, and the ID of the E-REG piping is smaller, at 4.3mm. If this happens during flight, as explained previously, the tank pressures are much less sensitive since propellants are already flowing out through the engine.

While a stuck regulator valve is the worst case scenario, other scenarios involving failures of the pres- sure transducer providing feedback could also occur. The regulator control board has a dedicated PT attached to the fuel tank, but can also read the pressure of two other PTs in the fuel and oxidiser tank across the CAN bus. Due to the risk of the regulator closing during flight causing an early engine shut- down, a 'half abort' and a 'full abort' structure has been implemented. The 'half abort' is triggered if any tank PT exceeds 55 bar or if any two become disconnected, and it stops any closed loop control of the regulator, and moves it to its lowest feed forward angle. A 'full abort' is triggered if any tank PT exceeds 65 bar or if all three become disconnected, and in this case the E-Reg valve is closed fully. The full abort should never end up being triggered during a launch attempt unless there is an issue with either main engine valve during ignition which prevents one of the propellants from flowing.

2.2.4 Liquid Bi-Propellant Engine (GOOFY)

GOOFY is a 6 kN liquid bi-propellant regeneratively cooled engine, built on ICLR's experience with 20+ hotfires of regeneratively cooled engines. GOOFY's design is further refined and optimised from the previous THANOS series of engines, with an additively manufactured AlSi10Mg thrust chamber, in-house machined oxidiser-centred pintle injector and head-end C-class solid rocket motor igniter. Race2Space 2025 saw seven successful hotfires of the engine, including a full duration 10s hotfire; and one integrated full-stack hotfire took place at Airborne Engineering.

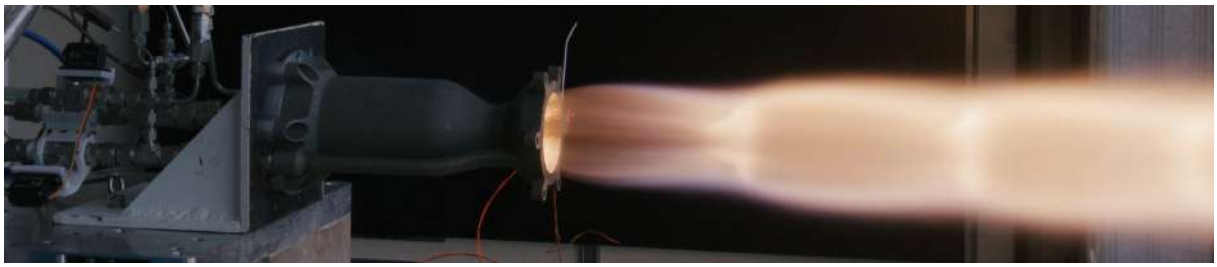

Figure 8: Exhaust plume of the GOOFY engine during the flight qualification hotfire

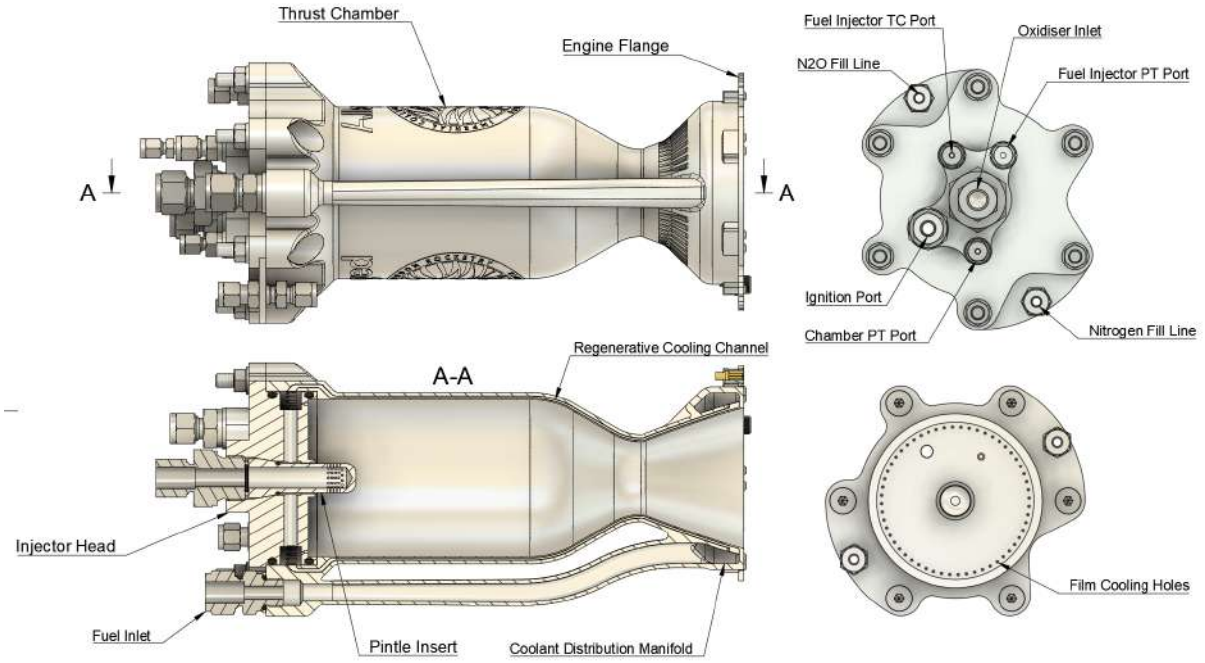

Figure 9: Cross Section of Chamber Assembly (left) & Top and Bottom Views of Injector Assembly (Right)

Pintle Injector

The pintle injector mixes the fuel and oxidiser through the use of a radial oxidiser fan and an axial fuel annulus, with mixing through impinging and shear, demonstrating a high c^* efficiency, $\eta_{c^*} = 0.96$ during hotfire testing. The injector consists of two main parts; the aluminium injector head and the stainless steel pintle insert, both manufactured using conventional machining. The pintle injector sits partially inside the thrust chamber, sealing the fuel injector manifold against the thrust chamber bore with two radial piston o-ring seals.

The injector head features a central 3/4" BSPP oxidiser inlet port, 3/8" BSPP ignition port and 3 1/8" BSPP ports for fuel injector pressure, fuel injector temperature and chamber pressure measurement. Additionally two Swagelok bulkhead fittings sit at the edges of the injector head to support the the N_20 and N_2 fill lines that run down to the engine flange.

The pintle insert fits into the back of the injector head and is held in place with the 1/2" Swagelok to 3/4" BSPP oxidiser inlet fitting, with a 3/8" BSPP bonded seal washer in between to seal the fitting to the pintle. The pintle insert also features a radial piston seal, to prevent fuel leakage out the back of the injector head. Combined, these provide two seals between the fuel and oxidiser with a vent in the middle through the oxidiser inlet thread, minimising the likelihood of propellant mixing inside the injector. Concentricity between the injector head and the pintle insert is achieved through a 10° tapered seat, aligning the two parts to form an even gap around

Table 3: Engine Specifications

Specification	Mass (kg)	Thrust (kN)	Chamber Pressure (bar)	O/F Ratio
Design	3.0	6.0	30.0	2.88
Stand-alone Hotfire	3.0	5.94	31.8	3.08
Flight Qual. Hotfire	3.0	4.8	25.4	2.30

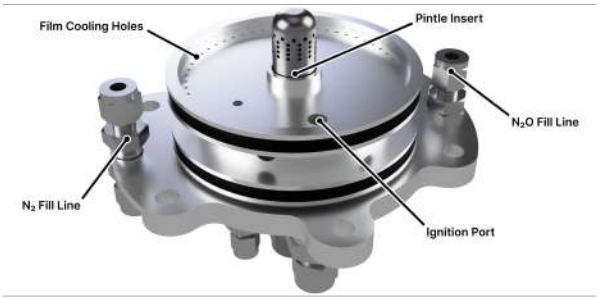

Figure 10: 3D View of the Injector Assembly

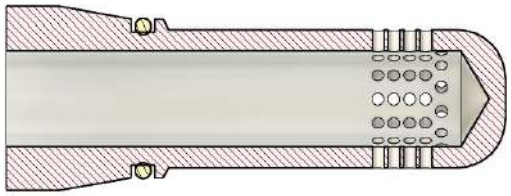

Figure 11: Cutaway of the Pintle Insert

the fuel injection annulus, ensuring fuel is distributed evenly into the combustion chamber.

Oxidiser injection is performed with 60 x 1.5 mm diameter radial holes near the tip of the pintle, with a measured discharge coefficient $C_d = 0.745$, providing a 2.33 kg/s mass flow rate with a pressure drop of 4.9 bar, 15.4% of chamber pressure. The oxidiser injection holes are arranged with 5 rows of 12 holes, as shown in figure 11, creating gaps between the columns of oxidiser injection holes for fuel to flow through and mix via shear, improving the mixing of the injector. The final row is offset to sit between the oxidiser columns above to catch any unmixed fuel.

Fuel injection is performed through the use of a primary annular orifice, and 56 secondary film cooling orifices, with a measured combined discharge coefficient $C_d = 0.723$. The main annular orifice injects fuel at a mass flow rate of 0.59 kg/s with a pressure drop of 6.9 Bar, 21.7 % of chamber pressure. The secondary film cooling orifices inject fuel near the edge of the combustion chamber to reduce chamber wall heat fluxes and temperatures. Fuel is injected here at a mass flow rate of 0.17 kg/s with the same pressure drop as the main annular orifice since they are both fed from the fuel injector manifold, this results in 22.6% of the total fuel mass flow rate used for film cooling.

Both propellant injectors have pressure drops above the typical minimum recommended value of 15% of chamber pressure to reduce the likelihood of coupled feed system - combustion chamber 'chugging' instabilities, with no combustion instability being observed in any hotfire tests.

Thrust Chamber

The AlSi10Mg thrust chamber is made through additive manufacturing by our sponsor Alloyed Ltd. The chamber features six M8 clearance mounting points on the top and bottom for injector mounting, post-machining, and hydrostatic testing, with a 3/8" BSPP fuel inlet port on the top. Fuel is delivered to the engine from a 1/2" Swagelok tube fitting, where it travels down into the coolant distribution manifold at the base of the chamber, and is subsequently distributed into the 50 regenerative cooling channels. The fuel then travels upwards through the regenerative cooling channels, exiting radially, where it enters the injector fuel manifold.

Furthermore, the thrust chamber features a water-jet cut flange plate attached to its base with 12 M3 screws, providing mounting points for the electronic and fluidic quick disconnects.

The thrust chamber guides the atomised fuel and oxidiser mixture through the combustion process and accelerates the combustion gases through its converging-diverging nozzle, with $L^* = 0.77$ m to give adequate hot gas residence time for combustion. The nozzle of the thrust chamber is made using Rao's parabolic estimation of the ideal nozzle geometry, with 80% the length of an equivalent conical nozzle chosen as a trade off between nozzle length and efficiency, and a design exit pressure of 1.3 bar, giving a slimmer aft end for the boat-tail fin can.

Thrust Chamber Cooling

The use of aluminium proves a challenge for regeneratively cooled rocket engines due to its low service temperature and sub-optimal thermal conductivity, compared to more conventional materials such as copper. Due to this, heat fluxes and temperatures must stay low to ensure the integrity of the chamber wall.

Thrust chamber cooling is achieved through the use of 3 methods: fuel regenerative cooling, fuel film cooling, and thermal barrier coating (TBC).

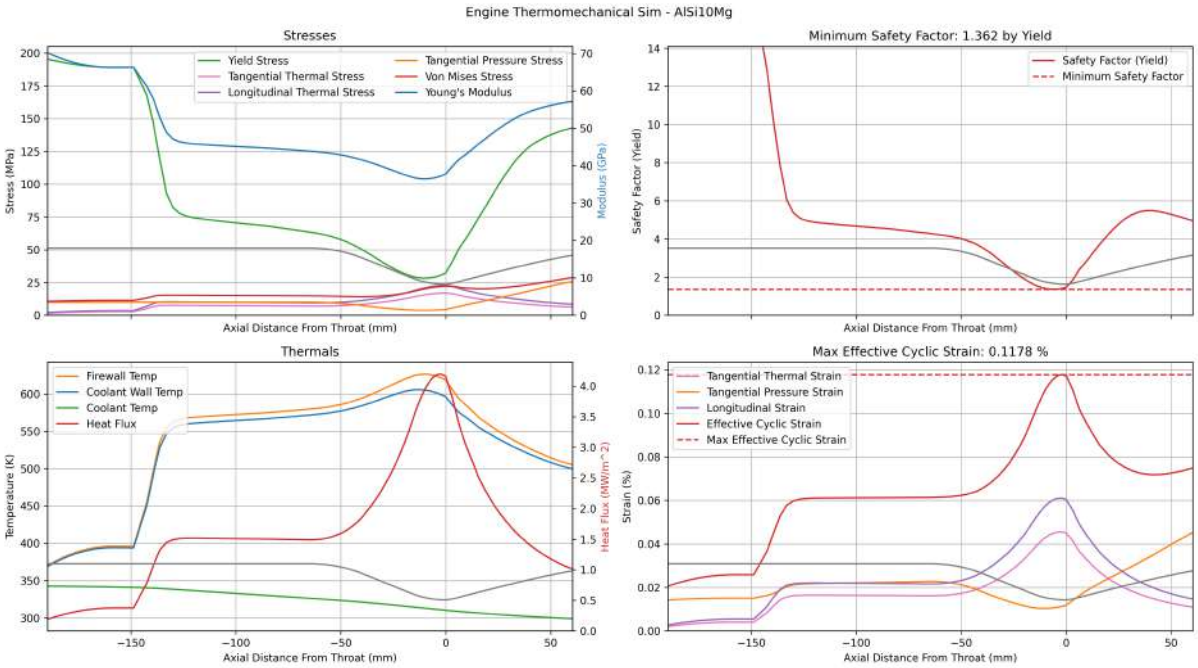

Figure 12: Engine Thermal Simulation, 20 micron TBC layer

The thermal barrier coating is achieved through the use of a small addition of silicone oil containing polydimethylsiloxane (PDMS) to the fuel, with a 98% Isopropyl Alcohol, 2% PDMS fuel composition by mass being used for all firings. The addition of PDMS to the fuel produces a thin regenerating layer of silica deposited on the chamber wall, acting as a thermal barrier coating.

Thermal analysis was performed using RPA (Rocket Propulsion Analysis), with mechanical analysis performed using the RPA output with in-house developed code.

Due to the uncertainty of the effect of PDMS addition to the fuel, two thermal-mechanical simulations are conducted. The TBC layer thickness is conservatively assumed to be 20 micron, with a thermal conductivity of 1.3 W/mK.

The results of the thermal analysis confirm the conservative simulated TBC, with the heat transfer rate reduction being only 4.2% relative to the 30% seen in literature. However this is already sufficient to prevent yielding of the chamber wall and increase our safety factor.

Ignition Method

The engine is ignited using a Klima C6-P solid rocket motor mounted in a stainless steel cartridge connected to the injector. The motor is ignited using an e-match which passes through the nozzle. Having the igniter hard mounted in the injector significantly reduces the chance of a hard start as it can't be ejected from the engine as the propellant flow rate is ramped up. A solid motor also gives a choked flame, meaning it operates independent of chamber conditions and can't be snuffed out. The solid motor fires directly into the well-mixed pintle impingement fan to guarantee a successful ignition. The igniter is fired 500 ms before the main valve open command is sent to ensure it is fully ignited before the valves open. The thrust then ramps up from below 300 N to max thrust in less than 100 ms as shown in Figure 51.

2.3 Airframe Subsystem

2.3.1 Overview

Pluto's airframe primarily consists of monocoques in the form of structural body tubes which are joined using Aluminium couplers. Structural tanks interface the upper monocoque sections and the lower skeletal airframe to which the engine is mounted at the base of the rocket.

The use of structural tubes saves mass as opposed to using stringers, stiffening rings and bulkheads. It also provides more space within the tube, which has been utilized by avionics bays.

However, for the lower feed system section below the structural tanks, aluminium stringers are used. These give easy access to the propulsion components with the fin can and boat tail removed, and serve as mounting points.

2.3.2 Bulkheads

In order to support the N_2 pressurant tank, 2 bulkheads were designed. The bottom N_2 bulkhead is designed to support the weight of the bottle, which was estimated to be 70N. Using Aluminium 6061-T6, the design was simulated in Abaqus and is well within safety factor limits. The top N_2 bulkhead is used only to hold the bottle in place.

2.3.3 Composites

Overview

Pluto uses multiple materials and multiple techniques to create various bodywork pieces. They very depending on mounted method,RF transparency and structural importance and dependency.

The bodywork has holes in certain places for assembly and priming the separation system. The placement of these holes was carefully done as to protect the composites.

Kevlar Body Tubes

The upper structural body tubes, for propulsion and recovery, are an RF-transparent Kevlar composite. The tubes, 120cm and 60cm long respectively, have a wall thickness of 2mm, and are composed of 5 plies of 300g, 2x2 twill kevlar cloth and an epoxy laminating resin, laid up by hand.

Both tubes are bonded to their aluminium bulkheads with structural epoxy: the lower tube has a Radax coupler between it and the upper tank; the two tubes connect at the separation system; and the upper tube connects to the nosecone. Each bonded surface is at least 220 square centimeters in area, suitably keyed and cleaned before bonding.

The upper tube containing the avionics bay has 2 small holes through which the rocket power keys are inserted, giving them on-rail access once the rocket is fully integrated.

Body Tube FEA Simulation

The body tubes were simulated in Abaqus 2024, using an anisotropic Aramid-reinforced epoxy resin composite material profile. At a load of 12kN, which is an overestimate for the loads the body tube will actually see, the maximum stress was found to be 35.23MPa and the maximum displacement was 0.2967mm, values which are reasonably within the material's structural properties. A conservative safety factor of 5700 was estimated for a buckling failure mode on a vertical load case with no external transverse loads.

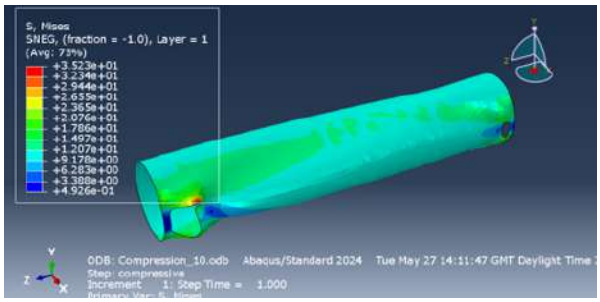

Figure 13: Upper body tube FEA showing stress distribution

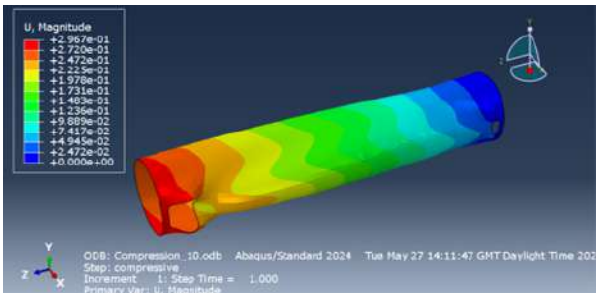

Figure 14: Upper body tube FEA showing displacement distribution

In reality, transverse loads such as airflow or ground impact can alter the buckling mode and decrease the safety factor. The fact that the tube is being made in-house without the use of resin infusion or pre-preg composites also means that the final tube will not be as strong as simulated. A high safety factor of 5700 ensures that even with a weakened tube, the strength is sufficient. Figure 70 and Figure 71 demonstrate the stress and displacement distributions within the tube, highlighting stress concentrations around the holes in the composite.

Carbon Fibre Fin Can and Boat Tail

The fin can and boat tail on *Pluto* are made using carbon fibre: they require greater strength because they do not have couplers that provide a complete adhesion to the rest of the rocket. Instead they are screwed into the bottom endcap of the tank and fit around the engine flange.

The boat tail has a complex geometry with multiple compound curves, so was laid up by hand internally inot a 3D printed mould, and vacuum bagged from the inside. The fin can is laid up by hand with the fins being cut from a CFRP sheet and epoxied on, before the final tip-to-tip hand lay up out over the fin can to secure the fins in place.

Glass Fibre Nosecone

The nosecone is made of 280g 2x2 Twill Glass Fibre cloth, screwed into the recovery body tube using anchor nuts in the cone. The tip of the nosecone is machined aluminium which screws into a thread also machined from aluminium and epoxied into the cone. The reason for a removable nosecone tip is to protect it during transport.

2.3.4 Tank-Tube Coupler

The top endcap of the fuel tank joins the 120cm Kevlar body tube at an Aluminium Radax coupler. The female side of the coupler and the tank endcap is one unibody part. The male side of

the coupler bonds to the Kevlar tube on a 227 square centimeter surface using a 2-part epoxy structural adhesive, giving a maximum predicted shear bond strength of 500kN.

The Radax coupler itself is secured using 9x M4 machine screws in Helicoil threaded inserts, with 4.4mm of thread engagement. The outer Radax screw holes are counterbored clearance holes, with 2.5mm of thread-contacting surface, and a further 4mm of head-contacting surface. One of the 9 machine screws is longer, and extends outwards to secure an aluminium launch lug. The coupler has a 2 machined slots to route plumbing and wiring through the 2 external raceways that sit outside the tanks. The bolt holes are exposed on the outside so may be plugged during flight for aerodynamic consistency.

2.3.5 Skeletal Airframe

Pluto's skeletal airframe is located between the structural tanks and the engine, consisting of 3 water-jet cut stringers and a generatively designed, additively manufactured engine truss.

The threefold symmetry of the stringers provides space in between to access the feed system, and aligns with the fins. Mounting points on the stringers have also been included to interface with avionics boards and mount the lower launch lug.

Stringers

Aluminium 6082-T6 was been chosen due to its high strength to weight ratio and affordable cost. The primary requirement for the stringers is to withstand the 6kN compressive force from the engine, distributed between the 3 stringers while being as light as possible and were optimized for this goal. The stringers are most prone to failure by buckling, therefore Euler Buckling theorem was first applied.

$$P_{\text{crit}} = \frac{\pi^2 EI}{L_{\text{eff}}^2} \tag{1}$$

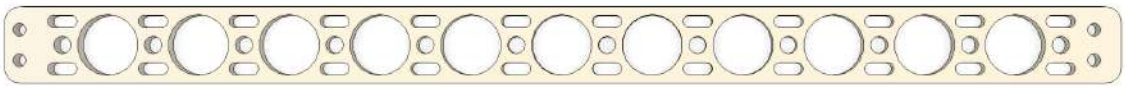

Figure 15: Mass Saved Stringer Design

After initial sizing, holes were cut into the stringers to remove mass. Buckling simulations were conducted in Abaqus CAE to determine whether a safety factor of 1.5 was achieved.

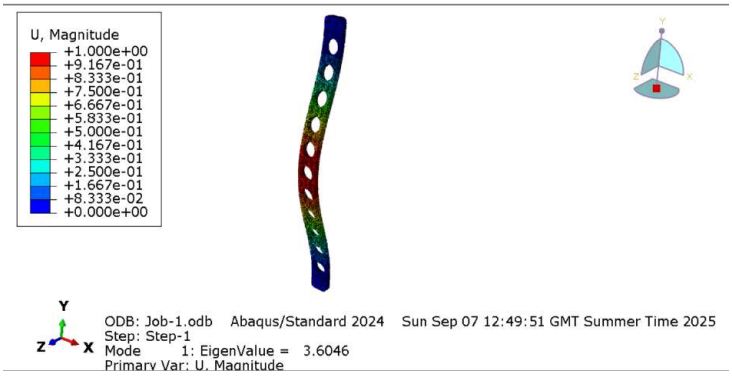

Figure 16: Stringer Mode 1 Buckling Simulation

The buckling simulations (H.2) gave a safety factor in mode 1 of 3.6046, thus meeting the ICLR standard of 1.5.

Engine Truss

The engine truss connects the engine to the rest of the rocket. Due to the tight packaging of the lower feed system along with some electronics, it was decided that generative design is the best way to create the truss. The truss was designed using Fusion 360 GenDes. The starting points being the connection to the engine and the 3 stringers.

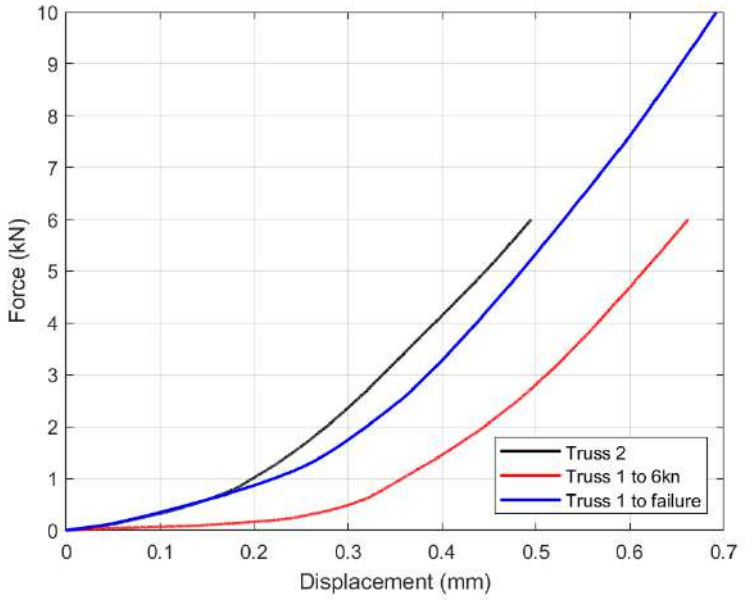

Figure 17: Initial Test of both trusses and overlay of test until failure

The truss is manufactured using aluminium additive manufacturing. To account for possible defects, two identical trusses were manufactured. They were tested under compression using a special testing jig to simulate the loads from the engine. The trusses were first loaded to 6 kN, which is the thrust that the engine is meant to produce. The truss which produced a higher displacement at a load of 6 kN was then selected for a test till failure, while the other became the flight truss. An FEA simulation was carried out in Fusion 360, which resulted in a minimum safety factor of 2.4, meaning the part is qualified for flight. Further details can be found in appendix H.4.

2.3.6 Hold-Down Mechanism

The rocket must reach it's target thrust of 5kN before leaving the launchpad, in order to achieve its target off-the-rail velocity. For the initial part of the burn, it will be held to the flame deflector, where the quick-disconnects for fuelling and power also lie. A Kevlar shock-cord will be used to hold the rocket down before thrust reaches required levels. The cord will be fixed to the base flange of the engine on one end, and an eye-bolt lower down the flame deflector on the other. The cord will be calibrated in an Instron tensile test machine to ensure correct breaking stress, altering the type of knot used (as that is where it is most likely to break) and the number of Kevlar strands used.

2.4 Recovery Subsystem

2.4.1 Separation Mechanism

Overview

The separation system lies between the upper proulsion section and recovery tube, which stores the parachute. It activates at apogee splitting the rocket, but keping them attached by the parachute and its shock cords.

Design

The separation system for *Pluto* consists of two couplers which are held together by 5 clamps across the 'rim' of the upper coupler. The clamps are engaged by a dyneema cord running through all clamps and to a spool. The spool is locked in place by a locking solenoid. During assembly, the clamps would be tensioned from the outside of the rocket using an Alan key. At apogee, the avionics will trigger the locking solenoid to unlock, causing the spool to undo and loosen the dyneema around the clamps. This causes the top and bottom halves of the coupler to separate and let the parachute naturally fall out in its reefed state. Besides the spool system, there is also a line cutter for the dyneema which is a COTS redundancy.

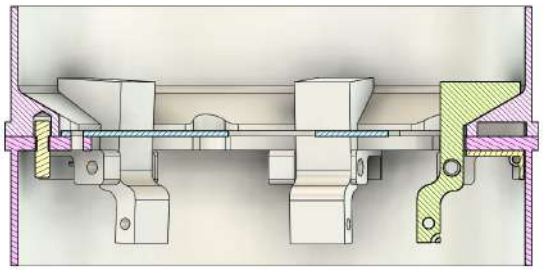

Figure 18: Clamp Engaged

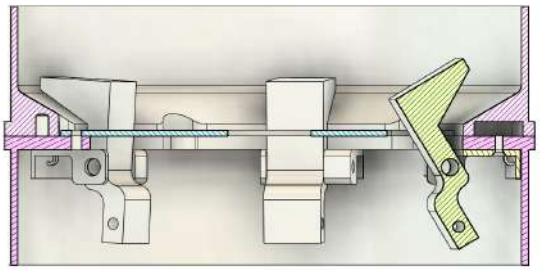

Figure 19: Clamp Disengaged

Dowel pins prevent the couplers from slipping laterally and in rotation. During assembly the dyneema pattern is adjusted by hand and tied together to ensure that the clamps tension evenly. The strength of how the system couples itself is based on how well the spool is tensioned during assembly. This is done through bench tests to investigate the number of turns needed to sufficiently tighten the separation system.

Manufacturing

Most parts were manufactured using Aluminium 6061 through CNC machining. Some parts such as the clamps and clamp holders were manufactured using aluminium 3D printing.

2.4.2 Parachute

The parachute is a COTS Toroidal Parachute. It has a total diameter of 10 ft and a drag coefficient of 2.2. The parachute is also reefed, so that the parachute is initially slowed down under drogue, and then further slows down when the parachute disreefs and the main deploys. The reefing mechanism includes reefing rings sewn onto the parachute using ripstop Nylon. The reefing line is a dyneema cord that runs through all the rings.

The line cutter is a separate 3D printed box that clamps onto the dyneema. It contains Nichrome wire wrapped tightly around the dyneema. To disreef, the nichrome burns the dyneema. The line cutter box carries its own battery and dedicated board, Crosshair. This is to prevent the disreefing mechanism from breaking in the event of a very violent shock upon separation.

2.4.3 Recovery Bulkheads

Overview

There are two recovery bulkheads used as part of *Pluto's* recovery system, one used to attach the parachutes outlined in section 2.4.2 to the main recovery tube of the rocket, and one to the nose cone and separated tube. They are designed around the various mounting points required of each; parachute shock cord and recovery system hardware for the lower recovery bulkhead, and just parachute shock cord for the upper recovery bulkhead. Both bulkheads were waterjet cut from aluminium 6061.

Design

Inspiration was taken from *Pluto's* predecessor, *Nimbus 24*, where a simple mass optimised plate with a central mounting point, outer bonding surface and connecting spokes was used. The design was adapted for a smaller outer diameter and further mass optimisation, resulting in the upper bulkhead seen in figure 20. The same m8 eye nut will be used for *Pluto*, so the central section did not require any changes, resulting in a final mass of 313.3g

However, for the lower bulkhead, components for the separation system described in section 2.4.1 such as the solenoid and spool assembly need to be fastened to it. Thus they were arranged around the central eye nut mounting point, and their fastener holes were added to the design with minimum mass in mind. This was allowable given that these fasteners will not be applying large loads to the bulkhead, and with an edge distance clearance of minimum 3mm, no edge effects will be prominent. This updated design, with a final mass of 317.5g can be seen in figure 21.

Simulation

Given the mission criticality of these components, significant effort was made to ensure that these bulkheads would not fail during flight. As such, FEA simulations were carried out on both bulkheads, which can be seen in figures 21 and 20. They were simulated at loads specified in Section 2.4.4, resulting in maximum stresses of 176 MPa and 157 MPa, and safety factors of 1.53 and 1.72 for the lower and upper bulkheads respectively, qualifying these designs for flight. Further details of the simulations can be seen in Appendix H.1.

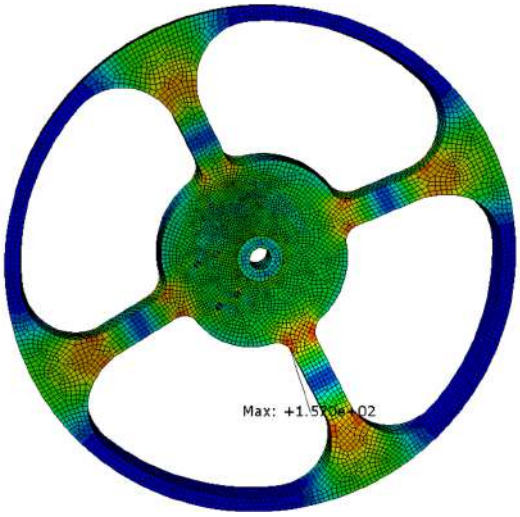

Figure 20: Upper Recovery Bulkhead FEA Simulation Showing Stress Distribution

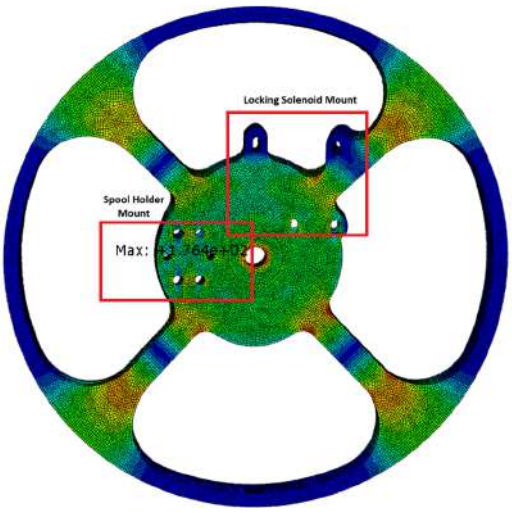

Figure 21: Lower Recovery Bulkhead FEA Simulation Showing Stress Distribution

2.4.4 Shock Load Calculations

The shock loads were calculated using multiple methods due to the structural failure experienced by Nimbus 2024 during parachute deployment, which led to preventing the parachute disreefing. The rocket touched down at a speed of ∼20 m/s. Therefore, the shock loads were calculated conservatively using a combination of the following methods:

1. **Hand calculations using *Nimbus 24* flight data:** Due to failure of disreefing of parachute, *Nimbus 24* gave the team data about the reefed parachute, included the shock loads experienced by *Nimbus 24*, video and images of parachute deployment, and the steady state descent rate date. The shock loads were calculated using *Nimbus 24's* IMU, with video to take account for the acceleration from heavy swinging and direction. At maximum load, the combination of all the shock forces experienced by the IMU was ∼7200 N. The vertical shock force experienced, taking into account any swinging motions, was ∼6500 N.
2. **OS-CALC program, which calculates the maximum drag force upon parachute inflation:** The inputs and the program can be seen in Appendix G.2.1. The program uses empirical data and a few parameters to calculated expected shock loads. The main limitation of this program is finding the estimated fall rate at line stretch, this can be calculated or tested. This is an important parameter and there is significant uncertainty around this value. This value was around 85 for Nimbus in order to give the right shock load.
3. 3 in-house programs; 2 in Python, 1 in MATLAB/Simulink. These all used similar methods, in which the spring constant, other key parameters were considered of the structure and environment. These were all inconclusive, differing between 2 kN and 10 kN. This was likely due to too many unknowns, like inflation time, simple trajectory simulations, and not enough test data to compare against. When these were standardised with *Nimbus 24* data, Shock loads given could still be way off depending which values were changed.

The first and second methods were predominately used to obtain the shock load values for parachute deployment as the in house programs were too early in development. Due to the high uncertainty of the shock loads found, A conservative team agreed value based on the previous experience, calculations and simulation of 8 kN was chosen. The recovery bulkheads and the eye nuts used are each simulated and rated to handle these loads. The shock load calculations are found in Appendix G.2.2.

2.5 Avionics Subsystem

Pluto 2025 utilises ICLR's fourth generation of the *Ricardo Avionics Ecosystem* (RAE). This year the electronics sub-team aimed to improve the robustness of the proven flight third generation system. RAE provides a unified hardware and software framework that scales seamlessly from simple, single solid-motor rockets to larger vehicles with advanced propulsion systems. Ongoing development has focused on improving reliability and reducing development time, enabling rapid deployment of fully featured avionics systems across ICLR, from rockets to ground support equipment. Over the past year, it has continued to perform well, enabling ICLR to perform various testing campaigns. The design of the Ricardo ecosystem is guided by three core principles:

1. **Distributed Architecture** – The avionics system is divided into discrete nodes, each with a single, well-defined responsibility. For example, while the flight controller may issue a command for a valve to move to a specific position, it is the responsibility of the valve control board to execute that action—whether by directly driving a servo or by adjusting the set-point of a more complex control loop. This clear separation of responsibilities enables straightforward expansion and upgrades.
2. **Configurability** – To ensure adaptability across rockets of varying complexity, both the hardware layout and the sequence of flight events must be configurable. Importantly, configuration can be adjusted at run-time such as at the launch site, rather than compile-time, greatly simplifying the process of adapting an avionics system to new rocket designs.
3. **Transparent Networking** – All nodes communicate over a network that is agnostic to the underlying physical layer. Since rockets often employ multiple communication layers, this transparency ensures that any node remains accessible from anywhere in the system. It also reinforces the principle of single responsibility: for instance, the flight controller focuses solely on flight operations, while tasks such as fuelling can be handled by separate nodes.

The electronics subsystem can be broken down into three main subsections: the flight system, the ground support system and the mission control system. The flight system is detailed below, whilst the ground systems are detailed in section 3.1.

2.5.1 Flight System

The goal of *Pluto's* avionics is to provide power, actuation, and sensor capabilities to the rocket.

An overview of the flight system is displayed in Figure 22, outlining the components onboard powering and controlling the propulsion and recovery systems and relaying vehicle telemetry to mission control. The system uses a central bus, *Ricardo Bus* (RBUS), providing logic power (5V), deployment power (14.2V nominal) to all actuators, and a CAN 2.0 bus to every component, enabling the onboard communications. CAN 2.0 provides a noise-tolerant and multi-master physical layer, supporting the goal of an extensible avionics system. Due to CAN's hardware arbitration, regardless of the number of nodes present on a bus, the packets deemed most important will always be prioritised. The deployment power rail is centrally controlled by a power distribution unit (PDU), therefore, turning off the rail ensures that the vehicle is in a safe state.

The flight system is powered by 2 packs of 2*s* 3000mAh Li-Ion batteries connected in series; each pack is capable of providing over 9 hours of system run-time. Each battery pack is connected to RBUS through an independent PDU, creating a redundant power system.

COTS Avionics

The CATS Vega board is used as the COTS redundant flight computer for recovery system actuation as well as official tracking. It is powered separately from the main power bus by a stand-alone

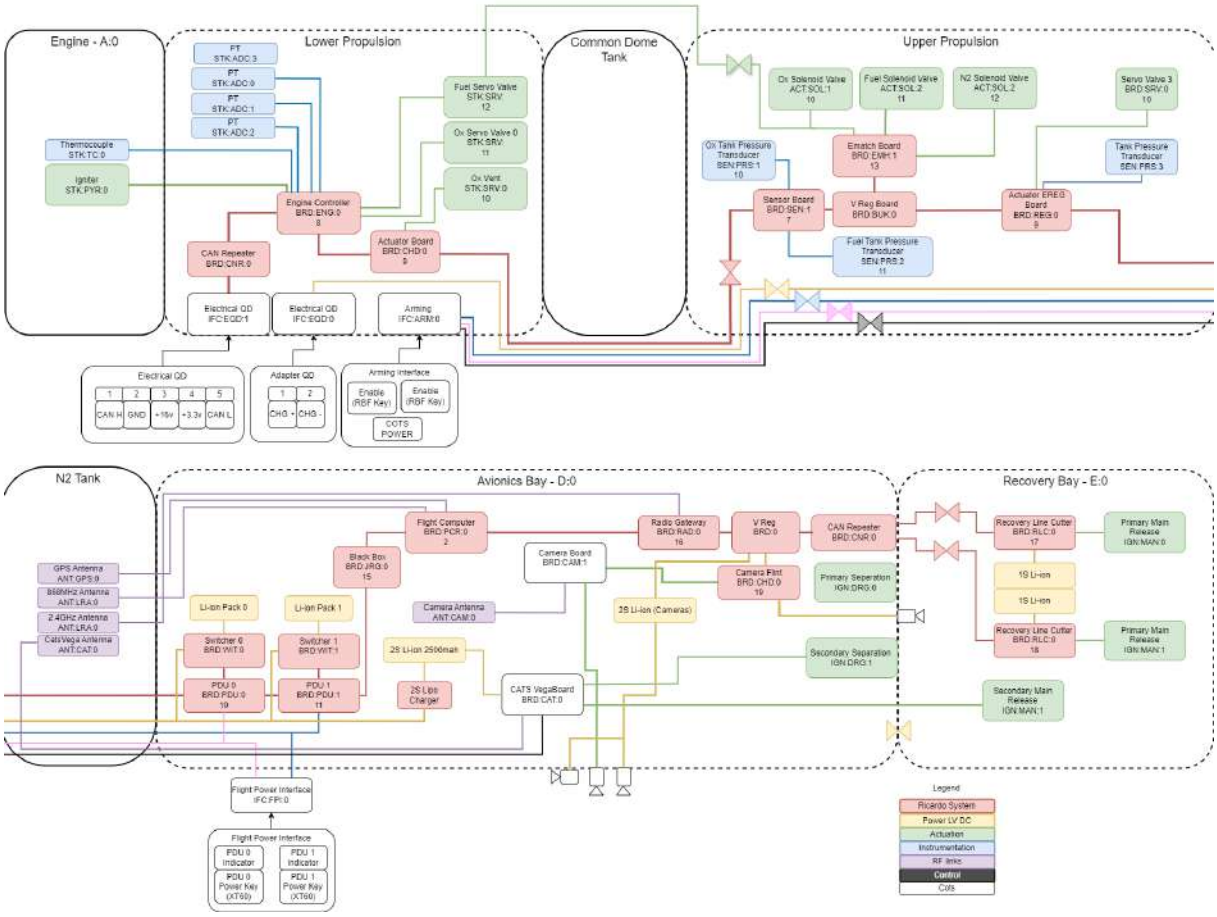

Figure 22: Electronics Systems Diagram

3s 2500mAh Li-Ion battery. A 3s charging circuit, connected to the COTS system battery, is additionally connected to ground power, allowing charging of the battery on the rail.

2.5.2 Hardware

The hardware developed for *Pluto* builds upon previous years with the modular Ricardo template (Section 2.5.3), providing a standardised schematic and layout for common components such as the ESP32 micro controller, power management and communication circuits. This standardisation provides a stable foundation to build hardware on top of, allowing development focus to be placed into the board's differentiating features. Additionally, the use of similar, well tested components across all Ricardo hardware ensures reliability while allowing the team to keep ample back-up stock of critical components.

2.5.3 Ricardo Hardware Template

The Espressif dual-core ESP32-S3 microcontroller has been used in the Ricardo ecosystem for the past two years for its fast performance and cost efficiency. A CAN transceiver is included to enable any board to access the rocket-wide CAN 2.0 bus.

The hardware template uses a buck-boost converter for logic power rectification, meaning that every board design can support logic power inputs from 1.8-5.5V, increasing tolerance to any power distri- bution faults. The layout of the converter and supporting passives is also provided in the template, as loop stability and EMI output of DC-DC converters are highly influenced by

Figure 23: Avionics Bay

Figure 24: Upper Feed 'Mini' AV Bay

component positioning and copper plane shape. The output of this converter is connected to a low dropout regulator (LDO) for post-rectification, resulting in a stable, low ripple 3.3 V local power supply. As the LDO may require a minimum 500 mV dropout voltage, the buck-boost converter is set to output 4.0 V, allowing enough headroom for the LDO to regulate down to 3.3 V.

Flight Controller - Pickle Rick V3

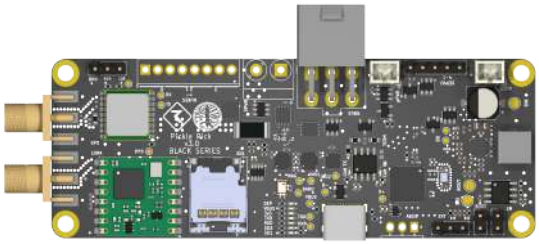

Figure 25: Flight Controller, Pickle Rick

Dimensions (mm)	100 x 37
Sensors	6 Axis IMU, Hi-g IMU,
-	3 Axis Mag, Baro, GNSS
Pyro Channels	4
Servo Channels	4
Input Voltage (V)	2.8 - 22

Table 4: Specifications of the flight controller

Pickle Rick is the primary flight controller of *Pluto*. The flight controller manages the propulsion and recovery systems during flight, computes the rocket's predicted apogee, records the trajectory and handles communications with mission control.

The flight controller integrates a 6-axis accelerometer and gyroscope, 3-axis magnetometer, a barometric pressure sensor, and a GNSS chip capable of receiving 4 different constellations, all for in flight telemetry and state estimation. During various flights of previous versions of *Pickle Rick*, it was found that the microSD card would either eject or crack during hard landings. Therefore, a lockable and shock resistant microSD card slot is included for logging of sensors and deployment events during flight. A buzzer is also included to provide auditory feedback of the flight computer's state.

Pickle Rick features a LoRA module operating in the 868 MHz band, providing a radio link between mission control and the rocket during flight. This module has a peak power output of +20 dBm, which can be configured lower to comply with local regulations. Coupling this with LoRA's excellent receiver sensitivity and signal to noise ratio capabilities enables the flight controller to return telemetry and tracking data at distances as high as 65km, even when using

omni-directional antennas as detailed in **??**. The flight controller logic power is provided by a similar architecture to the one described in Section 2.5.3, however with a different buck-boost converter allowing for input voltages up to 22V and therefore allowing the board to be powered by lithium batteries ranging from 1-5S. *Pickle* also includes pyro and servo channels (detailed in Table 4) which can also be powered from the same battery as logic power. The wide input range supported by the controller, as well as the inclusion of pyro and servo channels allows it to act as the sole flight and deployment controller on smaller rockets.

Engine Control Unit - Stark V2

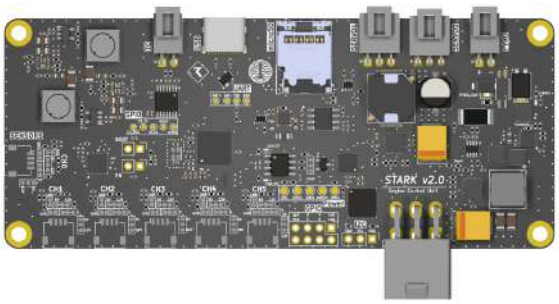

Figure 26: Engine Control Unit, Stark

Dimensions (mm)	117 x 49
Servo Channels	2
Servo Voltage (V)	6/7.4
Sensor Channels	6x (4-20mA, 5V,12V)
-	1 thermocouple
Pyro Channels	1
Pyro Voltage (V)	12
GPIO Breakouts	4

Table 5: Specifications of the engine control unit

Stark V2 is a new upgraded engine control unit (ECU), designed to fire and control the *GOOFY* engine. The controller follows a finite state structure, enabling precise execution of the ignition sequence. The integration of high rate data acquisition and controlled actuation in the same board enables the option of implementing closed loop throttle and OF control, as well as off-nominal abort cases without introducing load on the CAN bus.

The main engine servo actuated valves are power at regulated 6V and are independently calibrated to ensure the demanded angles in the ignition sequence correlate to the desired opening of the ball valves. Additionally, this demanded angle is relayed back through the telemetry packet which provides a useful debugging tool when configuring the ignition sequence at compile time. Additionally, both PWM control signals are transient protected using a TVS protection device. The pyro channel is supplied with regulated 12V with a high side switch and current monitoring for save operation. Additionally, continuous continuity checking on the pyro channel allows us to detect the integrity of the ignition e-match prior to propellant loading, hence reducing the chances of an undetected ignition failure.

The data acquisition on *Stark V2* includes a thermocouple channel to measure the desired engine temperature (configurable based on the type and location of thermocouple used). A 6-channel 24-bit resolution ADC is used to primarily measure pressure transmitter readings in the 4-20mA configuration. All data including sensor readings, valve angles, voltage and current monitors, as well as state transitions are logged locally on a locking MicroSD card. Additional features include 4 GPIO and an I2C breakout, providing extra functionality if required.

The ECU's design and control logic is an upgrade from *Stark V1* which has been tested in 20+ static hot-fires and cold flows. Additionally, V1 has also been flight tested as successfully ignited the engine onboard *Nimbus 24* at *EuRoC '24*. The V2 iteration has been tested in a cold flow, as well as the flight qualification hot-fire for *Pluto*.

High Powered Actuation Board - Flint & Steel

Flint & Steel consists of 4 actuation channels which are used for various applications within *Pluto*. These involve solenoid valves, used in the propulsion section, as well as Nichrome wire cutters, used in main separation and main parachute release.

N-channel MOSFETs with good thermal dissipation properties allow each channel to operate individually for long periods of time without overheating. *Flint & Steel* also incorporates a current shunt to monitor the output current, and a high side switch allowing power to connected actuators to be switched off entirely. This allows safety limits to be introduced which protect the rest of the rocket from a bus overload due to a malfunctioning actuator. A continuity check is also available on each channel to ensure that devices are connected correctly.

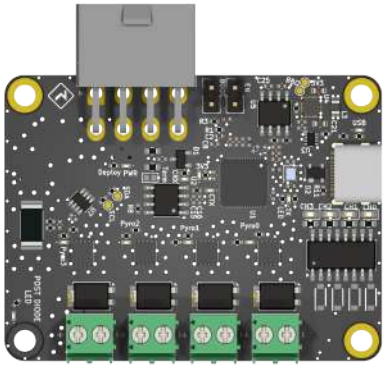

Figure 27: High Powered Actuation Board, Flint and Steel

Dimensions (mm)	58 x 44
Pyro Channels	4
Total Continuous Output Current (A)	20
Total Peak Output Current (A)	30

Table 6: Specifications of the high powered actuation board

Power Distribution Board - Lightning McQueen

Lightning McQueen is the Power Distribution Unit (PDU) responsible for regulating input voltage from the Ground Support System (GSS) or the onboard batteries to 3.3 V, which is required for the ESP32 microcontrollers. It also enables remote control over switching the logic and deployment power rails on and off, ensuring effective power management for the rocket's systems.

Additionally, Lightning McQueen features active power OR'ing, allowing automatic switchover between power sources in case of failure while facilitating load sharing. To protect electrical components and onboard batteries, the PDU also incorporates current limiting on the logic and deployment power rails during short circuit events.

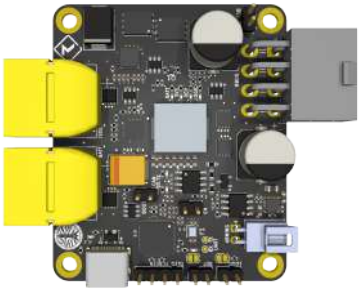

Figure 28: Power Distribution Board, Lightning McQueen

Dimensions (mm)	60 x 50
Input Voltage (V)	4-25.2
Maximum Deployment Current (A)	20
Maximum Logic Current (A)	10

Figure 29: Specifications of the PDU board

Servo Actuation Board - Chad

Each servo actuation board can control two servos, allowing only one board to be used if there are multiple servos in close proximity, thus easing integration.

The board is also used to read each valve's potentiometer, which provides direct feedback of the valve's absolute position. This allows to characterise the valve's backlash, detect valve failures and automate system checks.

The servos used are commercial RC servos, hence they require voltage regulation down to 6-7.4V to avoid damaging their integrated controllers, which *Chad* supplies through a buck converter. The position of such servos is set through a PWM signal, which is provided by the microcontroller.

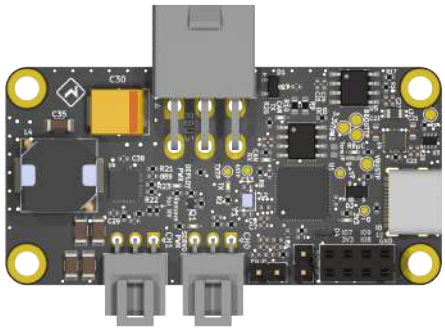

Figure 30: Actuator Board, Chad

Dimensions (mm)	60 x 30
Servo Channels	2
Potentiometer Channels	2
Servo Voltage (V)	6/7.4
Continuous Output Current (A)	12
GPIO Breakouts	6

Figure 31: Specifications of the servo control board

Electronic Pressure Regulator Board - Greg

Greg is a sensor breakout board for *Chad*. A single sensor channel can be powered using a regulated 5V or 12V supply. The signal is read by an analogue-to-digital converter on the *Chad* microcontroller, which is used for high data rate electronic pressure regulator, or E-Reg, pressure transducer feedback.

The identical GPIO pin configuration and sizing of both the *Chad* and *Greg* boards means that they can be integrated into a single unit using pin headers and stand-offs, which is the configuration used on the *Pluto* flight vehicle.

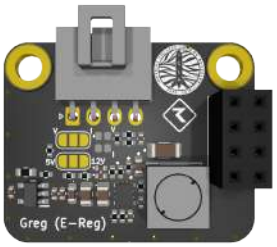

Figure 32: E-reg add-on board, Greg

Dimensions (mm)	30x24
Sensor Channels	1
Sensor Options	5V, 12V, 4-20mA

Table 7: Specifications of E-reg add-on board

Sensor Board - Kermit

Kermit is a sensor data acquisition board which features four analog-to-digital converter (ADC) channels sampled with a 24 bit resolution. The ADC channels are highly configurable, supporting both differential and single-ended readings, current sensing (4-20mA) and voltage sensing for 5V and 12V sensors.

This allows for any of the channels to be used to read a wide range of sensors. Additionally, power rails are supplied from boost converters which are post-rectified by linear regulators, thus preventing switching noise from propagating into sensor readings. Two thermocouple channels are also available, allowing temperature readings from any type of thermocouple.

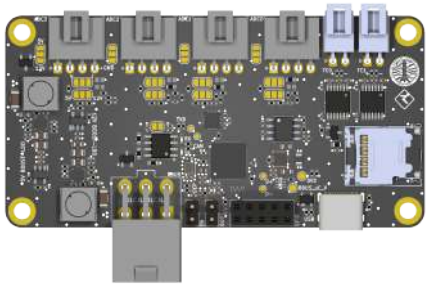

Figure 33: Sensor Board, Kermit

Dimensions (mm)	85x43
ADC Channels	4
Sensor Options	5V, 12V, 4-20mA
Thermocouple Channels	2
Nominal Data Rate (SPS)	500
Maximum Data Rate (SPS)	64000

Figure 34: Specifications of the sensor board

Power OR-ing Board - Witcher

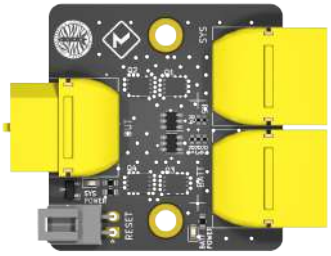

Figure 35: Power OR'ing board, Witcher

Dimensions (mm)	30 x 37
Maximum Input Voltage (V)	28
Maximum Continuous Current (A)	20

Table 8: Specifications of the Power OR'ing board

The power input OR'ing board, Witcher, is designed for switchover between the ground power and the onboard batteries. Ground power is favoured over the batteries, allowing the avionics system to have an indefinite runtime whilst on the rail. The batteries will only be used for flight and recovery, meaning they require less capacity and are therefore lighter. Additionally, *Witcher* allows for both power sources to be switched off, hence providing the rocket avionics with remote reset capabilities. The main design specifications of Witcher can be found in Table 8.

Parachute Line Cutter Board - Crosshair

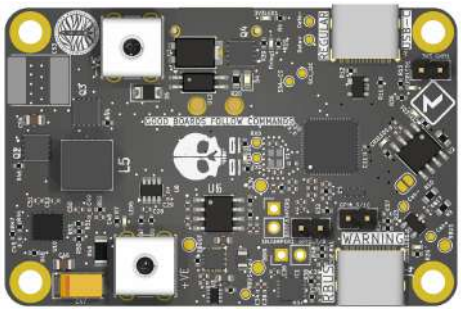

Figure 36: Line Cutter, Crosshair

Dimensions (mm)	40 x 61
Pyro Channels	1
Maximum Output Voltage (V)	36
Peak Output Current (A)	6
Maximum input Voltage (V)	5.5
Sensor Options	Barometer, Photo
GPIO Breakouts	4

Table 9: Specifications of the line cutter board

Crosshair is the board responsible for cutting the reefing line that encloses the parachute shock cord. A Quick Disconnect cable provides *RBUS* power and connection to the CAN 2.0 bus.

This board employs the use of finite states to enable parachute opening under the correct conditions. Initial states are determined by inputs from the *Pickle Rick* flight controller. Post separation, the board is powered by a 1S lithium battery, and states are triggered via the onboard sensor data.

It features a single pyro channel connected to a nichrome wire wound around the reefing cable. A buck boost converter is used to raise the voltage, ensuring enough power is dissipated in the nichrome to cut the reefing.

A MicroSD card locally logs the state transitions, as well as the data from the barometer, photo sensor, and the voltage and current monitors. *Crosshair* also features 4 broken-out GPIO channels for additional connectivity.

CAN Repeater

The CAN repeater allows multiple independent CAN buses to connect together, whilst also retaining hardware arbitration. A correctly set up CAN 2.0 bus requires both ends to be terminated to prevent signal reflections, and this termination can not be removed during a bus' runtime.

The CAN repeater provides termination at one end of the bus, and also retransmits any CAN packets across the electrical junction so that after QD disconnection both buses can continue to operate nominally. The CAN repeater also provides an option for galvanic isolation, eliminating ground loops.

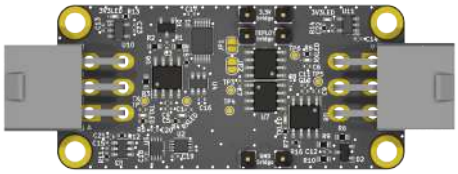

Figure 37: CAN Repeater

Dimensions (mm)	57 x 27
CAN	Yes

Table 10: Design specifications of the CAN Repeater

Radio Gateway - Hermes

Dimensions (mm)	65x43
Centre frequency (GHz)	2.4
Nominal Tx Power (mW)	100
Data-rate (Mbps)	1.0

Table 11: Design specifications of the radio gateway board

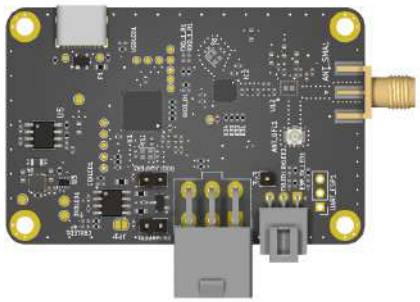

Figure 38: RF Gateway, Hermes

Hermes is a radio gateway designed to be able to downlink the full data-rate of the rocket CAN 2.0 bus. Inspired by the loss of *Nimbus 24* engine sensor data upon its hard landing, this is a step towards *Pluto*'s mission goal of recovering system telemetry regardless of mission outcome, enabling the team to maximise learning in off-nominal flight conditions. To avoid overloading the CAN bus, *Hermes* includes a direct, high data-rate connection to *PickleRick*.

Flight Recorder - Jolly Roger

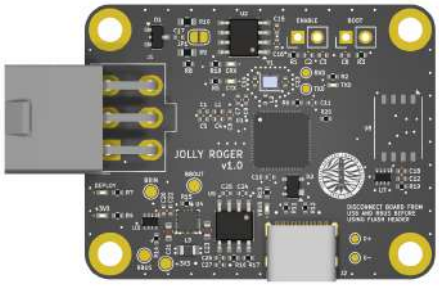

Figure 39: Flight Recorder, Jolly Roger

Dimensions (mm)	45 x 35
Flash Storage (Gb)	4

Table 12: Specifications of the flight data recorder

Jolly Roger is a flight data recorder designed to collect sensor telemetry from the rocket CAN bus. Its small size allows multiple *Jolly Roger* boards to be distributed throughout the rocket, increasing the likelihood of survival of at least one copy of the collected telemetry. This is another step towards *Pluto*'s mission goal of recovering system telemetry.

2.5.4 Antennas

Pluto features 4 separate antenna systems as seen in figure 22. The antennas are mounted in pairs on either side of the N2 tank for full radial coverage. Since the composite body tube is made from aramid, this section of the rocket is RF transparent. The SMA cables from the relevant boards are impedance matched to 50 Ω through a Wilkinson power divider. Refer to the radio test report for further detail on the SRAD flight controller telemetry antenna.

2.5.5 Software

The Ricardo avionics platform is built around a diverse, multi-language software stack. On the embedded side, systems powered by the ESP32-S3 run applications written in C++17 on top of FreeRTOS, a real-time operating system. Leveraging modern C++ ensures modularity, reusability, and access to high-performance libraries such as Eigen, which is used for efficient linear algebra operations. Middleware components, such as interface programs deployed on the GSS

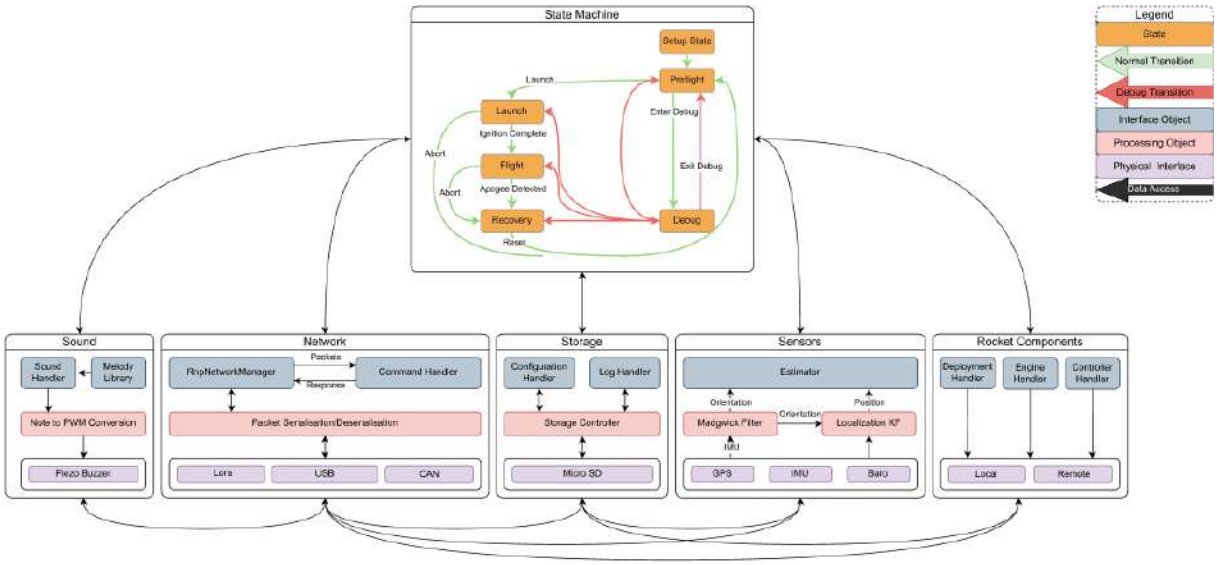

Figure 40: Overview of the Ricardo Software Stack

Raspberry Pi, are primarily written in Python to maintain cross-platform compatibility and make development more accessible to the wider team.

At the core of the software stack are three key libraries that underpin nearly all embedded code. LibRNP (Ricardo Network Protocol) implements a packet-based communication system, while LibRRC (Ricardo Rocket Components) models the rocket through two primary abstractions—actuators and sensors—simplifying representation of the flight system. A companion Python library, pylibRNP, extends LibRNP's functionality by offering tools for serializing and deserializing RNP packets in Python-based applications. To enforce consistency across hardware, the LibRICCORE (Ricardo Core Library) framework provides the base structure for every PCB. It introduces a generic "system" class that can be specialized for board-specific logic, enabling developers to concentrate on unique features without reinventing shared infrastructure.

In addition to these libraries, the framework incorporates several essential modules by default. These include: a finite state machine to organize program execution into well-defined stages, a LibRNP-based networking manager to provide communication on all nodes, a centralized command handler for registering and processing commands, a unified logging system for consistent message output, and a compact status-tracking object that manages error conditions using an efficient bit-field representation.

2.6 Apogee Detection Algorithm

Reliable detection of apogee is achieved through a polynomial fitting approach applied to altitude data generated by the flight computer's Kalman filter estimator. Altitude measurements are sampled at $50\,\mathrm{Hz}$ and processed over a sliding window of 100 samples. Within each window, a quadratic polynomial is fitted to the data via least-squares minimisation.

2.6.1 Polynomial Fitting Methodology

Let the altitude measurements be represented as (t_i, h_i) for $i = 1, \ldots, N$ with $N = 100$. A quadratic polynomial of the form

$$h(t) = at^2 + bt + c$$

is fitted to the data using Householder QR decomposition to solve the corresponding least-squares system. The resulting coefficients (a, b, c) provide a local characterisation of the vehicle's vertical

trajectory under an approximately constant acceleration.

As the vehicle approaches apogee, its vertical acceleration asymptotically approaches $-g$ (gravitational acceleration). Consequently, the quadratic approximation becomes increasingly accurate, and the fit converges to the true trajectory.

2.6.2 Apogee Estimation

The time of apogee, t_{apogee}, is obtained by identifying the maximum of the fitted quadratic, given analytically as

$$t_{\text{apogee}} = -\frac{b}{2a},$$

with the corresponding altitude

$$h_{\text{apogee}} = at_{\text{apogee}}^2 + bt_{\text{apogee}} + c.$$

At runtime, apogee is declared if the following conditions are satisfied:

1. The current time t_{current} exceeds t_{apogee}.
2. The current altitude h_{current} is less than h_{apogee}.

This criterion ensures a computationally efficient and noise-resilient detection scheme, avoiding sensitivity to short-term fluctuations in altitude estimates.

2.6.3 Safety Constraints

To improve robustness and prevent premature triggering, two additional safeguards are enforced:

- A minimum altitude threshold of $100\,\text{m}$ must be exceeded before the algorithm is enabled.
- A Mach lockout condition inhibits apogee detection while the vehicle is transonic or supersonic, mitigating false positives caused by shock-induced disturbances in the pressure-based altitude estimates.

2.7 Payload Subsystem

2.7.1 Overview

This year's payload, HORIZON (**H**igh-altitude **O**bservation & **R**ecovery for **I**nvestigating **Z**ero-G on **O**xygen & tra**N**sctriptome) is a 3U CubeSat hosting both technological and scientific experiments that build upon foundations set in previous years. These experiments can be split into three main modules:

CHIMERA: Investigating the effects of rocket launch loads on cyanobacteria samples by observing changes in fluorescence during flight and analysing genetic changes post-flight, assessing their potential for deep-space missions.

HYDRA: Secures the payload enables deployment via four servo-controlled pins that constrain the payload during launch.

2.7.2 Payload Structure

Last year's payload, FAWKES, presented a hybrid payload structure, comprising of aluminium stringers and bulkheads as primary load bearing components, with glass fibre reinforced polymer (GFRP) panels for aesthetics and some buckling resistance. HORIZON has transitioned to a full GFRP architecture, using 5 mm GFRP plates as both structural and functional members. This has

led to a 45 % weight reduction across the structure whilst maintaining the minimum 1.5 safety factor. Furthermore, using GFRP enables RF transparency throughout the flight, ensuring the flight computer, Pickle Rick, has constant signal to ground station.

The plate design itself utilises a bio-inspired lattice pattern in the form of a petal, derived from BCE curvature, designed to minimise mass whilst providing lower stress concentrations compared to a traditional X shape. Central 30 mm holes allow for camera's and external access to EQD's, whilst 3 mm mounting holes are arranged in a standardised pattern to allow customisability of the CubeSat's mounted components (i.e. PCB's, bulkheads etc). Constraining these panels is an upper and lower bulkhead, 3D printed from a nylon carbon-fibre composite material, Onyx.

2.7.3 Payload Electronics System

The electronic architecture of HORIZON is an evolution of FAWKES, centring around the use of *Pickle Rick* as the main flight computer, used for communications and storing experimental data from the CHIMERA experiment. Furthermore, a COTS spectrometer board equipped with six phase sensors and an LED driver is being used in the CHIMERA module to excite the cyanobacteria samples, measure their bioluminescence and send the data back to Pickle Rick.

2.7.4 CubeSat Experiments

CHIMERA

The CHIMERA module, a research investigation in collaboration with London's Natural History Museum and Imperial College London's Department of Life Sciences, builds upon the work of ICLR's 2023 payload, which investigated the effects of launch loads on algae samples. CHIMERA takes this a step further by analysing not only the transient response of cyanobacteria, but also their long term, transcriptome (epigenetic) response. This will provide insight into how high stress environments impact both the immediate strain samples but also how future strains DNA adapts to this stress. The results of this experiment will inform future feasibility studies into using various types of cyanobacteria samples for manned missions to space where cyanobacteria can produce oxygen and food for astronauts.

The independent variable for this investigation is the wavelength of light emitted during fluorescence by the chlorophyll (oxygen producing green pigment) of the strains. An expected wavelength range for healthy samples lies between 600 - 800 nm, with this wavelength being proportional to the amount of oxygen production. Four strains, two of each (one extremophile and and one engineered strand) of the same species, will be used. During flight, the samples are housed inside a 3D printed container with slots for the test vials and a rigid, opaque divider between them to prevent light contamination across samples. After landing, one sample set will be left out to analyse while the other is placed in a cool box for future analysis. This work will be conducted by scientists at The Natural History Museum using specialist genome tracing equipment.

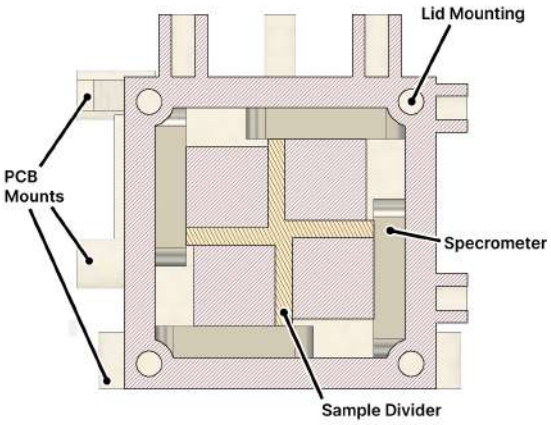

Figure 41: CHIMERA Top Section View

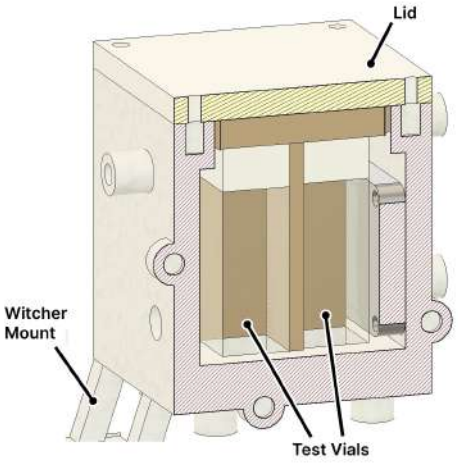

Figure 42: CHIMERA Side Section View

HYDRA

The HYDRA module was designed to enable payload deployment via four lock pins that rotate about a central hub, controlled by a single servo. These pins slot into circular holes in the recovery bulkhead, locking the payload to the rocket. When the mechanism is activated, the pins rotate out of the circular slots, unlocking the payload. However, since payload deployment has been cancelled, unlocking will only occur after the rocket has landed.

3 Ground Support Systems Architecture

3.1 Ground Electronics Architecture

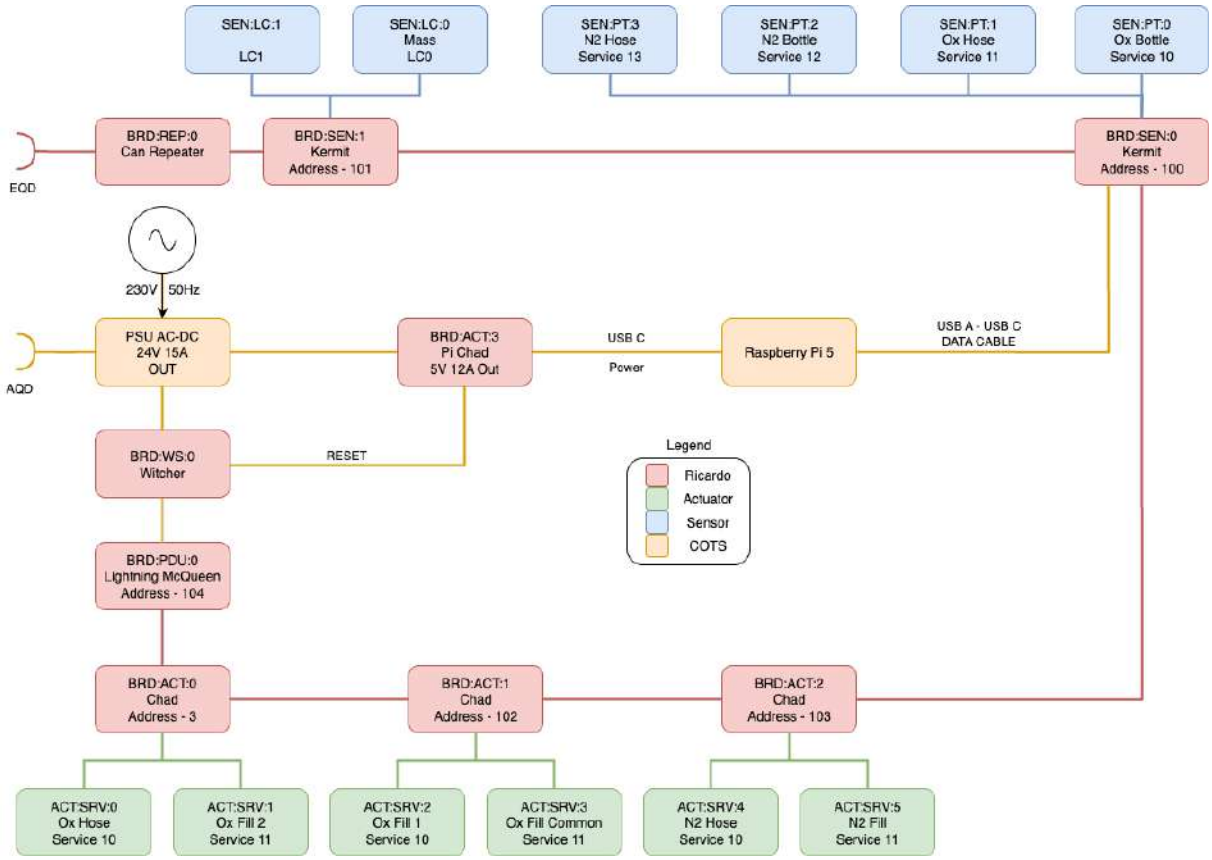

Figure 43: Overview of the Electronic Ground Support System

3.1.1 Ground Support Station

The Ground Support Station (GSS) electronics is a subsection of the same avionics system detailed in Section 2.5. A 24V AC-DC PSU powers the GSS, as well as the rocket while on the launch pad using an umbilical cable described further in Section 3.1.2. All power to the rocket and GSS can be reset using a switch on the GSS, allowing for a full bus hardware restart. There is also a CAN bus connection from the GSS to the rocket via a second umbilical. The primary function of the GSS is to provide a remote gateway from mission control to the filling station and rocket for all ground and pre-flight operations. This network interface will be described in Section 3.3.

3.1.2 Electronics Quick Disconnects

Pluto requires two electronics quick disconnects, providing a power and communications interface to the rocket when on the launch pad. These consist of passive, non-locking connectors which are ejected when the rocket lifts off.

The adapter power quick disconnect (AQD) consists of a dual-contact XT60 connector mounted on the bottom of the engine flange as seen in figure 45. This provides a retention force of $\approx$ 30N, with a maximum current rating of 60A. Since the GSS PSU current limits at 15A, an XT60 is suitable to use.

The electrical quick disconnect (EQD) enables communications and voltage feedback from the

rocket. It consists of 6 conductors as seen in Figure 44.

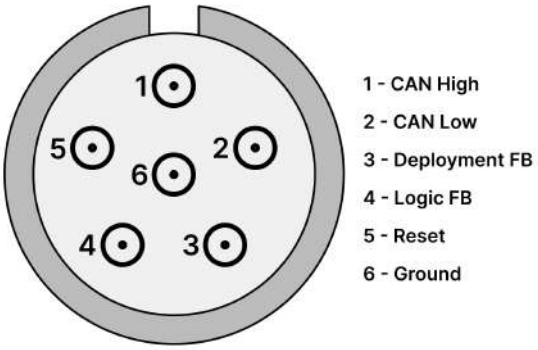

Figure 44: EQD Pinout

Figure 45: AQD

3.2 Ground Filling Station

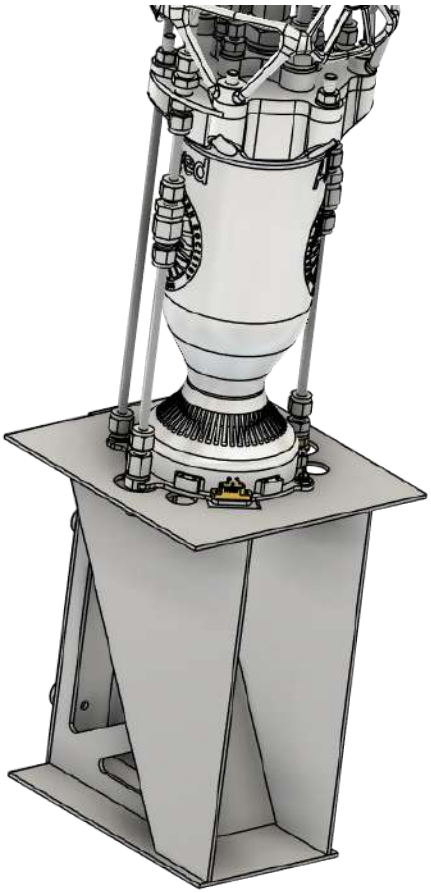

Figure 46: Fluid quick disconnects and flame deflector

3.2.1 Fluids System

The fluids system of the ground filling station (GFS) consists of separate nitrogen and nitrous oxide filling lines. This system connects the respective cylinders and the rocket, with Figure 47 containing the system P&ID.

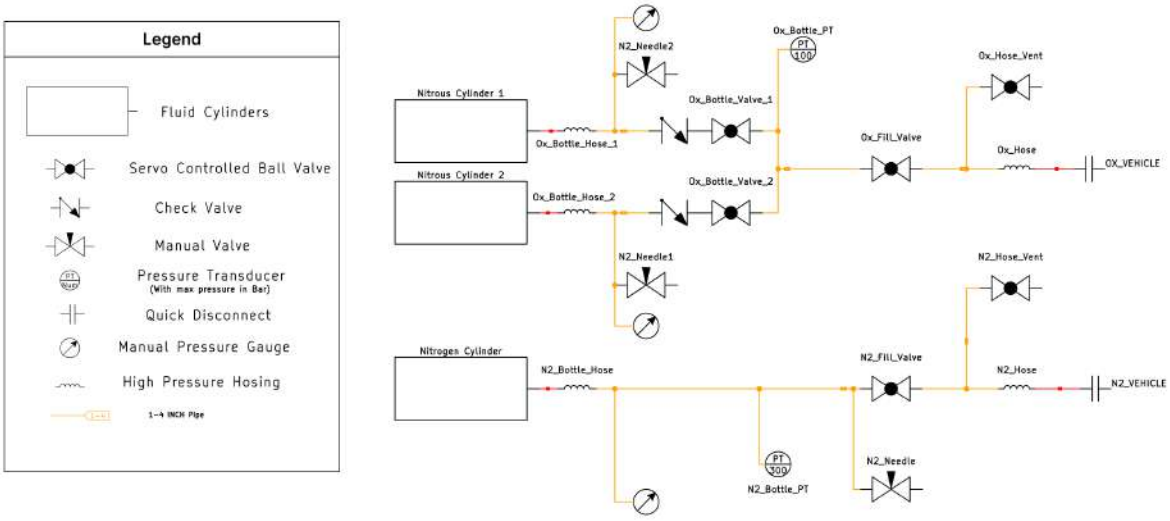

Figure 47: GFS Fluid System

Oxidiser System

Two nitrous oxide cylinders are connected in parallel to the system. By using nitrous oxide as a propellant the risk of self-pressurisation is always present. As the vapour pressure is dependent on temperature, venting to cool nitrous can be employed on *Pluto* to prevent tank pressures from exceeding nominal values. This is elaborated on further in Section 3.2.2, and a secondary nitrous cylinder is connected to the system as a reserve to accommodate the potential need for chill venting.

The individual nitrous oxide cylinders connect to manual pressure gauges, check valves and servo controlled ball valves before the pipes converge. The gauges will confirm to the Pressurised Fluids Specialist that the cylinders have been opened and inform them of the cylinder pressures. Check valves will act to prevent backflows in the event of a difference in cylinder pressures, and the immediate ball valves following cylinders (cylinder isolation valves) will ensure control over which cylinder is active at any moment. The flow paths combined and pass through a main oxidiser fill valve and into a quick disconnect with a manual quick release collar. The system also contains pressure transducers and both manual and servo actuated ball valve venting to be able to vent the GFS and the hose connecting it to the rocket. Important to note that whilst flow paths combine after the Nitrous bottles, only one isolation valve is ever opened at a time.

Nitrogen System

There is no risk of self pressurisation with nitrogen and as such fewer components are required in the nitrogen system than in the oxidiser system. The same combination of a manual gauge, pressure transducer, main nitrogen fill valve and the manual and servo actuated vents remains. A key difference between the systems safety wise is the use of different quick release connectors between the fluid lines, ensuring filling hoses cannot be connected incorrectly. Another difference lies in the pressure ratings of the components, with all components in the nitrogen system requiring a MEOP of at least 300 bar, compared to the 70 bar in the nitrous system.

3.2.2 Filling Procedure

1. Fuel

As specified in the checklist, first the fuel will be filled manually using a hand pump. During this operation, the fuel vent solenoid will be opened.

Fuel is measured before hand, to ensure the tank has appropriate ullage volume once filled.

Once fuel filling is done, the manual fuel fill valve and fuel vent solenoid are closed.

2. Bottles

After this, a visual and electronic check is done on all ground filling station and vehicle valves, to make sure they are all closed.

Then, both the nitrous bottles and N2 bottle are opened. Subsequently, all personnel clear the pad, and pressurised fluid filling will then commence.

3. N2 Pressurant

The second to be filled is the N2 COPV. To do this, the N2 Fill valve is actuated. Mission Control (MC) observe the filling rate using live data, and adjust the N2 Fill valve angle between fast and slow filling to keep the rate of N2 tank pressure increase slow.

Once a steady and slow rate of pressure rise is achieved, MC waits for equilibrium between the cylinder and the COPV. Crucially, the fuel and oxidiser tank pressures are periodically checked to see evidence of a leak through E-REG by any pressure rises. This is why it is imperative to have a slow fill initially. Once equilibrium is reached, the N2 Fill valve is closed.

It is worth noting that in the event that E-REG leaks through, N2 will be filled last, and automatically trigger venting if the propellant tanks start reading pressures above MEOP.

4. Oxidiser

Next, the Nitrous Oxide will be filled. To do this, the Ox Vent valve is opened on Pluto to its fast position. Then, one Ox Fill valve on the GFS is opened, after which gas will start venting from Ox Vent on Pluto as the tank fills.

Once N2O reaches the dip tube height within the tank, it will start venting through Ox Vent; visually this will look like a white plume coming from the rocket.

At this point MC closes the Ox Vent and Ox Fill valves, and check vapour pressure. If it is too high, which it often is after the first fill, Ox Vent is opened again irregardless of whether a plume is coming out of it.

Periodically it is closed to check the N2O vapour pressure, and once it reaches a target threshold value, i.e. 25 bar, Ox Vent is closed temporarily.

5. Oxidiser Top Up

Then, the top up procedure is started. Since one tank will now be mostly depleted, the second Ox Fill valve is opened to start draining the second N2O bottle.

Ox Vent is reopened in its slow vent position again, until a plume is spotted once more. Once the top up procedure is finished, Ox Fill is closed.

Finally, the Ox Hose valve is opened to vent the Ox QD hose.

6. Tank Pressurisation

E-REG is set to its pressurisation state, where it goes to a set angle and slowly pressurises the tanks. It then automatically closes when the fuel tank reaches the setpoint.

7. N2 Re-pressurisation

To account for any small pressure leaks from the N2 line, which may occur since it was first to be filled, a re-pressurisation procedure is done for the N2 COPV.

This entails opening the N2 Fill valve again on the GFS, and waiting for the N2 Tank pressure to equalise.

Lastly, the N2 Hose valve is opened to vent the N2 QD hose.

3.3 Mission and Launch Control

3.3.1 Ground Software

The ground software stack provides the primary interface between mission operators, the rocket, and associated ground support equipment (GSE). It consists of a combination of internally developed components, such as *Ricardo-Backend* and *Ricardo-CommandServer*, as well as established third-party solutions, most notably *Grafana*.

Each service within the stack is designed to function as a stand-alone native application, with inter-service communication occurring over Internet Protocol (IP) sockets. Despite this independence, the system is deployed within a containerised architecture to ensure reproducibility, simplify dependency management, and streamline software updates. The adoption of Infrastructure as Code (IaC) methodologies further accelerates deployment: a typical ground server, often a Raspberry Pi running Debian, can be fully provisioned in minutes with minimal manual intervention.

3.3.2 Ricardo Backend

Ricardo-Backend implements a translation layer bridging the Ricardo Network Protocol (RNP) network, used by flight and ground nodes, and the IP-based mission control network. This translation enables standard IP clients (e.g., laptops, tablets) to receive telemetry and issue commands without requiring direct knowledge of the RNP protocol.

A central component of *Ricardo-Backend* is its *Socket.IO* server, which provides a bidirectional publish–subscribe messaging interface. Multiple logical channels are supported, including:

- **Telemetry Channel:** Streams decoded telemetry data in real-time from the RNP network.
- **Packet Channel:** Allows clients to transmit encoded RNP packets to network nodes.

For clients without full *Socket.IO* support, a WebSocket-based fallback mechanism is provided.

Telemetry acquisition is handled on demand by the Data Task Request Handler (DTRH). The DTRH issues telemetry requests and deserialises responses from flight and ground nodes. Request specifications are defined in JSON configuration files, which describe the expected packet structure and any relevant bitfield mappings required for variable decoding. A browser-based frontend (Figure 48) permits dynamic modification of these tasks, enabling operators to create, edit, start, or stop tasks in real time. All received telemetry is persistently logged to disk to support post-flight analysis.

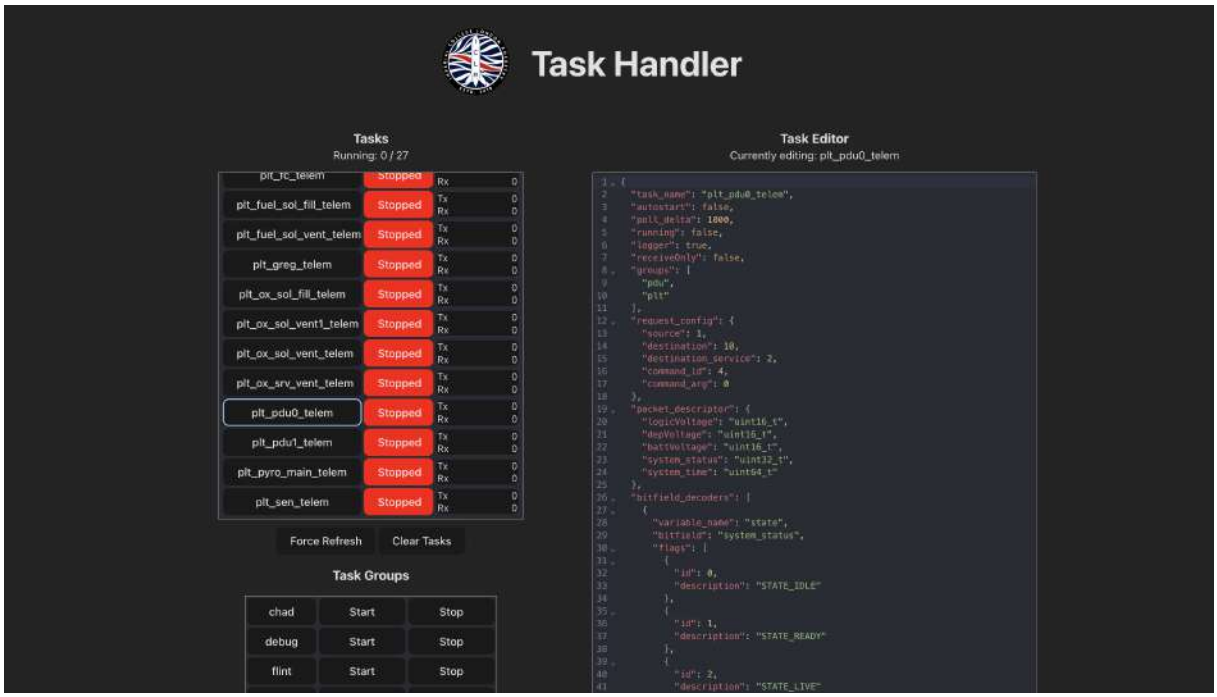

Figure 48: Task Handler UI

3.3.3 Ricardo Command Server

Ricardo-CommandServer provides a streamlined interface for transmitting commands to RNP nodes. It exposes a set of HTTP endpoints corresponding to predefined commands. These endpoints support a range of behaviours, including:

- Transmission of fixed, predefined commands to a single node.
- Parametrised commands accepting arguments via JSON payloads.
- Sequenced execution of multiple commands targeting multiple nodes.

This abstraction enables any HTTP-capable client to issue commands without requiring knowledge of RNP packet encoding or network topology. Consequently, operators and automated scripts can reliably interact with the flight system via a simple RESTful API.

3.3.4 Grafana

Grafana serves as the primary operator-facing interface for both telemetry visualisation and command execution. The platform's extensive plugin ecosystem facilitates integration with *Ricardo-Backend* WebSockets for real-time telemetry ingestion and supports the creation of custom dashboard elements, such as command buttons interfacing with *Ricardo-CommandServer*.

Well-structured dashboards are critical for rapid situational awareness, ensuring operators can access actionable information with minimal cognitive overhead. The ease of Grafana dashboard customisation allows rapid iteration of user interfaces based on operator feedback, enhancing reliability and operational safety. Figure 49 illustrates representative mission control dashboards employed during hot fire qualification testing.

3.3.5 Arming and Ignition

The arming and ignition sequence for the *Pluto* launch vehicle must follow a strict sequence to guarantee both nominal functionality and operational safety. Multiple independent arming

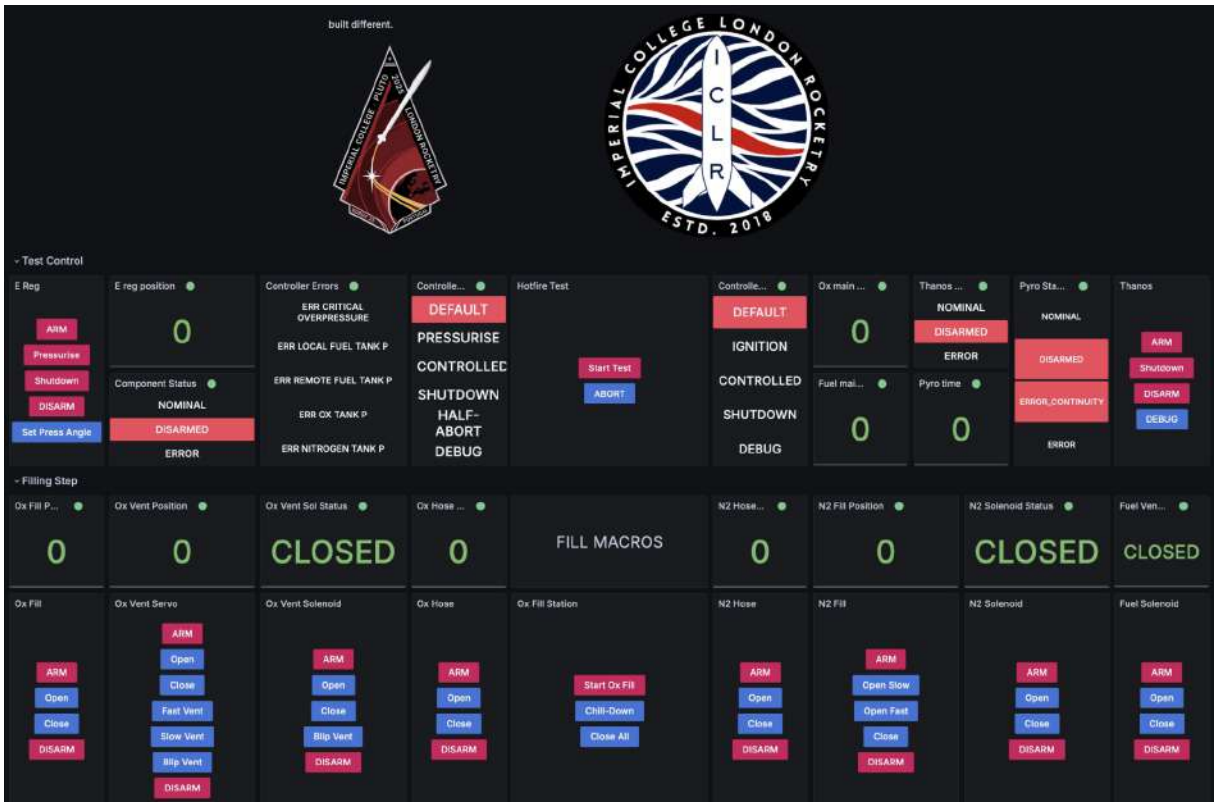

Figure 49: Grafana Hot Fire Dashboard

stages are enforced to minimise the likelihood of inadvertent actuation.

3.3.6 Power System States

The Power Distribution Unit (PDU) defines four discrete operational states:

1. **Off:** Both logic and deployment rails are disabled.
2. **Powered:** Logic rail enabled; deployment rail disabled.
3. **Ready:** PDU awaits explicit command to energise deployment rail.
4. **Deployment Live:** Deployment rail is energised and available for actuation.

In the *Powered* state, avionics controllers receive power via the logic rail while the deployment rail remains inactive, ensuring the vehicle remains in a safe configuration. Removal of the arming *remove-before-flight* (RBF) pins transitions the system into the *Ready* state, wherein the deployment rail remains inhibited. Once all personnel have vacated the launch vicinity, mission control issues a command to transition into the *Deployment Live* state.

Even with the deployment rail energised, each subsystem (e.g., ignition, separation mechanisms) requires an explicit arming command before actuation is possible.

3.3.7 Launch Sequence

Following propellant loading, the flight computer transitions into the *Launch* state and executes a pre-flight verification sequence. This process attempts to arm each subsystem; failure of any subsystem to report nominal status aborts ignition.

All ground-controlled operations, including enabling the deployment rail, arming components, and issuing the launch command, require multiple deliberate operator actions. This layered

safety architecture mitigates the risk of accidental triggers of potentially hazardous actuators, such as ignition or deployment events.

3.4 Flight Termination System

Pluto's flight termination system (FTS) uses thrust termination under two separate conditions as described below. This is commanded over the LoRa radio connection from mission control to the flight controller (*PickleRick*) if two hardware FTS buttons in mission control are pressed simultaneously.

If *PickleRick* does not detect lift-off but ignition is commanded, the FTS command disarms *Stark* which closes both engine valves to save fuel. The rocket will then be depressurised and N20 vented under propellant unloading procedures. This type of abort will likely occur if the hold down system does not release the rocket.

If liftoff is detected by *PickleRick*, a mid flight FTS command will result in a *Stark* shutdown which closes the oxidiser main valve, depleting fuel and pressurant through the engine. This is similar to the engine shutdown triggered post flight. As per the normal procedure, all vent valves will be opened prior to touchdown to allow sufficient time to boil off remaining oxidiser in the tank.

4 Mission Concept of Operations

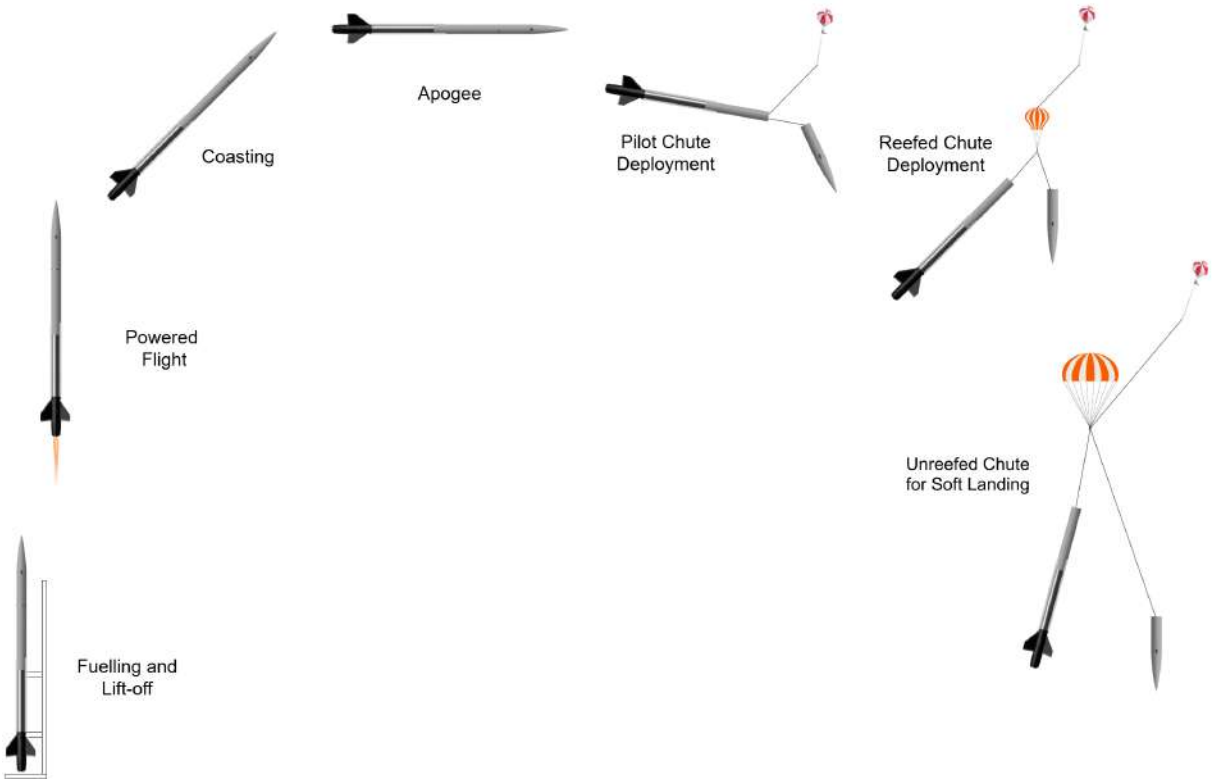

Figure 50: CONOPS diagram

1. ***Pluto* on rail (T-60 minutes)**:
   Pluto is placed on the launch rail with the ground electronics system already in place and quick disconnects attached. System checks are performed to ensure all systems are performing as expected post transport to the launch pad. The rail is then raised and all filling lines are connected. IPA filling occurs at this stage, after which the pad is cleared.

2. **Pre-Flight Operations (T-45 minutes)**:
   Ground support and actuators are armed, with the remote filling procedure commencing. The avionics then switch to their launch state given no anomalies during the final system checks.
3. **Lift-Off (T-0 to T+0.69 seconds)**:
   The engine ignites on the ignition command and shortly after reaches sufficient thrust for the rocket to accelerate upwards and begin flight safely. All quick disconnects detach upon lift-off. The avionics detect this event after acceleration exceeds 2 g and altitude exceeds 50 m.
4. **Powered Flight (T+0.69 seconds to T+9.1 seconds)**:
   The onset of powered flight is defined as the point when *Pluto* clears the rail. From this point onwards, the engine continues to burn until T+9.1 seconds, until an estimated altitude of 1610 m. During this phase *Pluto* reaches its peak velocity and acceleration.
5. **Coasting Flight (T+9.1 seconds to T+34.6 seconds)**:
   The engine flame quenches when all propellant is depleted. At T+30s, all vents open allowing any remaining propellants to vent off, especially if FTS is commanded.
6. **Reefed Parachute Deployment (T+34.6 seconds)**:
   At apogee, the avionics trigger the separation system to release the pilot chute, then the main parachute, initially in the reefed configuration. This will decelerate the rocket to a nominal descent speed in the range of 30-35 m s^{-1}. The COTS computer will act as a redundancy for this event.
7. **Parachute Dis-Reefing (T+160 seconds)**:
   At an altitude of 450 m AGL, the primary chute dis-reefs to slow the descent speed to 5.6 m s^{-1}. The event is triggered by the avionics system, again with the COTS computer used for redundancy.
8. **Touchdown and Recovery (T+239 seconds)**:
   The rocket will impact the ground at 5.6 m s^{-1} to ensure good condition post ground-impact and successful recovery. Similarly, the COTS computer will act as a redundancy to the SRAD avionics to transmit GPS signals on two frequencies along with an audible sound to determine the precise location to which the recovery team can travel.

5 Trajectory Analysis

OpenRocket v23.09 and RocketPy v1.10.0 were used to develop the simulations for this flight. OpenRocket and RocketPy give full 6 degree of freedom simulations of the rocket during ascent, with RocketPy also employing the same model fidelity on descent to model the flight of the rocket under both the reefed and unreefed parachute. Initially when sizing the rocket OpenRocket was used due to the more graphical nature of rocket design, before conducting more detailed simulations with RocketPy. The C_D vs Mach Number curve was exported from OpenRocket.

5.1 Nominal Thrust Curve

The thrust curve used in the final simulations was taken from the flight qualification burn performed on 01/09/2025. The thrust is shown in Figure 51, achieving a total impulse of 29,500 Ns over 9.18 seconds. This gives an average thrust of 3.23 kN and peak thrust of 5.23 kN at the start of the burn, high enough to ensure *Pluto* reaches the required off-the-rail velocity.

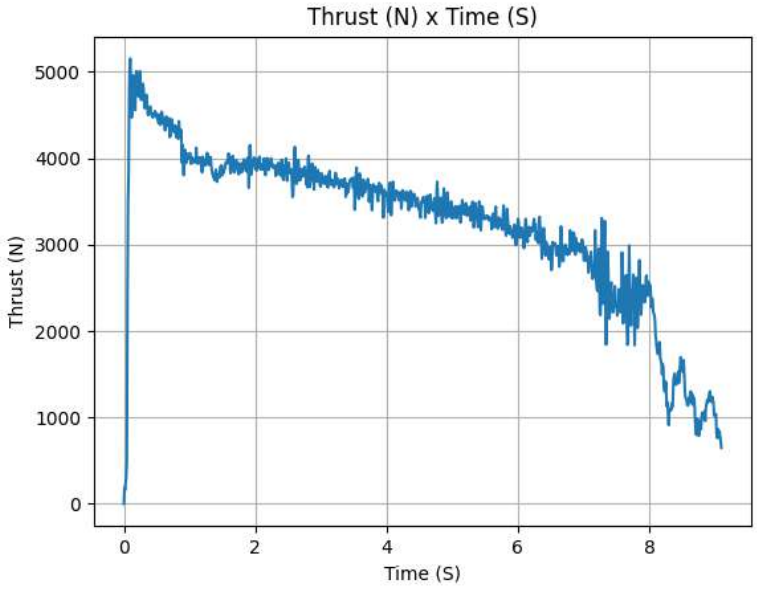

Figure 51: Flight Qualification Burn Thrust Curve

5.2 Trajectory Simulations

As per *EuRoC* specifications, RocketPy was used in the final simulations. Launch site parameters were used - the rail of length 12 m was positioned with a heading of 133° and elevation of 84°. The atmospheric model was based on the location of the launch site at Campo Militar de Santa Margarida at 39.2323°N 8.1720°W, with the surface wind defined as being 8.7 m/s in the direction of the launch corridor to model a worst-case drift scenario. The flight trajectory has been plotted in Figure 52. The vertical velocity and acceleration have been plotted in Figure 53.

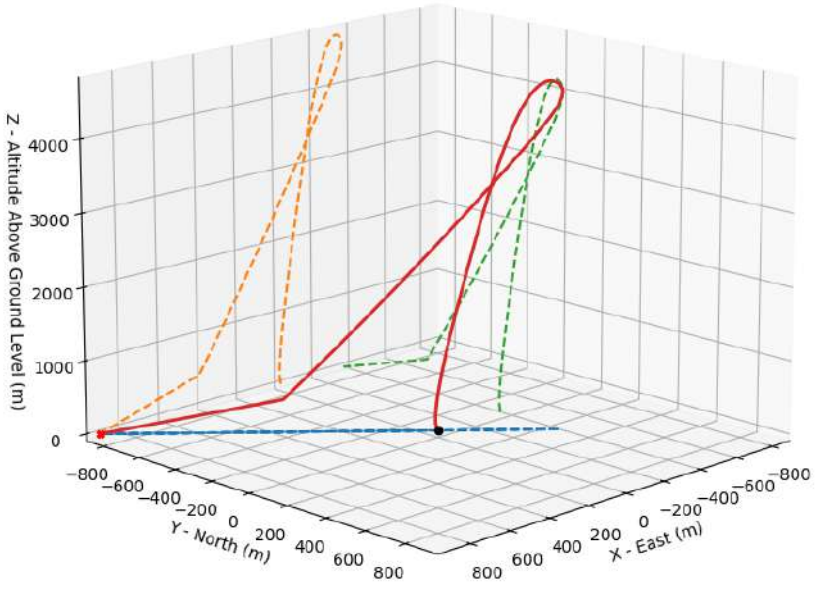

Figure 52: *Pluto* predicted flight trajectory

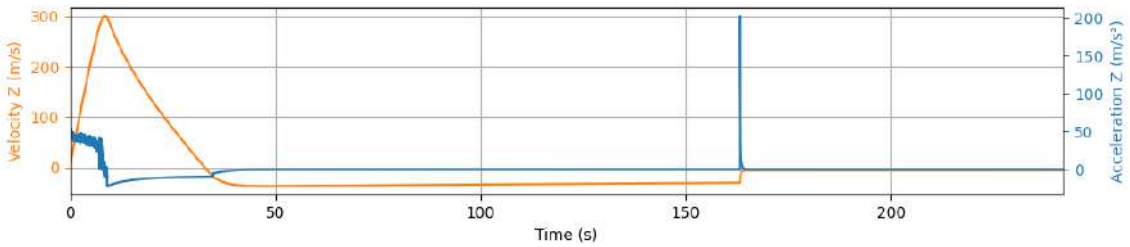

Figure 53: *Pluto* vertical velocity and acceleration

5.3 Stability Analysis

The initial stability margin of the rail is 2.22 cal, meeting EuRoC's requirement of a minimum of 1.5 cal. This continues to rise throughout the flight, reaching a maximum of 3.51 cal, which is well below the upper limit of 6 cal.

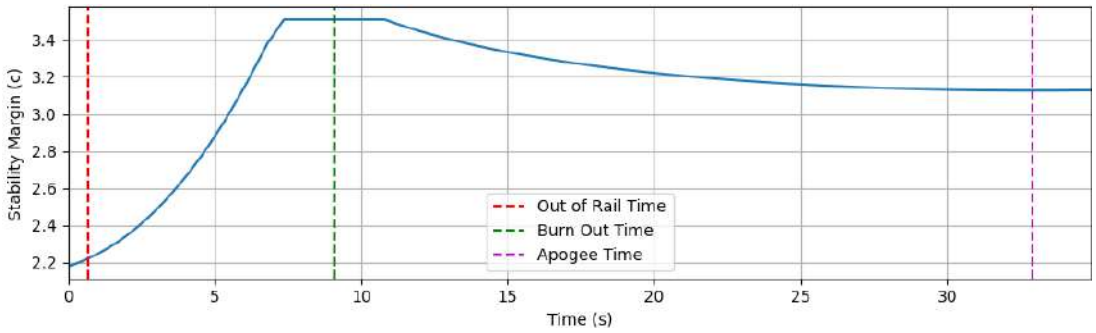

Figure 54: *Pluto* in-flight stability

5.4 Monte Carlo Analysis

Since the theoretical parameters used in the main simulation will likely be different for the launch, Monte Carlo analysis is carried out using RocketPy's 'Stochastic Objects', varying key parameters to observe their effect on the rocket's flight and launch conditions. The parameters to be varied are defined in Table 13 below, along with their standard deviation used in the simulations.

Table 13: *Pluto* Flight Parameter Standard Deviations

Mass	1 kg
Longitudinal Inertia	1.26 kg m/s^2
Rotational Inertia	0.01 kg m/s^2
Nose Cone Length	1 mm
Fins (all dimensions)	0.5 mm
Boattail (all dimensions)	1 mm
Main Chute C_DA	2.92 m^2
Drogue Chute C_DA	0.105 m^2
Rail elevation	0.5°
Rail heading	1°

The chutes and inertial properties of the rocket have the largest standard deviations relative to their values - this is due to effects such as atmospheric properties and the general unpredictability of the system. Variations in the inertia tensor were derived from those in mass, which was assumed to be 1 kg across the entire rocket. Manufacturable parts are much more likely to follow

the expected dimensions and therefore the changes in these values are lower, affecting results less. The variation in wind speed is accounted for with a 20% variability in all directions using a stochastic atmosphere model, with the mean value of 6 m/s at 330° being taken as an average at the launch site. Standard deviations of values resulting from these input distributions are given in Table 18.

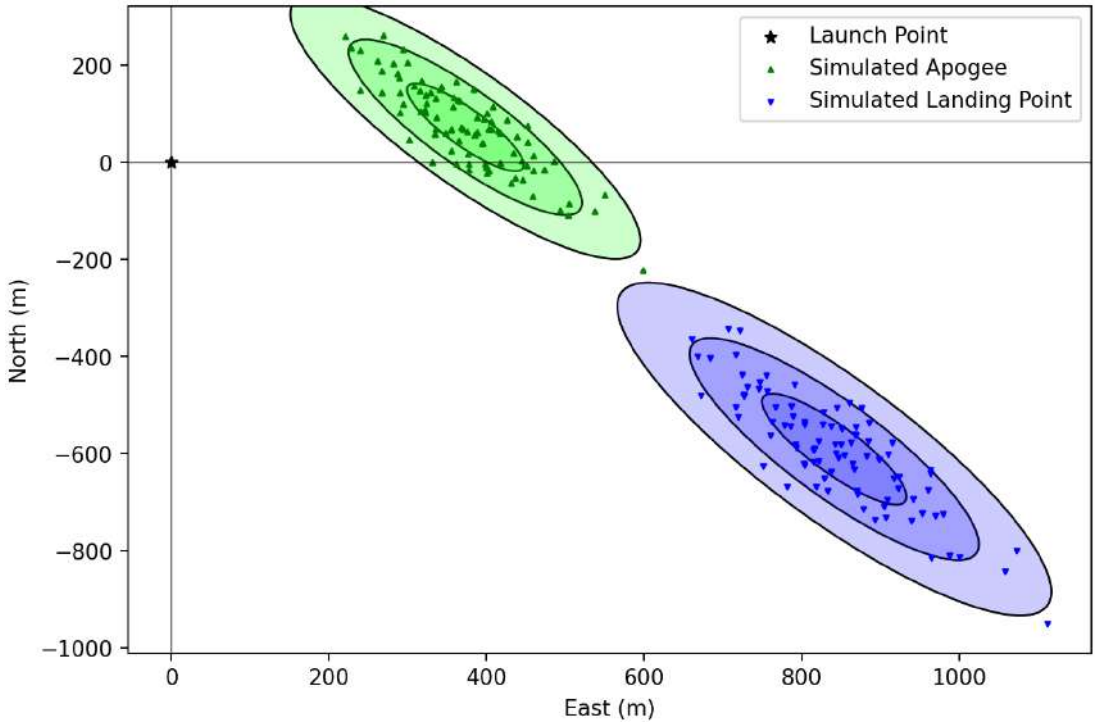

Figure 55: *Pluto* landing uncertainty ellipses

In total, 90 simulations were run. As expected, the mean values from the Monte Carlo simulations agree well with those from the nominal flight simulation. The standard deviations of flight parameters in 18 show that, with regard to *EuRoC* requirements, the rail departure velocity is above the minimum limit up to 3-sigma uncertainty. Minimum stability is high enough that even with this variability, it remains above the limit in all cases. The landing ellipses are shown in Figure 55, giving a drift of 1.46 km, again in a worst case for nominal flight at 3 standard deviations (the outer ellipse). All landing points lie well within landing requirements.

5.5 Simulations Summary

The key simulation outputs have been summarised in the below tables. Note the inclusion of the drogue-only case in Table 19, showing the maximum allowable wind speed to land within a 5 km radius of the launch site. This configuration represents recovery using only an unreefed COTS drogue parachute. This has been included to reduce the drift radius, and therefore allow for the launch of *Pluto*, in the case of very strong winds.

Table 14: *Pluto* Rail Departure States

Time	0.69 s
Velocity	30.85 m/s
Stability Margin	2.22 Cal

Table 15: *Pluto* Burn Out States

Time	9.1 s
Velocity	298 m/s
Altitude	1,629 m

Table 16: *Pluto* Apogee and Impact States

Apogee	4608 m (AGL)
Apogee Time	32.6 s
Time of Impact	238.8 s
Velocity at Impact	5.6 m/s
Maximum Drift	1320 m

Table 17: *Pluto* Ascent Maximum State Values

Maximum Speed	296 m/s at 8.55 s
Maximum Mach Number	0.88 Mach at 8.68 s
Maximum Acceleration	55.348 m/s^2 at 0.08 s

Table 18: *Pluto* Flight Standard Deviations

Rail Departure Velocity	0.28 m/s
Apogee	73.3 m
Impact Velocity	0.265 m/s
Drift Distance	241 m
Flight time	8.75 s
Time to Apogee	0.15 s

Table 19: *Pluto* Allowable Launch Winds

Nominal Flight	21.3 m/s
Drogue-Only	56.9 m/s
Unreef at Apogee	7.1 m/s

6 Conclusion

This report has presented a comprehensive overview of ICLR's 2025 EuRoC entry, *Pluto*. The report details the significant advancements built upon the lessons from the *Nimbus* series of rockets and shows the team's design decisions contributing to the overall mission objectives.

The liquid bi-propellant propulsion system, centred around the common bulkhead propellant tank and the GOOFY engine, has been successfully hot-fired seven times, including a full-duration flight qualification burn which achieved a peak thrust of 5.3 kN and a total impulse of 29,500 Ns. While this is just under the design target of 6.0 kN, it is sufficient to propel *Pluto* to the required rail departure velocity. Furthermore, the SRAD common bulkhead structural tank has been successfully proof-tested to 1.5 times its maximum expected operating pressure, demonstrating a mass-efficient architecture that effectively transfers flight loads without the need for an external airframe, a concept which can be refined in future vehicles.

The airframe's structural integrity has been validated through extensive simulation. The Kevlar composite body tube and aluminium stringers have been shown to withstand all expected flight loads, with buckling simulations of the stringers yielding a safety factor of over 3.6. This design has successfully integrated a hybrid monocoque and skeletal structure, providing both mass savings and crucial accessibility to internal components. Additionally, the successful compression testing of the generatively designed engine truss has proven the viability of this methodology for producing lightweight, robust components for high-stress applications.

The recovery system has been redesigned for improved reliability, addressing the failures experienced by its predecessor. The novel, clamp-based separation mechanism demonstrates a robust, SRAD system that operates without blackpowder, allowing for safe and repeatable ground testing. FEA simulations on the recovery bulkheads, using conservative shock load estimates derived

from previous flight data, have confirmed their ability to withstand deployment forces with safety factors of 1.53 and 1.72. This provides confidence in the system's ability to ensure a safe recovery, which can be further affirmed with future flight testing.

Through the design, testing, and validation of Pluto's subsystems, ICLR has progressted towards a more robust and capable vehicle architecture. The project successfully demonstrates the viability of a structural common-bulkhead tank, a redesigned non-pyrotechnic recovery system, and a refined liquid bi-propellant engine. These advancements provide a critical foundation for future missions as the team progresses towards its long-term goals.

6.1 Closing Remarks

ICLR would like to thank in particular Dr. Aaron Knoll who has invaluably supported and guided the team continuously since its inception, taking us through the difficulties of navigating and managing an ever-evolving team. We are incredibly grateful to James MacFarlane, Adam Greig, Iain Waugh, Iain Laine, Ed Moore, Malcolm, Phil, and Helen, at Airborne Engineering, as without their critical assistance and provision of their test facility, ICLR would never have made it to EuRoC 2025.

A thank you is owed to the Student Teaching Workshop technicians Eddie, Paul, Steve, Aslan, Neil, who were vital in manufacturing many of our most critical components, including our propellant tanks. We would like to extend a large thanks to Ela Sapinska-Elise and Daisy Antonioni for assisting us to seamlessly integrate and grow the finances of ICLR over the past year with the Aeronautics department. We would also like to thank the Aeronautics technicians Jordan Farrar, Mark Thornton, Ian Pardew and Roland Hutchins for their contributions, and assistance with CNC milling processes and manufacture of the airframe. Thank you to the Imperial Hackspace technicians, especially Fred, for their ongoing manufacturing assistance and also of course Sam, Gary Senior, Mark, and Harry at Mech Eng Stores, for dealing with the unending deliveries we order.

Finally, to all of our sponsors, academic partners, individual contributors, and especially ICLR's hard-working team members, from the veterans of past EuRoC's to new freshers, thank you - it would not be possible without you.

References

[1] Safety W. Hybrid Assembly®;. Available from: https://www.wehberg-safety.de/bursting_discs_hybrid_assembly.html.

[2] ICLR. Pluto Concept Report. Imperial College London; 2025.

[3] Abnahmebeauftragter. Inspection Certificate 3.1 - DIN EN 10204:2005. Unna, Germany: Aluminiumwerk Unna AG; 2023.

[4] MakeItFrom com. 6082-T6 Aluminum Material Properties; 2025. Available from: https://www.makeitfrom.com/material-properties/6082-T6-Aluminum.

[5] Hicks TG. Bolted Joint Analysis; 2025. Available from: https://mechanicalc.com/reference/bolted-joint-analysis.

[6] Young WC, Budynas RG. Roark's Formulas for Stress and Strain. 8th ed. New York: McGraw-Hill; 2012.

[7] McGinty B. von Mises Stress;. Available from: https://www.continuummechanics.org/vonmisesstress.html.

[8] Supplies TR. Bolts-Commercial grade;. Available from: https://tridentracing.co.uk/product/bolts-commercial-grade/#:~:text=12.9%20grade%20Socket%20Cap%20heads,75%2C000%20(517MPa)%20shear%20strength.

[9] Austin Sennott CS. How to Design Pressure Vessels, Propellant Tanks, and Rocket Motor Casings. Half CAT rocketry;.

A System Data

Table 20: General Specifications of *Pluto*

Length	4510 mm
Diameter	191 mm
Wet Mass	81.3 kg
Dry Mass	57.8 kg
Stability Off-the-Rail	2.22 cal
Predicted Off-the-Rail Velocity	30.85 m/s
Predicted Apogee	4608 (AGL) m
Predicted Max Acceleration	55.348 m/s^2 (5.64 g)
Predicted Max Velocity	296 m/s (Mach 0.88)
Flight Time	238.8 s

Table 21: *Pluto* GOOFY Engine Specifications

Total Impulse (Ns)	31779
Specific Impulse (s)	155
Maximum Thrust (N)	5304
Burn Time (s)	7.0
Oxidiser Type	Nitrous Oxide
Fuel Type	Isopropyl Alcohol
Oxidiser Mass (kg)	15.9
Fuel Mass (kg)	5.2
OF Ratio	3.0
Chamber Pressure (bar)	30
Tank Pressure (bar)	50

Table 22: *Pluto* Parachute Specifications

Type	Annular
Diameter(Disreefed)	10 ft
Coefficient of Drag	2.2

Table 23: *Pluto* Mass Breakdown

Section	Mass (kg)
Payload	1.8
Electronics	9.5
Airframe	6.3
Recovery	4.8
Propulsion	35.4
Propellant	23.5
Dry Mass	57.8
Wet Mass	81.3

Table 24: *Pluto* Battery Specifications

Name	Cell Configuration	Capacity (mAh)	Nominal Voltage (V)
Rocket	$2 \times$ 4s 1p	3000	14.8
Reefing Line Cutter	$2 \times$ 1s 1p	2000	3.7
Payload	2s 1p	2500	7.4

Table 25: *Pluto* Avionics Specification

Nominal Battery Voltage	14.8 V
Battery Type	Li-ion
Battery Capacity	3000 mAh (Redundant)
Endurance	9 hours
RF protocol	LoRa
Maximum RF Transmission power	100 mW, 100 mW
Tested range	65 km
Estimated maximum range	100 km
RF frequency	868 MHz, 2400 MHz
Rocket antenna type	Patch
Rocket antenna gain	-2.4 dBi
GCS antenna type	Rubber Ducky
GCS antenna gain	+2.7 dBi
Maximum bit rate	37.5 kbps, 1000 kbps
Kalman filter refresh rate	200 Hz

B Test Reports

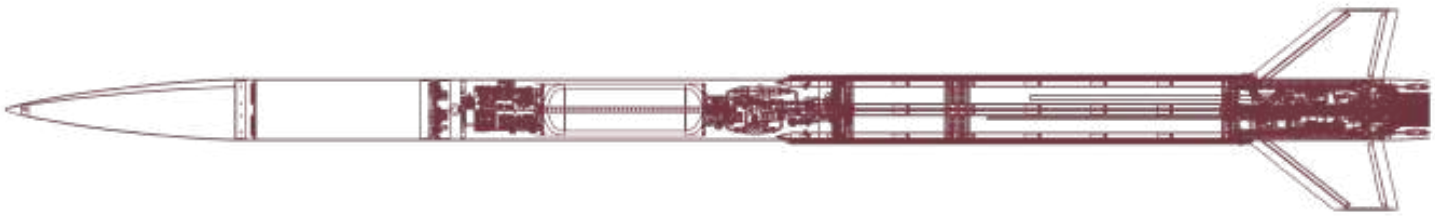

PLUTO
Test Report

Team 18 Test Report
to the 2025 EuRoC

September 14th 2025

Supervised by Dr. Aaron Knoll

Department of Aeronautics, Imperial College London

IMPERIAL COLLEGE
LONDON ROCKETRY

Contents

1 Propulsion Test Reports

1.1 Tensile Testing of SRAD Pressure Vessel Bulkhead Material

Test Name: Bulkhead Material Testing

Version: 1

Date: 30/06/2025

Location: Dynamic Fracture and Forming (DFF) Lab, Imperial College London

Conducted by:

Rohan Woodcock	Hardik Modi	Jason Aretaios
Propulsion Engineer	Propulsion Engineer, SFO	Propulsion Lead

Aims

The aim of this test is to experimentally determine the yield strength and temper of the Al 7075 stock material used to manufacture the tank bulkheads.

Procedure

1. Measure dimensions of each testing sample.
2. Calibrate video extensometer.
3. Stick marker dots to the reduced width sections of the samples for use with the video extensometer.
4. Clamp samples to testing machine, with the machine actively moving to ensure 0 stress.
5. Wear safety glasses.
6. Begin test, recording load cell force data and strain data from the video extensometer.

Results & Conclusion

3 ATSM E8M Subsize samples were CNC machined from the bulkhead stock material. They were each tested to failure. The 0.2% proof stress was taken as the yield strength for the material, as Aluminium does not exhibit a clear yield point.

Images & Data

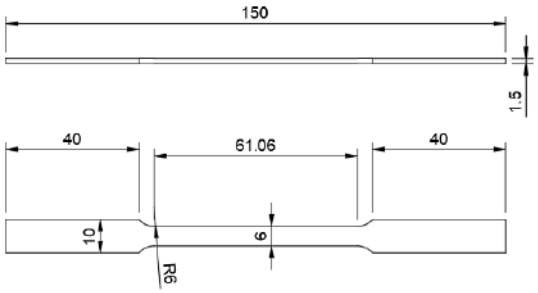

Figure 1: Sample Dimensions

Figure 2: Test Setup

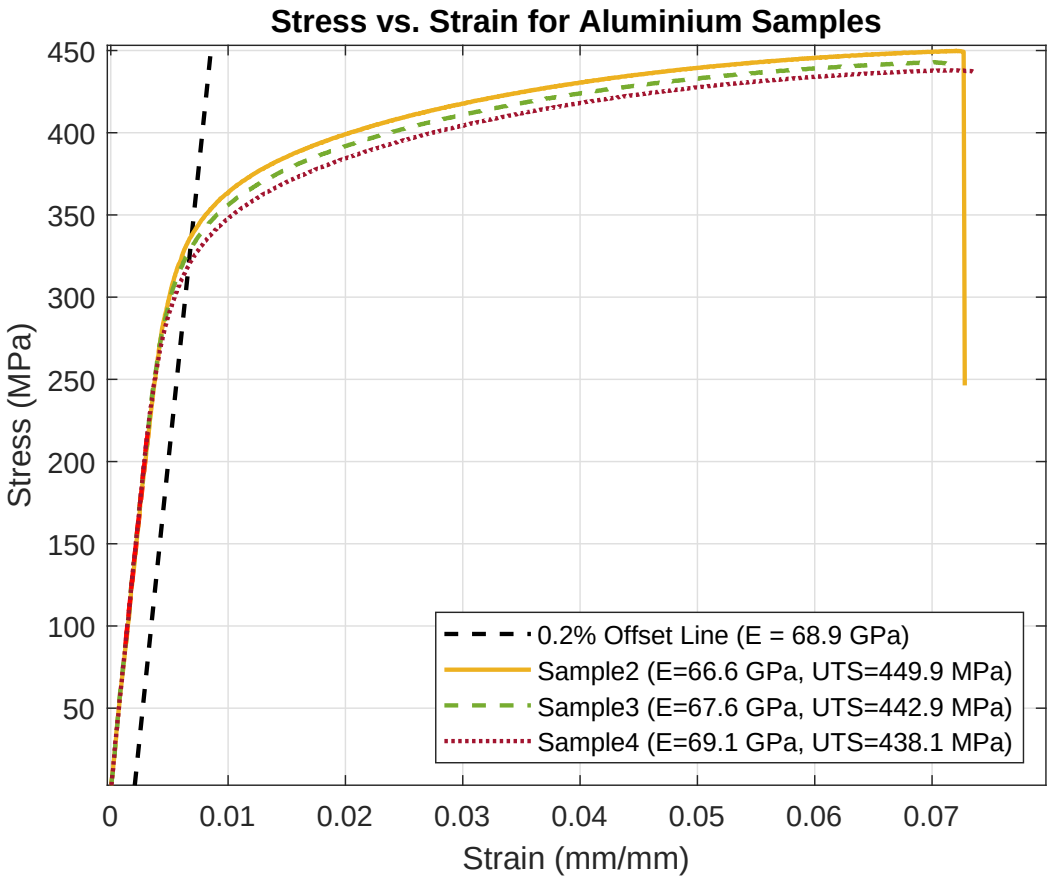

Figure 3: Stress-Strain Graph

Test Outcome

This test was declared a success. Completion is signed for by the following responsible engineers:

Rohan Woodcock

Propulsion Engineer

Hardik Modi

Propulsion Engineer, SFO

Jason Aretaios

Propulsion Lead

1.2 Hydrostatic Testing of SRAD Common Bulkhead Pressure Vessel

Test Name: Hydrostatic Tests of Oxidier and Fuel Tanks

Version: 1

Date: 24/08/2025

Location: Silwood Park, Imperial College London

Conducted by:

Rohan Woodcock	Hardik Modi	Soham Moore
Propulsion Engineer	Propulsion Engineer, SFO	Electronics Lead

Aims

Demonstrate that the SRAD pressure vessel can withstand a hydrostatic pressure 1.5 times the Maximum Expected Operating Pressure (MEOP) for 60 minutes (twice the maximum expected operating period). Conduct the fuel tank and oxidiser tank tests separately to ensure the maximum load scenario (90 bar dP across common bulkhead).

Procedure

1. Connect fittings to tank and ensure tightened.
2. Test solenoid pressure release valve actuation.
3. Zero pressure transducers to absolute pressure (1 bar).
4. Fill tank with water vertically.
5. Prime the hydrostatic pump and connect to the tank, minimising trapped air volume.
6. Shift tank to horizontal position.
7. Increase pressure to 60 bar (MEOP), ensuring that pressure on hydrostatic pump gauge and transducer are consistent.
8. Shift toggle to high pressure mode and continue operating handles until pressure gauges read 90 bar.
9. Watch pressure gauges for any leaks for a period of 60 minutes.
10. Release pressure by remotely actuating solenoid valve.

Results & Conclusion

The fuel tank was tested first. The reading on the pump gauge and pressure transducer were inconsistent at 20 bar. An additional digital pressure gauge was then attached to the system, which matched the pump pressure gauge reading. The test was restarted and performed as expected, with no pressure loss over a 60-minute period.

The oxidiser tank was tested with a new pressure transducer and performed as expected with no pressure loss over a 60-minute period.

Images & Data

Figure 4: Test setup

Figure 5: Fuel Tank Test Pressure Reading

Figure 6: Oxidiser Tank Test Pressure Reading

Test Outcome

This test was declared a success. Completion is signed for by the following responsible engineers:

Rohan Woodcock

Propulsion Engineer

Hardik Modi

Propulsion Engineer, SFO

Soham More

Electronics Lead, CTE

1.3 Hydrostatic Testing of COTS COPV

Test Name: Hydrostatic Test of COTS pressurant tank.

Version: 1

Date: 24/08/2025

Location: Thermofluids Lab, Imperial College London

Conducted by:

Baboucarr Jeng	Hardik Modi	Soham More
Propulsion Lead	Propulsion Engineer, SFO	Electronics Lead

Aims

Verify that the COTS COPV used to store the pressurant can withstand a Maximum Expected Operating Pressure (MEOP) of 300 bar for 60 minutes (twice the maximum expected operating period).

Procedure

1. Calibrate pressure transducers at 1 Bar.
2. Test the servo actuated pressure release ball valve actuation.
3. Fill tank with water vertically.
4. Connect fitting to tank and ensure tightened.
5. Prime the hydrostatic pump and connect to the tank, minimising trapped air volume.
6. Shift tank to horizontal position.
7. Increase pressure to 250 bar, ensuring that pressure on hydrostatic pump gauge and transducer are consistent.
8. Shift toggle to high pressure mode and continue operating handles until pressure gauge reads 300 bar (MEOP).
9. Watch pressure gauges for any leaks for a period of 60 minutes.
10. Release pressure by remotely actuating the servo ball valve.

Results & Conclusion

The COTS COPV was tested with a pressure transducer and performed as expected with no pressure loss over a 60-minute period.

Images & Data

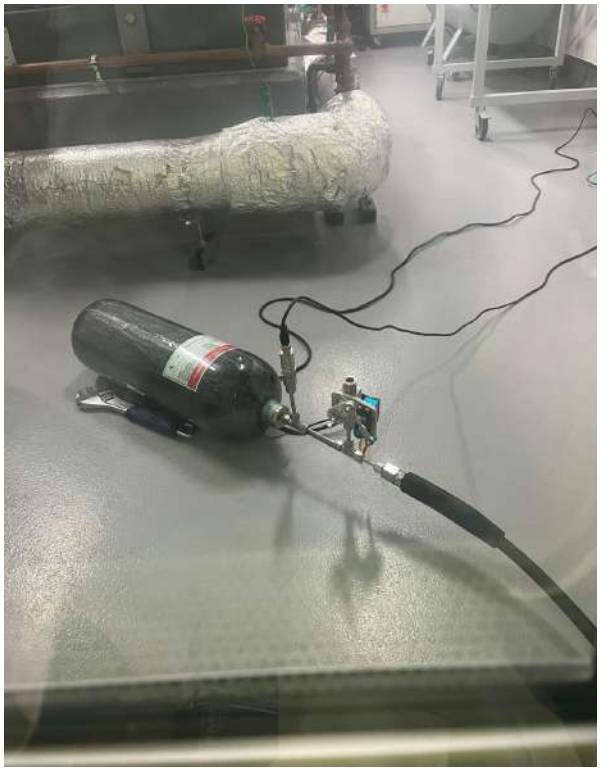

Figure 7: Test Setup

Figure 8: COTS COPV Test Pressure Reading

Test Outcome

This test was declared a success. Completion is signed for by the following responsible engineers:

Baboucarr Jeng

Propulsion Lead

Hardik Modi

Propulsion Engineer, SFO

Soham More

Electronics Lead, CTE

1.4 Hydrostatic Testing of GOOFY Combustion Chamber

Test Name: Hydrostatic Testing of GOOFY Combustion Chamber

Version: 1

Date: 13/09/2025

Location: Aeronautics Workshop, Imperial College London

Conducted by:

Baboucarr Jeng	Rudra Nakade	Raghav Ramkumar
Propulsion Lead	Propulsion Lead	Propulsion Lead

Aims

Demonstrate that the GOOFY engine combustion chamber can withstand a hydrostatic pressure 1.5 times the Maximum Expected Operating Pressure (MEOP) for 30 minutes

Procedure

1. Fill engine with water.
2. Prime hydrostatic pump and connect to engine, minimising trapped air volume
3. Increase pressure to 30 bar (MEOP) using the test pump
4. Shift the toggle to high pressure mode and continue operating handles until desired pressure (45 bar) is achieved
5. Stop increasing pressure and monitor pressure gauge for any leaks over a period of 30 minutes
6. Release pressure by loosening fine adjustment valve and then main pressure release valve

Results & Conclusion

Test performed as expected, no pressure loss was observed over the 30 minute test period.

Images & Data

Figure 9: Test pressure reading

Figure 10: Sealed engine

Figure 11: Testing setup

Test Outcome

This test was declared a success. Completion is signed for by the following responsible engineers:

Baboucarr Jeng	Rudra Nakade	Raghav Ramkumar
Propulsion Lead	Propulsion Lead	Propulsion Lead

1.5 Fuel Loading and Offloading Test

Test Name: Fuel Loading and Offloading Test

Version: 1

Date: 13/09/2025

Location: Aeronautics Workshop, Imperial College London

Conducted by:

Baboucarr Jeng	Lea Liu	Raghav Ramkumar
Propulsion Lead	Propulsion Engineer	Propulsion Lead

Aims

Demonstrate capability to load and unload fuel from *Pluto*, and that both procedures can be completed on the launch pad.

Loading Procedure

1. Fill hand pump to upper 9L line with required fuel mixture.
2. Connect hand pump to manual valve on fuel line.
3. Close fuel main engine valve and open fuel vent solenoid.
4. Open manual valve and pump hand pump to fill the fuel tank.
5. Stop pumping when fuel level reaches lower marked line on filling tank and close manual valve, the difference in volume is pre-measured to be the required fuel volume (6.7L).
6. Disconnect filling tank

Offloading Procedure

1. Connect compressed air system to fuel vent solenoid - this will be through an air compressor at the launch pad.
2. Connect filling tank to manual valve and uncap the pump.
3. Close fuel main engine valve and open fuel vent solenoid.
4. Open manual valve.
5. Turn on air compressor to force fuel from tank to filling tank.
6. Turn off compresssor once air begins to be pumped into filling tank.
7. Close manual valve.

Results & Conclusion

Both loading and offloading were completed using the above described procedure. The mass of the filling tank was measured pre-loading and post-offloading, with a 0.3% reduction in mass.

Images & Data

Figure 12: Testing Setup

Figure 13: Filling tank with hand pump

Figure 14: Compressed air gauge

Test Outcome

This test was declared a success due to successful loading of required fuel volume and near 100% of volume offloaded. Completion is signed for by the following responsible engineers:

Baboucarr Jeng

Propulsion Lead

Lea Liu

Propulsion Engineer

Raghav Ramkumar

Propulsion Lead

1.6 Pressurant and Oxidiser Loading and Offloading Test

Test Name: Pressurant and Oxidiser Loading and Offloading Test

Version: 1

Date: 24/08/2025

Location: J2 Test Facility, Airborne Engineering Ltd.

Conducted by:

Raghav Ramkumar	Rudra Nakade	Andrei Paduraru
Propulsion Lead	Propulsion Lead	Electronics Lead

Aims

Demonstrate capability to load and unload pressurant (N2) and oxidiser (Nitrous Oxide) from *Pluto*, and that both procedures can be completed remotely through the Ground Filling Station (GFS).

Loading Procedure

Nitrous oxide is loaded prior to nitrogen loading.

Nitrous Oxide

1. Pre launch, Mission control and Launch Control will determine based on environmental conditions whether one or two nitrous cylinders will be required for launch.
2. The nitrous cylinder(s) is/are opened before leaving the pad, with oxidiser fill and vent valves on the GFS closed.
3. Open rocket oxidiser vent valve to fast position
4. Open GFS oxidiser fill valve
5. Keep filling until white plume is seen coming from oxidiser vent valve
6. Rocket oxidiser vent valve and GFS oxidiser fill are closed.
7. MC check vapour pressure - if too high oxidiser vent is reopened
8. Oxidiser vent is periodically closed to asses vapour pressure, and once target threshold reached ($\sim$25 bar), oxidiser vent is closed.
9. In the event that both nitrous cylinders were decided to be needed, the oxidiser fill valve of the second nitrous cylinder is now opened and the first cylinder's fill valve is closed.
10. The rocket oxidiser vent valve is reopened in its slow vent position, and closed once white plume is spotted
11. The oxidiser fill valve is closed.
12. GFS oxidiser hose vent is opened to depressurise the hose between the rocket and GFS.

Nitrogen

1. Nitrogen cylinder is opened before leaving the pad, with N2 fill and vent valves on the GFS closed.
2. N2 fill valve on GFS is actuated, and Mission Control (MC) observe and adjust valve angle to keep the rate of N2 tank pressure increase slow.
3. Once steady and slow rate of pressure rise is achieved, MC waits for equilibrium between the cylinder and the nitrogen COPV, then closes N2 fill valve.
4. GFS N2 hose vent is opened to depressurise the hose between the rocket and GFS.

Offloading Procedure

In the event offloading is required, Nitrous oxide will be offloaded before nitrogen is offloaded.

Nitrous Oxide

1. Oxidiser vent valve is opened to fast vent.
2. Oxidiser vent solenoid is opened.
3. If there is an issue meaning the rocket cannot be immediately reloaded then the oxidiser main engine valve is also opened.

Nitrogen

1. N2 vent solenoid is opened, allowing nitrogen to vent.
2. The fuel vent solenoid and both oxidiser vent solenoid and vent servo are opened.
3. The EREG is opened, allowing nitrogen to additionally vent through the fuel and oxidiser vent valves, and oxidiser main engine valve if that was opened during oxidiser venting.

Once both propellants have been offloaded and the rocket is confirmed safe by launch control, the Pressurised Fluids SPecialist (PFS) will approach the launch pad and close both nitrogen and nitrous oxide cylinders, as well as open the respective manual vents on the GFS.

Results & Conclusion

Both loading and offloading of oxidiser and pressurant were able to be completed using the above described procedure.

Images & Data

Figure 15: Full testing setup

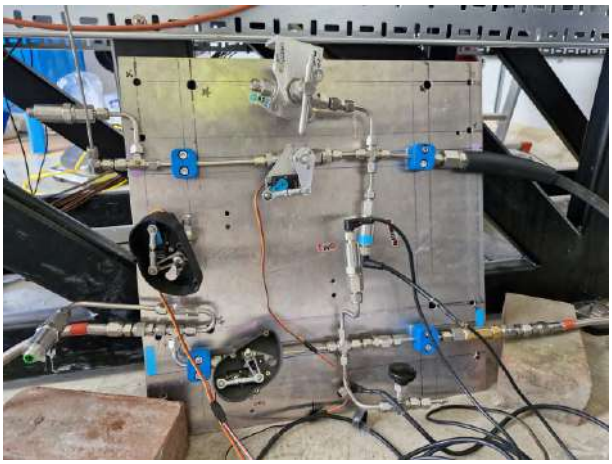

Figure 16: Ground Filling station

Test Outcome

This test was declared a success due to successful and safe loading and offloading of oxidiser and pressurant.

Raghav Ramkumar	Rudra Nakade	Andrei Paduraru
Propulsion lead	Propulsion Lead	Electronics Lead

1.7 SRAD Electronic Pressure Regulator Testing

Test Name: Full Stack E-REG Testing

Version: 1

Date: 24/08/2025

Location: J2 Test Facility, Airborne Engineering Ltd.

Conducted by:

Raghav Ramkumar	Rudra Nakade	Andrei Paduraru
Propulsion Lead	Propulsion Lead	Electronics Lead

Aims

To validate Electronic Pressure Regulator (E-REG) performance with flight-like flow rates, pressures and tank ullage volumes. Also to prove that E-REG can safely keep tank pressure at the desired set-point, while avoiding large spikes, which could cause tank overpressure and burst disk activation. For this test, the E-REG tank pressure set-point is 40 bar. The previous version of this E-REG system was tested over 20 times last year, as part of the *Nimbus '24* testing campaign.

Procedure

1. Assemble sub systems including, thrust table, engine assembly, engine feed system, rocket feed system, electronics, filling system
2. Perform electrical system checks, including actuator control, sensor readings, and data acquisition
3. Perform propulsion system checks, by tightening fittings and performing leak checks with inert pressurant
4. Perform exact fuel mixture and fuel tank filling with Isopropyl Alcohol mixture, filling with 5.2 kg of fuel
5. Perform connection of oxidiser and pressurant gas cylinders to the filling system
6. Begin remote filling procedures as outlined by the EuRoC checklist in the *Pluto* Technical Report.
7. Perform propellant tank pressurisation
8. Arm the ignition, confirm all stations and operators are GO/NO GO with audible statements, and commence engine firing procedure
9. Begin countdown and send command for engine ignition
10. Hot-fire until depletion of propellants
11. Safe the system venting all tanks ensuring no operator approaches until fully depressurised
12. Approach to close oxidiser and pressurant cylinders

13. Vent the lines
14. Perform post test inspections and review data

Results & Conclusions

Initial tank pressurisation proceeded nominally, with E-REG pressurising both tanks to 40 bar. After pressurisation, a steady decrease in the fuel tank pressure was seen, with no visible liquid leak on cameras, indicating a leak in the fuel tank pressurisation plumbing. After monitoring the leak rate, it was decided to proceed with testing, with tank pressurisation immediately before the sequence start to keep the fuel tank pressure as close as possible to the set-point.

For the cold-flow, the main valves were partially closed to best represent the lower mass-flows experienced during hot-fires, allowing more accurate testing conditions for characterising E-REG.

When the sequence starts, the fuel tank pressure dropped then spiked to 46 bar, which is expected behaviour for E-REG. After that the pressure steadily drops as the N2 tank runs in blow-down.

The ox tank pressurised nominally too, notably with no leak. However once flow started, it drops sharply below the tank set point. Although this is not cause for concern from a tank overpressure perspective, it is not normal behaviour. This year, the tank volume is a lot higher and there is a long 1/4" N2 pressurant raceway going to the bottom bulkhead for the ox tank. These two combined means that the pressure drop through the Ox pressurant line is too high, and the Ox tank doesn't experience the necessary N2 mass-flows to sustain pressure. E-REG prioritises the fuel tank pressures since it is closest to the E-REG valve, and hence would experience the highest pressure. The raceway was then changed to a 3/8" raceway to reduce the pressure drop down the Ox pressurant raceway. In the future, possible fixes include the addition of a secondary E-REG.

Overall, the E-REG showed its ability to regulate high pressure down to a set-point. The small pressure spike on the fuel tank allowed us to proceed to a higher pressure hot-fire, with the take away that the pressure set-point would be lowered slightly under nominal to account for the spike in fuel tank pressure.

Images & Data

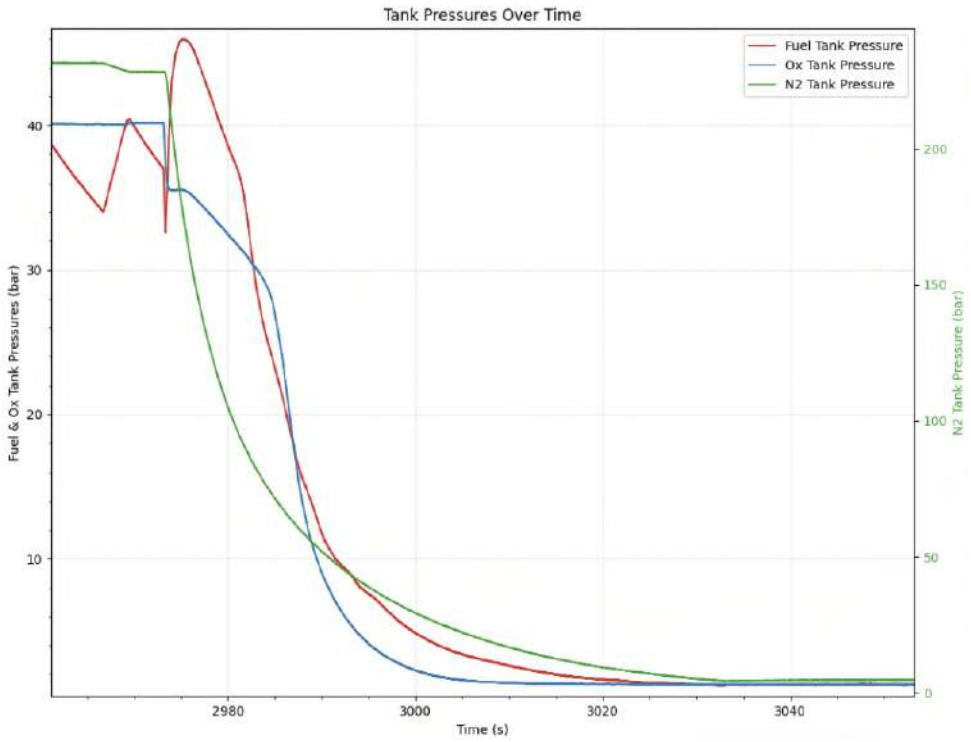

Figure 17: Cold-flow tank pressures

Test Outcome

This test was declared a success. Completion is signed for by the following responsible engineers:

Raghav Ramkumar	Rudra Nakade	Andrei Paduraru
Propulsion Lead	Propulsion Lead	Electronics Lead

1.8 Flight Qualification Hotfire of the *Pluto* Propulsion System

Test Name: Full-Stack Hotfire of *Pluto's* propulsion system

Version: 1

Date: 24/08/2025

Location: J2 Test Facility, Airborne Engineering Ltd.

Conducted by:

Raghav Ramkumar	Rudra Nakade	Andrei Paduraru
Propulsion Lead	Propulsion Lead	Electronics Lead

Aims

To characterise the exact performance of the flight propulsion system, demonstrate reliable ignition and firing of the *GOOFY* engine, verify nominal E-REG performance during hotfire, while also practising procedures such as fuel loading, oxidiser loading, tank pressurisation, and tank venting after firing. The purpose of the test is to also confirm that the *GOOFY* engine will reach target performance in flight configuration, and meet off-the-rail startup requirements, including: Peak thrust of 5 kN, and sustained thrust of over 3.5 kN.

Procedure

1. Assemble sub systems including, thrust table, engine assembly, engine feed system, rocket feed system, electronics, filling system
2. Perform electrical system checks, including actuator control, sensor readings, and data acquisition
3. Perform propulsion system checks, by tightening fittings and performing leak checks with inert pressurant
4. Perform exact fuel mixture and fuel tank filling with Isopropyl Alcohol mixture
5. Perform connection of oxidiser and pressurant gas cylinders to the filling system
6. Begin remote filling procedures outlined by the EuRoC checklist in the *Pluto* Technical Report
7. Perform propellant tank pressurisation
8. Arm the ignition, confirm all stations and operators are GO/NO GO with audible statements, and commence engine firing procedure
9. Begin countdown and send command for engine ignition
10. Hotfire until depletion of propellants
11. Safe the system venting all tanks ensuring no operator approaches until fully depressurised
12. Approach to close oxidiser and pressurant cylinders

13. Vent the lines
14. Perform post test inspections and review data
15. Perform trajectory simulations with full flight configuration hot fire data

Results & Conclusions

The propulsion and avionics sub-systems in flight configuration successfully ignited and hot-fired *GOOFY*, demonstrating the reliability and safety of the systems. The integrated avionics system performed nominally during the test, thus adequately verifying the updated engine controller design. The successful test adds to the extensive testing record of the avionics system, reinforcing its suitability for safety critical applications.

The E-REG system successfully regulated the pressure and stopped any major spikes in pressure beyond 60 bar MEOP of the propellant tanks.

With a peak thrust of 5.2 kN, achieved within 100 ms of ignition, satisfactory off-the-rail thrust was achieved. Due to additional feed system pressure drop, caused by extra plumbing required to connect to the engine in a horizontal configuration, such as long hoses, sharp bends and pipes, thrust in this configuration is lower than the flight configuration.

Near the end of the test, burn-though of the engine combustion chamber wall was observed. This was caused by an oxidiser-rich shutdown due to a lower than expected oxidiser flow rate, tracing back to low oxidiser tank pressure from limitations with E-REG mentioned previously. This resulted in the fuel tank depleting first before the oxidiser. Consequently, this meant that the engine experienced a sustained high O/F ratio from T = 7s onwards, leading to reduced thrust and burn-through.

For the flight propulsion system, a backup engine combustion chamber of identical design will be used.

Images & Data

Table 1: Tank pressures 100 ms after main valves open

Fuel Tank	Ox Tank	N2 Tank
44.31 bar	33.92 bar	198.15 bar

E-REG mitigated any large pressure spike, with a large pressure difference between N2 and fuel tank.

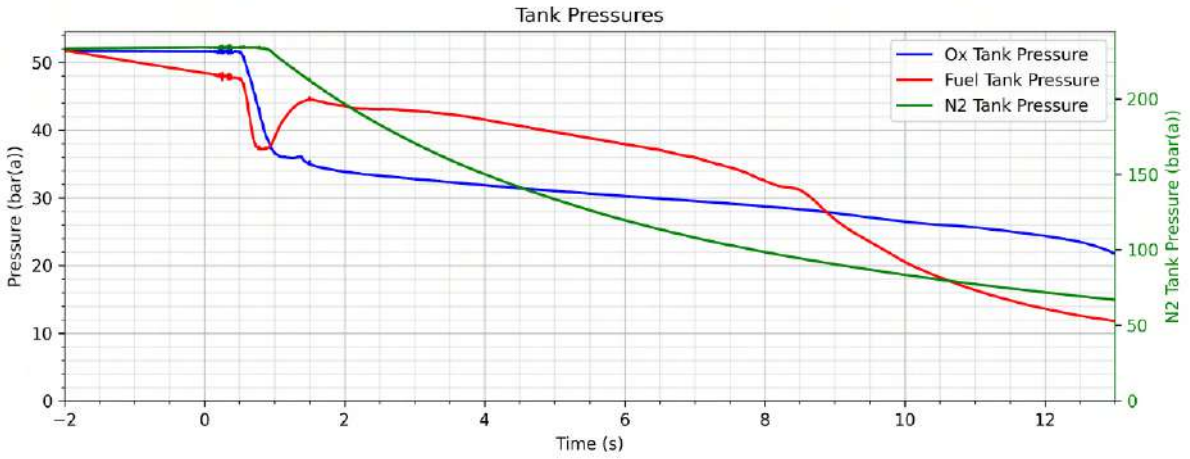

Figure 18: Tank pressures during hot-fire

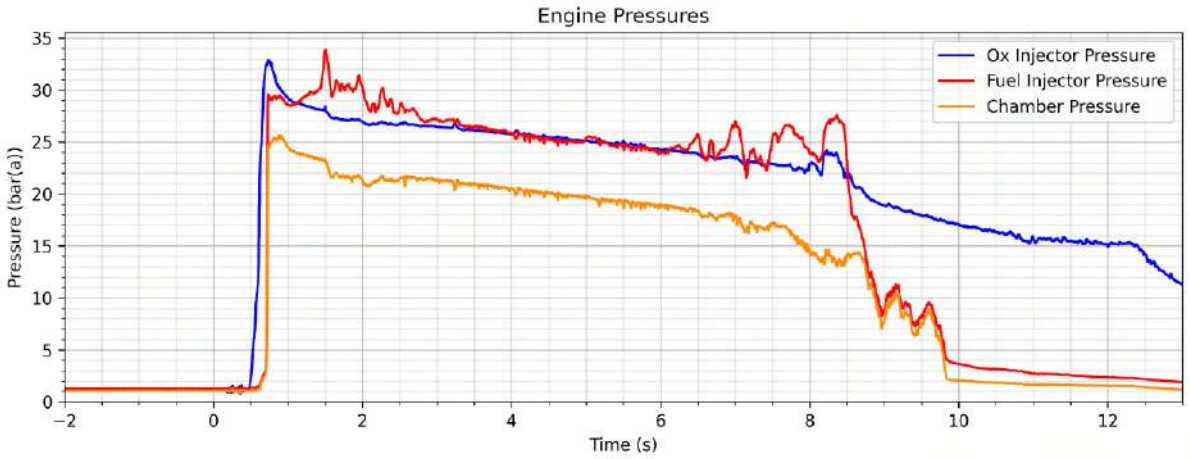

Figure 19: Engine pressures during hot-fire

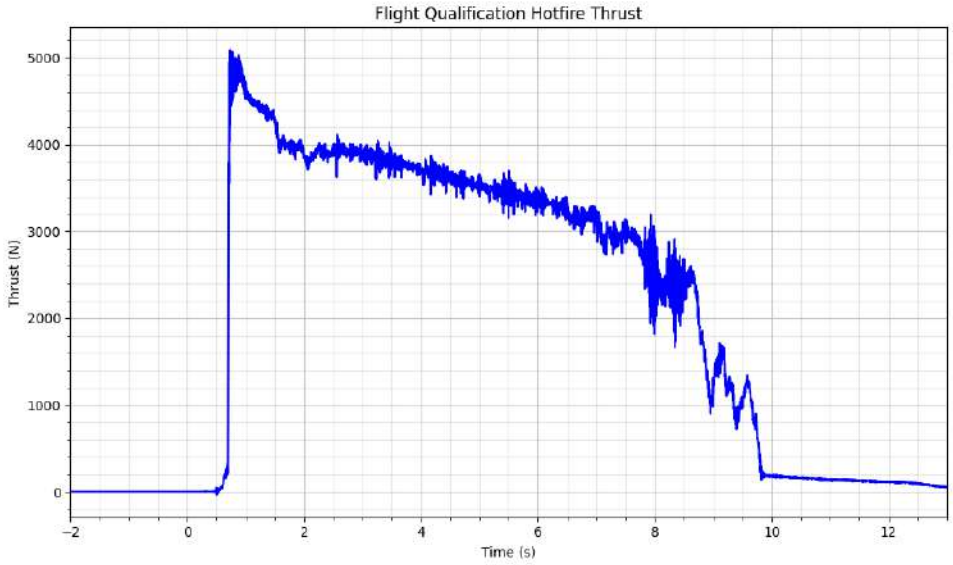

Figure 20: Flight Qualification Hot-fire Thrust Curve

Figure 21: Flight Qualification Hot-fire

Figure 22: Full stack test setup showing overall view (left) and details: thrust table, ground systems, and filling station (right).

Test Outcome

This test was declared a success. Completion is signed for by the following responsible engineers:

Raghav Ramkumar

Propulsion Lead

Rudra Nakade

Propulsion Lead

Andrei Paduraru

Electronics Lead

2 Airframe Test Reports

2.1 Hold-Down Tether Test

Test Name: Kevlar Tether Static Tensile Failure test

Version: 1

Date: 12.9.2025

Location: Imperial College London

Conducted by: Zak Leek - Airframe & Recovery Lead

Aims

To calibrate a hold-down configuration that would break between 4kN and 4.5kN in a static test. This involves finding the thickness of Kevlar cord required, and the most suitable knots.

Procedure

1. Attach an eye-bolt and load cell in series with the lower crosshead of the tensile test machine.
2. Connect the load cell to 'Kermit' (data acquistion unit), and configure the live plotting dashboard on a PC.
3. Lower the top crosshead as much as possible (this will allow for the greatest displacement range when the cord stretches).
4. Tie the cord specimen to the eye bolt, and pass it up through the hole in the top crosshead, tying off against a carabiner to stop it going back through the hole.[1]
5. Gently increase the crosshead displacement until failure.
6. Observe the maximum load recorded by the load cell on the dashboard, as well as the number and nature of subsequent breaking spikes shown on the load/time graph.
7. Record relevant data and reset specimen configuration, altered as necessary to get closer to the target breaking load.

Results & Conclusion

Two different configurations were tested: A loop, where a single piece of cord was wrapped around the eye-bolt and carabiner with its ends tied together on a straight section; and a single strand, which had one end tied to the carabiner and one tied to the eye-bolt. Unsurprisingly, the single strands failed at approximately half the breaking load of the loops. The final tether will be a loop, as it is easier to tie and tension correctly, and you can get the same strength with two thinner cords as you can with one thicker cord, so the mounting holes can be smaller.

[1] This method was necessary due to the tensile test machine not having enough travel to fit two eye-bolts and a load cell between the crossheads.

3 different knots were tested, each in different configurations.

- The first was a standard Overhand Knot on a bight (OAB), which slipped and untied before cord failure when in the loop configuration (meaning the two strands on one side of the knot were being pulled in opposite directions, same-side loading). The overhand OAB would have been stronger in the single strand configuration (opposite side loading), but was untested. The Overhand knot will not be used on the final tether, as it is too weak.
- The second knot was the Figure of Eight on a Bight, tested both in loop and single-strand configurations. The figure of eight is much less prone to slipping than an Overhand providing there is enough tail left as excess, although if not properly dressed can invert and become harder to untie. The figure of eight held in all tests, both loop and single-strand, and the cord broke below the knot each time. The Figure of Eight OAB was chosen to be the knot used on the final tether.
- The final knot tested was the Bowline. In the loop configuration, with the Bowline's loop being loaded in opposite directions, the knot slipped dramatically at just 400N. The bowline should not be loaded in this way. In the single-strand test, a bowline was used on each end, and held nicely before the cord broke at a mid-point between the two knots. The Bowline will not be used in the final tether because it is incompatible with the loop configuration, it is harder to check than a Figure of Eight, and risks untying when unloaded.

The final independent variable in our testing was the thickness of Kevlar cord. We had purchased 2.9mm braided Kevlar cord, and varied its thickness by pulling a different number of strands out of the braid for each specimen. We tested with 0 1, 2 and 3 strands removed; and found that the double-loop of cord broke within our target range (4kN to 4.5kN) when configured such that 3 strands had been removed. The other configurations broke at too high a load.

Images & Data

Figure 23: Loop specimen during fracture, red and black dial indicators show maximum and current load.

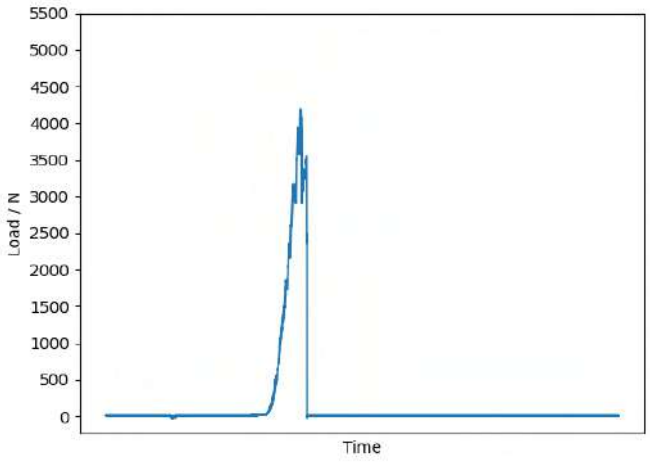

Figure 24: Load graph depicting 4.18kN fracture

Config	Knots	Strands / Thickness	Breaking Force (kN)	Failure Mode
Double	Overhand OAB	Full	3.6	Knot slipped, some fraying
Double	8 OAB	Full	5.33	Failed in 3 stages, broke below the knot
Double	8 OAB	1 tow out	5	Failed in 3 stages (5, 3.2 and 1.8), broke below the knot
Single	2x 8 OAB	1 tow out	3.7	Not full failure, maxed out strain
Double	8 OAB	2 tows out	4.5	Knot slipped a lot
Double	8 OAB	One Single tow	0.66	Failed then stuck due to fibre friction
Double	8 OAB	3 tows out	4.18	Snapped mostly on the first peak, then a couple of minor breaks
Double	Bowline	Full	0.4	Knot slipped
Single	2x Bowlines	3 tows out	2.556	Clean break

Table 2: The failure loads and modes for each tested tether configuration

Test Outcome

This test was declared a success, resulting in a final configuration being selected for the hold-down tether: 2.9mm braided cord with 3 strands removed, as a loop, tied with a Figure of Eight on a bight. Completion is signed for by the following responsible engineers:

Zak Leek	Shaeel Akhtar	Andrei Paduraru
Airframe & Recovery Lead	Airframe & Recovery Lead	Electronics Lead

2.2 Engine Truss Compressive Test

Test Name: Engine Truss Compressive Test

Version: 1

Date: 17/07/2025

Location: DFF Lab, Imperial College

Conducted by:

Shaeel Akhtar	Lothaire Valex	Charlie Aveline
Airframe & Recovery Lead	Airframe & Recovery	Airframe & Recovery

Aims

To compressively test two engine trusses which are additively manufactured to select one for flight and one for a compression-till-failure test.

Procedure

1. Assemble the engine truss jig that allows for even application of load.
2. For the first test, place jig within testing machine. Begin applying load to an initial value to account for imperfect assembling of jig. Apply load till 6kN. Perform this test on both trusses.
3. Compare load versus displacement plots. The truss that performs 'worse' that is, has higher displacement for same loading will be destructively tested in the second test.

Results & Conclusion

It can be observed from the load vs displacement plot that truss 1 has a higher displacement for the same load. Both trusses, however, have higher displacements than predicted. This is to be expected due to the additive manufacturing process. Truss 1 was then compressed till failure. However, we were unable to record data past 10 kN due to a data logging issue. But observing the curve, the truss should still have a high enough safety factor

Images & Data

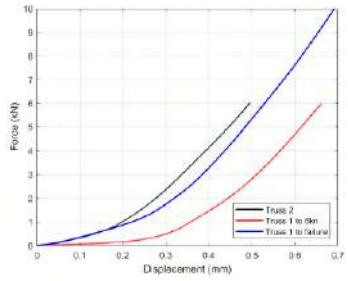

Figure 25: Load vs Displacement

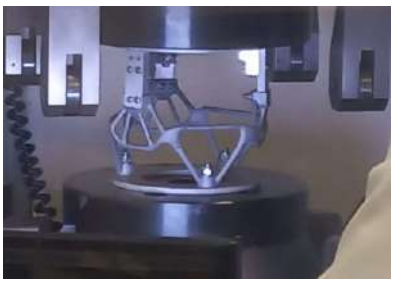

Figure 26: Truss jig

Figure 27: Failed truss

Test Outcome

This test was declared a success. Completion is signed for by the following responsible engineers:

Shaeel Akhtar	Lothaire Valex	Charlie Aveline
Airframe & Recovery Lead	Airframe & Recovery	Airframe & Recovery

3 Recovery Test Reports

3.1 Parachute Disreefing Test

Test Name: Parachute Disreefing Test

Version: 2

Date: 11/09/2025

Location: Lasham Airfield, Alton

Conducted by:

Shaeel Akhtar	Vera Overhauser	Roshan Frost
Airframe & Recovery Lead	Airframe & Recovery Engineer	Electronics Engineer

Raghav Ramkumar	Rohan Woodcock
Propulsion Lead	Propulsion Engineer

Aims

The aim of this test is to validate *Pluto's* reefing deployment by which the main rocket's parachute transitions from the its reefed state to its fully opened state.

Procedure

1. Mount the main parachute carabiner to the test vehicle tow bar.
2. Connect a load cell in series with the shock cords.
3. Connect the reefing actuation cables to the reefing dyneema.
4. Twill the nichrome wire around the dyneema chord within the reefing case.
5. Connect the actuation cables to the Flint and Steel board located in the test vehicle.
6. Accelerate to 30 mph. Once the parachute is inflated and stable, activate the dyneema cutter.

Rocket Disreefing System

The main chute disreefing system has multiple redundancies built in, as can be seen in Figure 28:

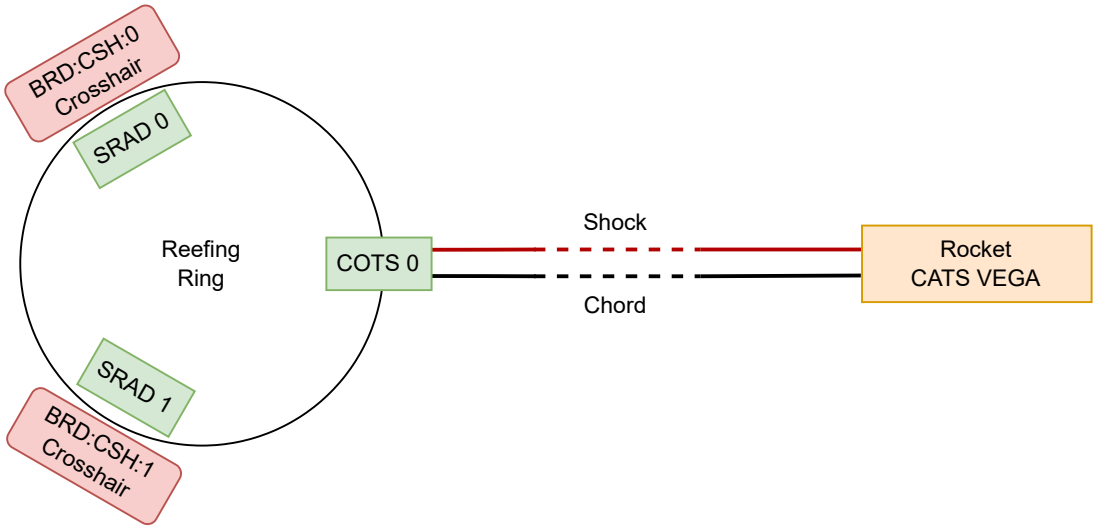

Figure 28: Direefing system redundancy overview

Firstly, one nichrome cutter is connected to the rocket CATS Vega through a cable running the length of the shock chord which acts as the COTS disreefing mechanism. Although this is the same as the failed *Nimbus 24* disreefing line, the team has updated the strain relief strategy for this connection, thus preventing the same failure as the one experienced during *EuRoC '24*. For the SRAD side, each nichrome case integrates a nichrome cutter, a li-ion battery, and a *Crosshair* board. Upon separation and thus removal of the rocket quick disconnect from the *Crosshair* boards, the disreefing command is enabled, ensuring disreefing does not occur on ascent.

Results & Conclusion

Two runs were performed on the test day. The first run's objective was to demonstrate the disreefing system is flight read and that the shock cords can sustain the shock loads induced. The parachute was mounted as detailed in the procedure section. After reaching 30 mph, the pyro command was sent to the line cutter to cut the dyneema. The parachute successfully disreefed and fully inflated into main configuration. Figure 31 show the reefed states of the parachute.

Figure 29 shows the data recorded on the first test. Due to a gusting wind and the low mounting point of the shock cord, the parachute frequently contacted the runway surface during the test. This led to the noisy load cell data seen in the graph. A 2 second delay was observed from the initial current surge (when the nichrome cutter was activated) to the first spike in load cell force reading. This delay was consistent with bench tests of the system and demonstrates reliable operation of the line cutting system.

The second run's objective was to demonstrate the robustness of the reefing method at high velocities. The nichrome line cutter was attached but not activated, allowing the parachute to stay in the reefed state. The parachute stayed reefed for the duration of the second run, demonstrating the effectiveness of the reefing method.

Images & Data

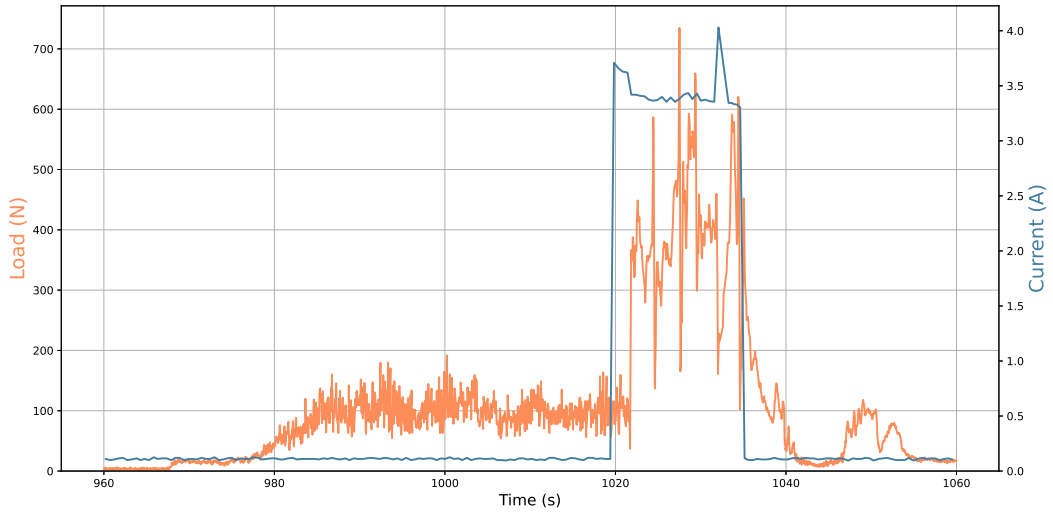

Figure 29: Load-cell and Nichrome Current Data from first test

Figure 30: Setting up parachute test

Figure 31: Reefed parachute on 1st run

Test Outcome

This test was declared a success. Completion is signed for by the following responsible engineers:

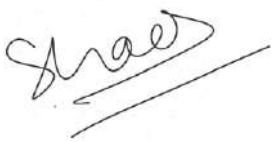

Shaeel Akhtar

Airframe & Recovery Lead

Vera Oberhauser

Airframe & Recovery Engineer

Roshan Frost

Electronics Engineer

Rohan Woodcock

Propulsion Engineer

Raghav Ramkumar

Propulsion Lead

3.2 Separation System Bench Test

Test Name: Separation System Bench Test

Version: 1

Date: 10/09/2025

Location: Aero Student Workshop, Imperial College

Conducted by:

Zak Leek	Shaeel Akhtar	Roshan Frost
Airframe & Recovery Lead	Airframe & Recovery Lead	Electronics

Aims

To ensure separation system design works effectively.

Procedure

1. Assemble separation system and tension Dyneema spool. Ensure all clamps clamp down evenly.
2. Connect locking solenoid to power supply set to a lower voltage and current.
3. Gradually increase voltage but not above 24 V. Once voltage is set increase current limit until locking solenoid successfully disengages and allows for separation.

Results & Conclusion

The solenoid requires at least 18V to trigger whilst fully engaged with the separation mechanism, however this wasn't consistent and occasional tests at 18V failed, or required some shaking. The only voltage where the solenoid disengaged 100% of the time, even with the separation mechanism at the highest tension, was 24V (requiring 2.3A). With a consistently working solenoid, the rest of the separation mechanism worked flawlessly, including the setting procedure where the pulley is turned and the cable tightens. The spring-loaded solenoid acted as a ratchet to make tightening easier, and a knot could be placed to mark where the rope sat on the pulley so that a complete number of turns could be made before nominal tension was achieved.

Voltage / V	Required Current / A
24	2.3
20	2.4
18	2.5
12	N/A

Table 3: The required current for the solenoid to trigger separation, given a fixed voltage.

Images & Data

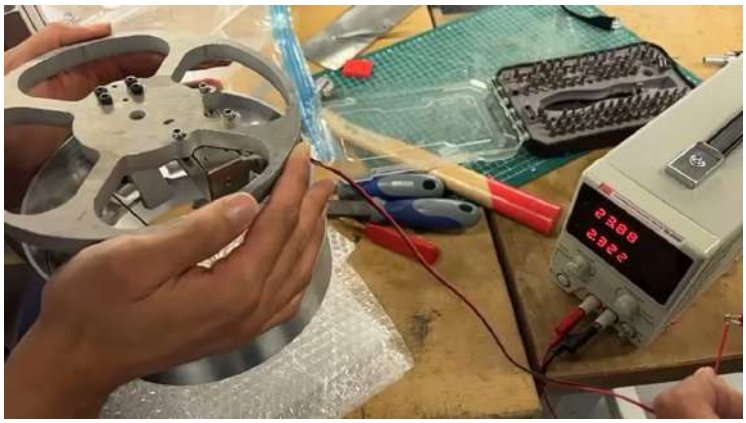

Figure 32: Test at 24 V and 2.3 A

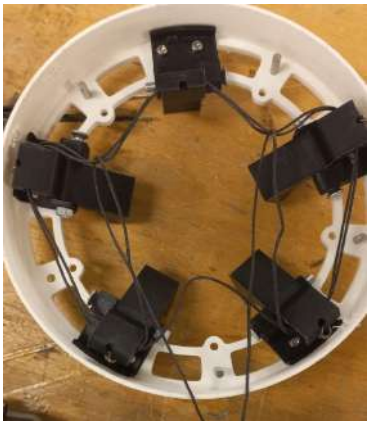

Figure 33: Tie pattern on 3D printed prototype

Test Outcome

This test was declared a success. Completion is signed for by the following responsible engineers:

Zak Leek

Airframe and Recovery Lead

Shaeel Akhtar

Airframe and Recovery Lead

Roshan Frost

Electronics

4 Avionics Test Reports

4.1 SRAD Avionics - Flight Test

Test Name: SRAD Avionics Integrated Flight Test

Version: 1

Date: 11/10/2024

Location: Santa Margarida, EuRoC '24

Conducted by:

Andrei Paduraru	Shiven Chandarana	Soham More
Flight Director	Launch Control Lead	Launch Control Avionics

Aims

To flight test the fully integrated SRAD *Ricardo* avionics system for nominal operation during all flight phases.

Procedure

1. Power the rocket using the PDU master keys.
2. Conduct pre-flight actuator and sensor checks.
3. Begin propellant loading and pressurisation.
4. Arm the flight controller and status check all relevant components when the rocket is flight ready.
5. Launch the rocket using the launch command.
6. Analyse flight logs and sensor data.

Results & Conclusion

All avionics systems onboard *Nimbus '24* performed nominally at *EuRoC '24*. This includes hardware, software and networking interfaces for ground and flight operations. Figure 34 shows a dataset from the Extended Kalman Filter used onboard the SRAD flight controller, *Pickle Rick*. The system logs analysed post flight showed that apogee and main parachute deployment were also triggered at the correct times. The same flight controller board and software will be used for *Pluto*. Additionally, figure 35 shows successful tank pressure regulation using the electronic pressure regulator in flight.

Images & Data

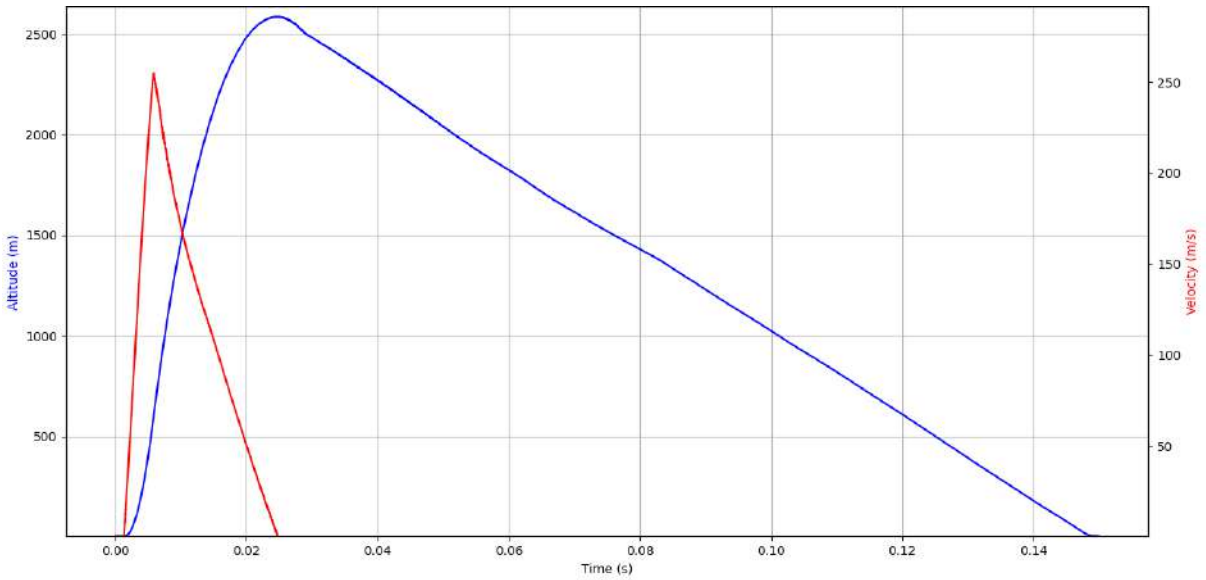

Figure 34: *Nimbus '24* flight controller recorded trajectory estimation

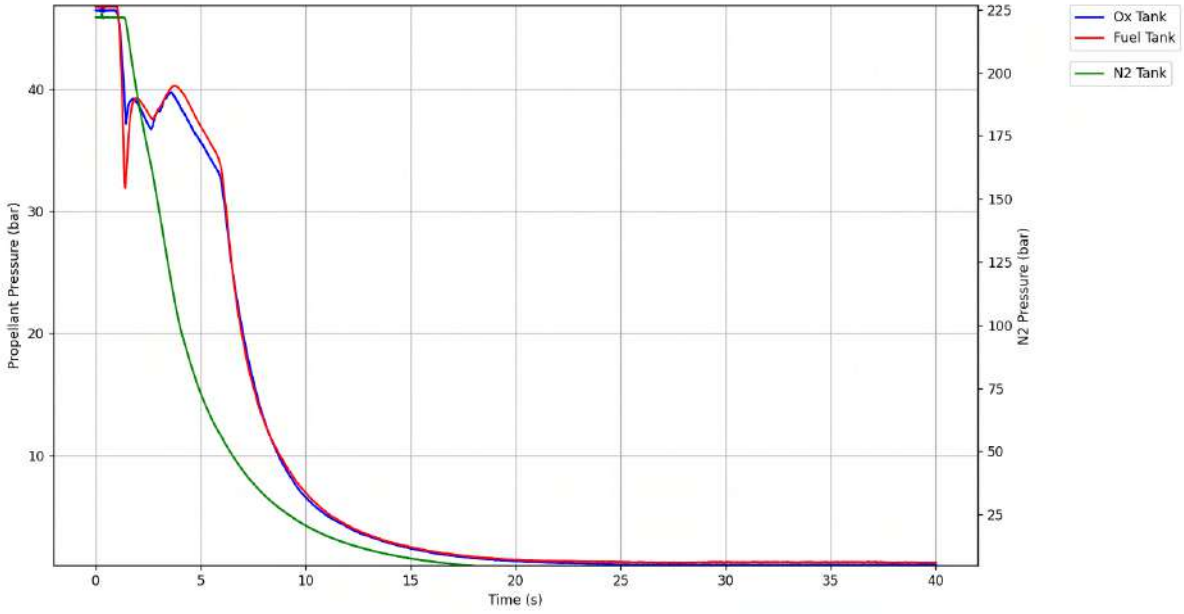

Figure 35: *Nimbus '24* flight tank pressure regulation data

Test Outcome

This test was declared a success. Completion is signed for by the following responsible engineers:

Andrei Paduraru

Flight Director

Shiven Chandarana

Launch Control Lead

Soham More

Launch Control Electronics

4.2 SRAD Avionics - High Temperature Test

Test Name: High Temperature test of Ricardo Avionics

Version: 1

Date: 09/09/23

Location: London, United Kingdom

Conducted by:

Shiven Chandarana	Kiran de Silva	Andrei Paduraru
Electronics Lead	Electronics Lead	Electronics Lead

Aims

The avionics are expected to perform in the high temperature environment in Portugal as well as the increased heat environment inside the fully assembled rocket. To ensure this is the case the avionics can be subjected to higher temperatures to ensure full working capability during these expected conditions.

Parts List

- Pickle Rick Flight Controller
- Computer
- Ricardo-Backend
- Thermocouple attached to a multimeter

Procedure

1. The oven was preheated to approximately 70 degrees Celsius.
2. The Ricardo avionics flight controller was put inside the oven, on a heatproof soldering mat.
3. The sensors on the flight controller were continuously monitored during the test for any inconsistencies that may be due to temperature.

Results & conclusion

The flight controller - Pickle Rick performed nominally both measuring data and relaying it to the connected computer as seen in Figure 36. The flight controller also maintained command response ensuring command-ability during high temperature conditions. Due to the inherent Faraday cage properties of the oven, GPS and LoRa were not tested but both before and just after (still approximately 50 degrees Celsius) antennas were connected and both systems worked nominally.

Images & Data

Figure 36: Sensor readings of flight controller under high temperature conditions

Test Outcome

This test was declared a success. Completion is signed for by the following responsible engineers:

Shiven Chandarana (09/09/23) Kiran De Silva (09/09/23) Andrei Paduraru (09/09/23)

4.3 SRAD Avionics - Low Temperature Test

Test Name: Extremely Low Temperature test of Ricardo Avionics

Version: 1

Date: 31/08/23

Location: London, United Kingdom

Conducted by:

Shiven Chandarana	Kiran de Silva	Andrei Paduraru
Electronics Lead	Electronics Lead	Electronics Lead

Aims

To demonstrate full controllability of the flight controller and the high powered actuation board under extreme low temperatures. Inside the rocket the tanks and plumbing will be subject to low temperatures and the avionics system is expected to operate in these conditions.

Parts List

- Pickle Rick Flight Controller
- Flint and Steel High Powered Actuation Board
- Computer
- Ricardo-Backend
- Dry Ice
- Nichrome
- Dyneema

Procedure

1. Dry Ice was placed in an insulated foam box.
2. A string of Dyneema was tensioned with a spring and a nichrome wire was encircled.
3. The nichrome wire was screwed into the high powered actuation board.
4. Both the high powered actuation board and flight controller were placed into the solid dry ice mass.
5. The temperature will be left to reach equilibrium. Command-ability and data retrieval will be tested many times during this test.
6. The final test being to command the ignition of a pyro channel for 5 seconds.

Results & conclusion

The flight controller performed nominally, measuring data and relaying it to the connected computer as seen in Figure 38. The flight controller and high powered actuation board also maintained command responsiveness. During the test the ambient temperature reached equilibrium at approximately -60○C. At this temperature the pyro was fired successfully and the Dyneema separated releasing the attached spring.

In an effort to stress test the Ricardo Avionics System solid dry ice was placed on top of the flight controller to visualise the absolute minimum limits as seen in Figure 37. The controllers' sensor readings instantly jumped from -60 Degrees Celsius to -90 Degrees Celsius and continued to operate nominally. During the test it was not possible to get much colder without more apparatus therefore was deemed a huge success of the Ricardo Avionics System. Although conditions re-enacted are somewhat of an exaggeration of the low temperatures the opportunity to test under this condition was presented and therefore was tested successfully. Nonetheless this test gives the approval of the use of the Ricardo Avionics system at temperatures up to -90 Degrees Celcius. It is worth mentioning the fact that alike the high temperature test (subsection 4.2) Lora and GPS could not be tested due to the interference in the box as well as the box being made from metal walls. After the test was concluded, both GPS fix and LoRa radio were tested successfully after.

Images & Data

Figure 37: Pickle Rick Flight controller with dry ice

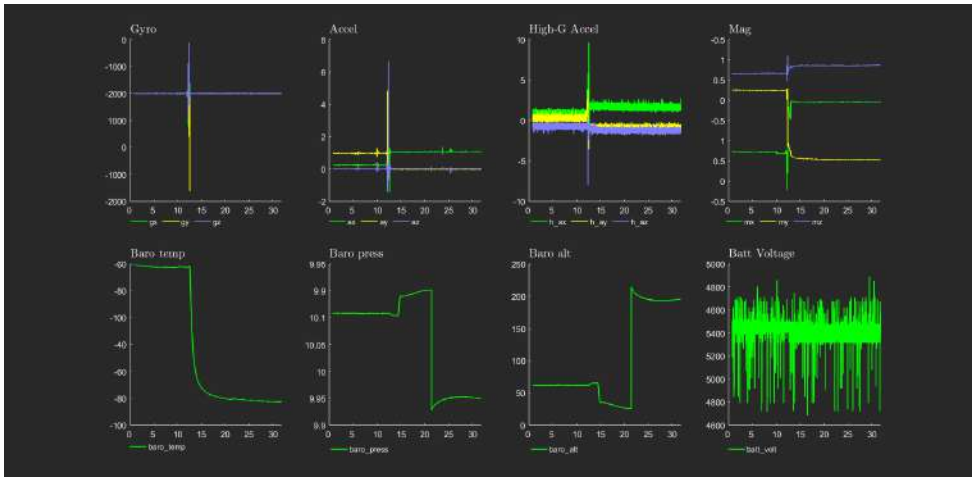

Figure 38: Sensor Readings for Flight Controller under extreme low temperature conditions

Test Outcome

This test was declared a success. Completion is signed for by the following responsible engineers:

Shiven Chandarana (31/08/23) Artem Sheykin (31/08/23) Andrei Paduraru (31/08/23)

4.4 COTS Avionics - CATS Vega Nichrome Recovery Actuation Test

Test Name: CATS Vega Pyro testing

Version: 1

Date: 20/09/24

Location: London, United Kingdom

Conducted by:

Shiven Chandarana	Andrei Paduraru	Soham More
Electronics Lead	Electronics Lead	Electronics Engineer

Aims

To ensure the CATS Vega is a suitable secondary flight computer on nichrome based separation systems

Parts List

- CATS Vega
- CATS ground station
- 2x 2.4GHz LoRA antenna
- 15 cm, 0.2mm diameter nichrome
- 2 mm Dyneema rope
- 2 pin Molex nanofit connector

Procedure

1. The nichrome wire will be setup in a 3D printed casing as designed for flight.
2. This will be integrated in the clampband with Dyneema with the separation coupler.
3. The nichrome is connected to the CATS Vega via a 2 pin nanofit connector.
4. Using the inbuilt testing mode in the CATS Vega ground station, the pyro channel will be fired remotely for 5 seconds to assess the ability for nichrome to cut Dyneema and separate the rocket.
5. We will examine the integrity of the nichrome wire and housing post test and make changes if required.

Results & conclusion

The system performed nominally allowing for the nichrome wire to heat up to red-hot without breaking and to successfully cut the dyneema rope. The result provided evidence to approve the use of the CATS Vega on *Pluto*'s separation system and parachute disreefing.

Test Outcome

This test was declared a success. Completion is signed for by the following responsible engineers:

Shiven Chandarana (08/08/23)

Soham More (08/08/23)

Andrei Paduraru (08/08/23)

4.5 SRAD Avionics - Radio Range Test

Test Name: Telemetry and tracking system range test

Version: 1

Date: 22/06/2024

Location: London, United Kingdom

Conducted by:

Kiran de Silva	Andrei Paduraru	Artem Sheykin
Electronics Lead	Electronics Lead	Electronics Lead

Aims

To test the maximum range of the telemetry and tracking subsystem with omni-directional antennas at maximum output power (100mW).

Parts List

- *Pickle Rick* Flight Controller
- Antenova SRF2I019-100 -2.4 dBi patch antenna
- *Pickle Rick* Ground Station
- Rubber Ducky +2.7 dBi antenna
- 2x SMA GNSS antenna (any)
- Ricardo-Backend

Radio settings

- Spreading Factor - 7
- Bandwidth - 200 kHz
- Power - +20 dBm
- Frequency Band - 868 MHz

Procedure

1. Connect both LoRa and GNSS antennas to the *Pickle Rick* ground station
2. Connect both LoRa and GNSS antennas to the *Pickle Rick* flight controller
3. Start telemetry request on both the ground station and flight controller, and verify radio link is functional at short range.

4. Move one or both radio nodes to an elevated position, such as a hill, so that the radio horizon is above the test range
5. Orient the antennas so that there are no major obstructions between them.
6. Repeat the procedure, and move one or both nodes to different locations to test at higher distances.

Results & conclusion

Telemetry from both flight controller and ground station was successfully received by both stations via radio at distances up to 65 km every 0.5 s. The operating signal to noise ratio (SNR) at 65 km suggests that it is possible to achieve radio communications at higher distances. However no suitable locations in the vicinity of the 65km test locations were found, and as such the system was not tested any further.

It is important to note that this maximum range was achieved with an output power of 20 dBm (100mW), which is only legal for unlicensed use in a narrow band of 869.4-869.65 MHz. As such, if this frequency band is congested, the output power needs to be reduced to 14 dBm (25mW) to operate in the rest of the 868 band. Since the received power varies with R^2, this means that the achievable range is reduced to 32.5 km, which is still adequate for tracking *Pluto* throughout its flight.

Images & Data

Figure 39: Ground support system radio station during test.

Test Outcome

This test was declared a success. Completion is signed for by the following responsible engineers:

Andrei Paduraru (22/06/2024)

Kiran De Silva (22/06/2024)

Artem Sheykin (22/06/2024

C Hazard Analysis

Material/Component	Potential Hazard	Control Measures	Risk Level
C/D-Class Klima Ignition Motors	Unintended combustion	Sealed in fireproof box prior to use. Ignition sources stored separately. Only EuRoC certified personnel permitted to handle ignitors, under supervision of lead pyrotechnic technician.	Low
E-matches	Accidental ignition causing fire or burns	Connected to tested firing systems. Activation requires multiple deliberate actions. Handled by certified personnel, under supervision.	Low
Li-Ion Batteries	Fire from overcharge, overdischarge, or puncture	Charged with proper chargers, balance charged. Careful handling to avoid puncture, properly soldered and insulated wiring. Stored in Li-ion safe bags	Low
Nitrous Oxide	Dizziness, unconsciousness, cold burns, explosions	Stored in certified vessels, used in ventilated areas. Plumbing and vessels cleaned and tested. Gloves used to prevent frostbite.	Low
Ethanol	Fire, Incapacitation from inhalation/congestion.	Stored in original sealed container away from ignition sources. Protective gear worn during handling. Pumped using low-pressure spray bottle, handled outdoors for ventilation.	Low
High Pressure Nitrogen	Explosion from overpressure, asphyxiation	Loaded last. Components rated for 300 bar. Gas bottles opened slowly, used outdoors for ventilation.	Low

D Risk Assessment

Failure Mode	Mission Phase	Mitigated			Team's Comments and Justification
		Probability	Severity	Risk	
Airframe					
Buckling of stringers	Ascent	1	3	3	Buckling of stringers results in a critical failure of the structural integretiy of the rocket. This is unlikely to occur as the stringers are designed against the maximum load, with the resulting simulations indicating a safety factor of at least 1.5.
Engine truss structure failure	Ascent/Apogee	1	3	3	The engine truss was designed with large buckling and yield strength safety factors. Two identical trusses will be compression tested, one truss to failure to validate the design and ultimate load (15Kn). The other flight truss will be tested to the design load to identify any manufacturing defects.
Bending of the airframe due to weaker joints and couplers near the top	Pre flight, Apogee	1	2	2	A strong aluminium internal frame increases stiffness and reduces the need for couplers. All joints use machined interfaces to ensure good tolerances. A stiff CFRP skin also reduces deflections due to bending.
Airframe bending when being carried		1	2	2	Bolts within sections are tightened and checked before launch day. Checklist ensure bolts between sections are all tightened correctly. Minimum of 4 people required to carry the rocket at all times to ensure load is supported evenly.
Shearing of bolts that screw into body tube and/or body tubes and bulkhead due to shock loads	Mid flight - Chute deployment	1	3	3	Bolts appropriately sized to make sure they do not shear. Components along the critcial load path simulated with a resulting safety factor of 1.98. Screw holes in the composite tube placed sufficiently far away from the edge so as to not cause any damage to the tubes mid flight.
Separation mechanism disengages prematurely due to axle shearing	Ascent	1	2	2	During the engine burn, the compressive load will keep the rocket together if the separation mechanism opens. If post-burn, then it's possible the two stages could separate due to drag, although the majority of the drag is on the nosecone so most likely not.
Hold-down tether breaks prematurely due to shockload	Pre-flight	2	1	2	The rocket will still launch, albeit at a slightly lower initial velocity. All measurements on the tether are rounded so that it is more likely to break than not.
Hold-down tether never breaks	Pre-flight	1	3	3	Could result in launch failure, damage to the rail and ground station umbilicals. Will essentially be a static vertical hot-fire test, so the rocket shouldn't be harmed. Very unlikely considering the statement above.
Recovery					
Disconnection of nichrome recovery actuators	Ascent	1	3	3	Molex Nanofit connectors are used to connect the nichrome to the electronics cables which are positivley locking hence are unlikely to be experienced in flight.
Nichrome wire melts before cutting dyneema due to over-heating	Ascent/Apogee	1	3	3	Ground tests show that each nichrome heating element can be reused multiple times, therefore the probability of a section of nichrome snapping is very low.
Parachute ripping	Descent	1	3	3	The parachute is made of rip-stop nylon, which is specifically chosen to prevent ripping under the expected shock loads.
Airframe frailure from shock	Descent	1	2	2	The airframe is made from a mixture of aluminum, carbon fibre and glass fibre. The airframe was designed to take the maximum shock load in bending with a safety factor of more than 1.9 against yield.
Recovery bulkhead failure	Descent	1	3	3	The recovery bulkhead was designed against the maximum shockload with reference to previous Nimbus 24 loads and further analysis using dedicated and open source software with a safety factor of more than 2 against yield of maximum load found.
Reefed parachute not opening	Descent	1	2	2	The parachute transitions from its reefed state into its fully opened state by using the same nichrome acutation method used in the main seperation method and previous recovery systems. The full reefing system has been ground tested and pull tested from a car. Failure to un-reef results in the rocket desending faster than expected, but this should not result in a critical severtiy risk.
Dyneema knot comes loose mid flight	Ascent	1	2	2	The dyneema is tied with a reef knot which a strong knot commonly used for this loading condition. Tests have been performed with the clamp band showing that the knot is strong and unlikely to come undone in flight.
Electronics					
Quick Disconnect Detaches Prematurely	Pre-Launch	2	1	2	Connectors and Cable harness tested multiple times including a flight test at EuRoC '24. Proper connection verifed at launch pad physically and electrically during pad operations. Backup communication link allows for independent control of the rocket if quick disconnect detaches.
Deployment power failure	Pre-Launch - Flight	1	2	2	Two independant and redundant power management boards and battery packs on the rocket with automatic switchover reduce the likelyhood. Independent battery system for COTS recovery system ensures power failures in primary avionics sytem do not propagate.
Logic power failure	Pre-Launch - Flight	1	3	3	Two independent and redundant power management boards and battery packs on the rocket. Logic power isolated from deployment power mitigating risk of brownout during high current output of acutators.
Batteries depleted	Flight	1	3	3	Battery level monitored through power management boards. Quick disconnect and umbilical present for on-the-pad charging. Over 6hr battery life on each battery pack.
Telemetry Link Failure	Pre-Launch - Flight	1	1	1	Independent SRAD and COTS telemetry links. Hard wired telemetry link present for ground operations. Range testing of radio systems. During flight, the flight controller pre-programmed with all deployment events so no live commands are required for succesful flight.
Firmware Crash	Pre-Launch - Flight	1	3	3	Firmware thoroughly tested during real world tests with hardware. Independent COTS flight computers used to ensure recovery and multi-step igntion implemented to prevent un-intentional vehicle ignition. Constant monitoring of all flight boards during ground operations.
COTS recovery power failure	Flight	1	2	2	COTS battery system charged using main power umbilical however still fully independent of main power system. A good compromise between complete independence of the COTS system and practicality was sought. For this reason, even though the COTS recovery system has its own independent battery pack, it is charged through the main power umbilical in order to ensure infinite battery life on the pad. Primary avionics system powered speratley ensuring power failures do not propagate between systems.

Deployment Power Brownout	Launch - Flight	1	2	2	The power system has been sized and tested to support multiple igniters firing on a single battery pack. Current limited output channels ensure the current draw from a dead short is limited. Dual battery packs give failover redundancy. The battery chemistry used, as well as the bulk capacitance present on each board was designed to be able to handle the current draw of the deployment events. Primary and secondary avionics systems powered seperately ensuring brownouts do not propagate between systems.
Electronics heating due to high temeperatures	Pre-Launch - Flight	2	1	2	Adequate space between electronics boards designed and appropriate thermal control measures such as heatsinks used. Simulated hot enviorment testing. Thermal imagery used to investiage hot spots on boards. While previous launches during hot, sunny days have not affected the electronics due to its relatively low power usage, several mitigations are in place.
Configuration of electronics with erroneous settings	Pre-launch - Flight	1	2	2	Electronics configured before-hand with flight configuration verified with hardware-in-the-loop flight simulations as well as wet dress rehersals. Version control system (git) used to track any changes. Final configuration only verified on launch day. Checklists are used.
Electrical fire	Pre-Launch - Flight - Recovery	1	3	3	Appropriate insulation present for the voltages used. Connectors designed such that dead shorts through erroneous orientation is not possible.
Li-Ion battery fire	Pre-Launch - Flight - Recovery	1	3	3	Battery voltage monitoring. Over current and over voltage protection implemented on power distribution units. Batteries balanced charged in LiPo Safe bag.
Propulsion					
GSS N2O Filling Valve Actuation Failure	Pre-flight	1	2	2	Redundant power systems and prior tests ensure that a valve failure is unlikely. Consequences of filling valve failure are low as vehicle can be vented and approached to facilitate repairs.
GSS N2 Filling Valve Actuation Failure	Pre-flight	1	2	2	Redundant power systems and prior tests ensure that a valve failure is unlikely. Consequences of filling valve failure are low as vehicle can be vented and approached to facilitate repairs.
Rocket N2O Vent Valve Actuation Failure	Pre-flight	1	2	2	Redundant power systems and prior tests ensure that a valve failure is unlikely. Should the vent valve fail, vehicle can be vented through normally open solenoid valves and approached to facilitate repairs. Should both the vent valve and solenoid valve fail, a calibrated SPRV (Safety Pressure Relief Valve) and burst disc ensures the tank does not fail due to an overpressure event. Consequences of vent valve failure are low as N2O can be offloaded via main engine valve (through a separate board) with ignition and fuel valve disarmed and approached to facilitate repairs.
Rocket Fuel Solenoid Vent Valve Actuation Failure	Pre-flight	1	2	2	COTS solenoid valve and Prior tests ensure that a valve failure is unlikely. Calibrated SPRV (Safety Pressure Relief Valve) and burst disc ensures the tank does not fail due to an overpressure event. Consequences of vent valve failure are low as valve is normally open, resulting in a safe system state in the event of a valve failure. Vent valve only vents from above the maximum liquid level in the tank, meaning no liquid is lost during a valve failure.
Rocket N2 Solenoid Vent Valve Actuation Failure	Pre-flight	1	2	2	COTS solenoid valve and Prior tests ensure that a valve failure is unlikely. Consequences of vent valve failure is low as valve is normally open, resulting in a safe system state in the event of a valve failure. Nitrogen COTS COPV can also be vented via the electronic regulator through fuel and oxidiser tank venting systems, to ensure rocket is safe to approach.
Main N2O Valve Actuation Failure	Pre-flight, Ascent	1	2	2	Redundant power systems and prior tests ensure that a valve failure is unlikely. Consequences of valve failure are low as vehicle can be vented and approached to facilitate repairs. If valve fails during ignition, ethanol will be dumped and burnt off immediately presenting low risk. During flight, valve is intended to remain open to full vent all fluids from the rocket. During flight, tank vents are automatically opened to ensure rocket is safe to approach.
Main Fuel Valve Actuation Failure	Pre-flight, Ascent	1	2	2	Redundant power systems and prior tests ensure that a valve failure is unlikely. Consequences of valve failure are low as vehicle can be vented and approached to facilitate repairs. If valve fails during ignition, nitrous will be dumped from the rocket. During flight, valve is intended to remain open to full vent all fluids from the rocket. During flight, tank vents are automatically opened to ensure rocket is safe to approach.
Engine Combustion Chamber Explosion	Ascent	1	3	3	Engine designed with appropriate safety factors, and tested over 16 times at all expected operating points, as well as some tests both above target maximum thrust (112%) and for extended durations (12s) . Engine hydrostatic tested to 1.5x the MEOP. Due to the nature of this failure, there is no way to reduce the severity.
Engine Combustion Coolant Channel Failure	Ascent	1	2	2	The regenerative cooling channels can fail if the heat transfer to the coolant is insufficient. This can lead to a structural failure of the channel wall where coolant can leak into the comubstion chamber. This will reduce the efficiency of the engine as more fuel is dumped than nominal, but should not compromise anything else on the rocket, hence is not a critical failure. Test data from instrumented engine indicates critical parameters within expected design region (e.g fuel injector flow temperature) indicating this failure mode is unlikely.
Ignition Failure	Pre-flight	1	1	1	Ignition method tested successfully numerous times over the past 3 engine development cycles. COTS motors with well fitting COTS ematches proven to be reliable. Consequences of ignition failure are low as vehicle can be vented and approached to facilitate repairs and swapping ignition cartridges.
SRAD N2O Tank Section Explosion	Pre-flight, Ascent	1	3	3	Tank designed with appropriate safety factors, and tested numerous times integrated in flight system. Tank fitted with a calibrated SPRV and burst disc to vent overpressure. Bust disc sized to 4 times the area of the filling pipe. Furthermore, it is designed to fail in a specific manner, wherein radial bolts fail in shear-out, allowing end-cap to pop out and tank to de-pressurise. Due to the nature of this failure, there is no way to reduce the severity.

SRAD Fuel Tank Section Explosion	Pre-flight, Ascent	1	3	3	Tank designed with appropriate safety factors, and tested numerous times integrated in flight system. Tank fitted with a calibrated SPRV and burst disc to vent overpressure.Bust disc sized to 4 times the area of the filling pipe. Furthermore, it is designed to fail in a specific manner, wherein radial bolts fail in shear-out, allowing end cap to pop out and tank to de-pressurise. Due to the nature of this failure, there is no way to reduce the severity.
Fluid system leak	Pre-flight, Ascent	1	2	2	Fluid system components will be hydrostatically tested and full propulsion system leak tested with nitrogen. Procedure has been developed using industry standards. If leak occurs during pre-flight phase, vehicle can be vented and approached to facilitate repairs. During flight, nothing can be done to fix leakage, however consequences are low as the system only needs to hold pressure for a few seconds after liftoff.
GSS Filling Hose Vent Valve Failure	Pre-flight	1	1	1	Redundant power systems and prior tests ensure that a valve failure is unlikely. Consequences of valve failure are low as vehicle can be vented and approached to facilitate repairs.
Quick Disconnect Failure	Ascent	1	3	3	QD collar is held in place allowing rocket to disconnect it as it launches. Redundant cable and bracket system used to ensure collar is well secured to the launch pad. Ground tests have been performed to characterize the expected pull out force and ensure the collar works as intended so failure is very unlikely. Consequences of failure would damage filling lines on both the rocket and ground support system, likely requring extensive repairs.
Electronical Regulator Failure	Pre-flight, Ascent	1	2	2	Redundant power systems and prior tests ensure that a valve failure is unlikely. Consequences of valve failure are low as vehicle can be vented through normally open solenoid valves and approached to facilitate repairs. If valve opens unintentionally or by too much, high pressure nitrogen can enter the low pressure plumbing parts, where the SPRV and burst disc will fail first before anything else. Bust disc sized to 4 times the area of the filling pipe.
Common Dome Tank O-Ring Seal Failure – Propellant Mixing within tank cavities	Pre-flight, Ascent	1	3	3	The O-ring seal separates N_2O and ethanol in the common dome tank. If the seal fails, liquid propellants may mix inside the tank, leading to uncontrolled combustion. Dynamic loads and thermal cycling during ascent may compromise the seal. The tank is hydrostatically tested before flight to detect leaks via dye coloration. No mitigation is available in flight. The interpropellant region uses a double O-ring configuration for redundancy. Passive venting in the downpipe and dome sidewall helps prevent cross-contamination by safely relieving any leakage to atmosphere, reducing the chance of in-tank mixing.
Leaking Propellent Vappor Mixing and Combustion Outside of the Rocket	Pre-flight, Ascent	1	3	3	If N_2O and ethanol vapours escape the common dome region and accumulate outside the tank—such as near fittings or in enclosed volumes—there is a risk of vapour-phase mixing followed by ignition. This could occur due to seal degradation, vent line backflow, or minor leakage. Ignition sources may include static discharge, nearby electronics, or hot surfaces. The system includes passive vent paths at the dome and downpipe to direct leaks away from enclosed areas. All seals are leak-checked pre-flight, and static discharge risks are mitigated via vehicle grounding and controlled fluid handling procedures.
Ethanol Freezing/Crystalisation post venting of the Oxidiser tank	Pre-flight	1	2	2	After full oxidiser venting , the surrounding tank and dome structure and pipe can undergo rapid chilling. This may cause ethanol near the dome and around the pipe to freeze or crystallise, potentially impacting seal function, restricting flow in or blocking engine channels. Although the freezing point of ethanol is low at 114 C, it is possible that the tank reaches that temperature after full vent. The system is passively insulated, and the duration between oxidiser vent and engine start is minimized to limit exposure, in case of a full vent.
Thermal Shrinkage of Dome O-Ring Material Post Oxidiser Venting	Pre-flight	1	2	2	Rapid chilling of the common dome region after oxidiser venting may cause thermal contraction of the O-ring material, potentially reducing seal compression and allowing minor leakage. The interpropellant section uses two O-rings for redundancy. Passive venting is incorporated in the dome sidewall and downpipe to safely relieve any minor leakage. The O-ring material is selected for compatibility with the expected temperature exposure, and the system would be fully disarmed in the event of a full vent.
Payload					
Strucutral failure of payload	Ascent, Descent	1	3	3	The payload and deployer has been designed considering the expected loading conditions with a safety factor of at least 1.5. While this severity is critical to the payload, it is not expected to have any significant impact on the launch vehicle.
Avionics failure	Pre-flight, Ascent	1	2	2	Flight Battery tested with multimeter before installation on launch day. Communication with SRAD flight controller and COTS tracker verifed before launch in pre-launch checklists.
Cyanobacteria experiment failure	Pre-flight, Ascent	1	2	2	Leakage of the cyanobacteria samples is prevented through a two layer seal system that sees the samples placed inside sealed test tubes, within a sealed 3D printed container housing. This minimises the risk of any sample leaking out of the CHIMERA module.

E Compliance Matrix

Requirement reference	Title	Text	Compliance	Remarks	Verification Method	Test needed?
EuRoC-LV-RQT-0010	Non-toxic propellants	Launch vehicles entering EuRoC shall use non-toxic propellants.	Fully compliant	The launch vehicle uses nitrous oxide, ethanol and nitrogen	Simple confirmation	N
EuRoC-LV-RQT-0020	Air-start ignition circuit electronics	All upper stage and secondary ignition systems shall comply with the recovery systems redundant electronics and safety critical wiring requirements specified in Sections 5.1 (EuRoC-LV-RQT-0240 to EuRoC-LV-RQT-0280) and 5.4 respectively.	N/A	The launch vehicle only has one stage.	N/A	N
EuRoC-LV-RQT-0030	Ground-start ignition circuit arming distance	All ground-started propulsion system ignition circuits/sequences shall be capable of being armed and disarmed with no personnel within 15 m of the launch vehicle.	N/A	We don't ground start.	N/A	N
EuRoC-LV-RQT-0040	Clustered vehicle release system	All clustered vehicles shall have a launch release system ensuring lift-off only occurs if a minimum threshold force is met.	N/A	The launch vehicle is not clustered.	N/A	N
EuRoC-LV-RQT-0050	Clustered vehicle stability proof	All clustered vehicles shall be capable of performing a stable flight for any lift-off force above the minimum threshold value.	N/A	The launch vehicle is not clustered.	N/A	N
EuRoC-LV-RQT-0060	Clustered vehicle arming	For vehicles with a "main" and several "secondary" propulsion systems, the arming function of the secondary propulsion systems shall only be armed by launch detection (i.e., air-start).	N/A	The launch vehicle only has one main propulsion system.	N/A	N
EuRoC-LV-RQT-0070	Air-start ignition circuit arming	All upper stage and "secondary" (i.e., air-start) propulsion systems shall only be armed by launch detection.	N/A	The launch vehicle only has one main propulsion system.	N/A	N
EuRoC-LV-RQT-0080	COTS solid motors	All COTS solid motors shall be selected from the official EuRoC Motors List [RD02].	Fully compliant		Simple confirmation	N
EuRoC-LV-RQT-0090	Ignition systems for solid motors	All solid motors shall use the electronic ignition system provided by EuRoC.	N/A	The launch vehicle uses an SRAD liquid propulison system.		N
EuRoC-LV-RQT-0100	Active pressurization	All gaseous and liquid propellant systems shall be able to be externally pressurized with inert gas.	Fully compliant	Nitrous oxide and ethanol are pressurised usign nitrogen	Simple confirmation, inspection	N
EuRoC-LV-RQT-0110	Loading lines disconnection	Systems employing any gaseous or liquid propellants shall perform propellant tank pressurization after all propellant and pressurant loading lines are disconnected.	Partially compliant	Fill valves closed before pressurisation	Simple confirmation, inspection	N
EuRoC-LV-RQT-0120	Dissimilar connections	All loading lines, used for pressurization gases or propellants, shall feature dissimilar connectors.	Fully compliant	All loading lines use dissimilar connectors.	Simple confirmation, inspection	N
EuRoC-LV-RQT-0130	Remote-controlled loading mechanism and respective emergen	Any remote-controlled loading mechanism for gases or liquid propellants shall feature a clearly marked and labelled, single action, hand actuated, "Emergency Release Mechanism".	N/A	No remote controlled loading lines.	N/A	N
EuRoC-LV-RQT-0140	Filling/loading/unloading connections	Any filling/loading/unloading connections for fluid propellants shall be readily accessible from the ground, when the rocket is in vertical launch position.	Fully compliant	All filling/loading/unloading connections are located below the engine's flange or in the lower propulsion area.	Simple check	N
EuRoC-LV-RQT-0150	Filling/loading/unloading timing	Teams shall demonstrate that the filling/loading/unloading of the liquid fuels can be done to be ready for the launch window (maximum 90 minutes for liquid propellant loading, including pressurization).	Fully compliant	All filling/loading/unloading operations can be completed in 10 minutes as demonstrated during our wet dress rehearsal.	Reasoned argumentation, test	Y
EuRoC-LV-RQT-0160	Venting	For hybrid and liquid motors, teams shall facilitate oxidizer tank venting to prevent over-pressure situations.	Fully compliant	Ox vent servo and solenoid	Simple confirmation, inspection	N
EuRoC-LV-RQT-0170	Passive PRD in isolated sections of pressurized lines	All isolated sections of pressurized lines (including pressure vessels) shall incorporate a passive pressure relief device (PRD) with an opening set point below the maximum tested pressure of that line section.	Fully compliant	SPRVs on SRAD Tanks	Inspection, calculations	N
EuRoC-LV-RQT-0180	PRD discharge coefficient	All pressure relief devices shall have a discharge coefficient equal to or higher than any other fluid interface on the respective pressurized section in which they are installed.	Fully compliant	Vent faster than you can fill	Reasoned argumentation, calculations	N
EuRoC-LV-RQT-0190	Propellant offloading after launch abort	Hybrid and liquid propulsion systems shall implement a means for remotely controlled venting or offloading of all liquid and gaseous propellants in the event of a launch abort.	Fully compliant	NO solenoids and remote servo vent	Reasoned argumentation	N
EuRoC-LV-RQT-0200	Combustion chamber pressure test	SRAD and modified COTS propulsion system combustion chambers shall be designed and tested according to the SRAD pressure vessel requirements defined in Sections 0 and 6.3, respectively.	Fully compliant	Hydrostatic test plus hotfire test	Test	Y
EuRoC-LV-RQT-0210	Combustion chamber leak proof	Combustion chambers shall be designed allowing to be closed off in a leak-tight manner for testing at any section between the throat and the exit section of the nozzle.	Fully compliant	Engine can be sealed for hydrostatic testing	Reasoned argumentation, test	Y
EuRoC-LV-RQT-0220	Hybrid and liquid tanking test	SRAD and modified COTS propulsion systems using liquid propellant(s) shall successfully (without significant anomalies) have completed a propellant loading and offloading test in "launch-configuration", prior to the competition.	Fully compliant	Wet Dress Rehearsal	Test	Y
EuRoC-LV-RQT-0230	Static hot-fire test	SRAD propulsion systems shall successfully (without significant anomalies) complete an instrumented (chamber pressure and/or thrust), full scale (including system working time) static hot-fire test prior to EuRoC.	Fully compliant	Flight Qualification Burn	Test	Y

EuRoC-LV-RQT-0240	Redundant recovery system electronics	Launch vehicles shall implement fully redundant recovery system electronics, including sensors/flight computers and "electric initiators", with a separate power supply (i.e., battery).	Fully compliant	The launch vehicle features fully redudandant recovery system electronics. It includes both COTS & SRAD recovery activation on seperate power supply.	Simple confirmation	N
EuRoC-LV-RQT-0250	Redundant COTS recovery electronics	At least one redundant recovery system electronics subsystem shall implement a COTS flight computer.	Fully compliant	The redundant recovery system electronics subsystem includes a CATS Vega flight computer.	Simple confirmation	N
EuRoC-LV-RQT-0260	Recovery electronics access panel	All electronics switches or connectors that need to be manually operated shall be accessible from outside the vehicle via either access panels or direct mounting on the outer skin.	Fully compliant	No manually operated recovery electronics.	Simple check	N
EuRoC-LV-RQT-0270	Recovery electronics location	All electronics switches or connectors that need to be manually operated shall be readily accessible from the ground, when the rocket is in vertical launch position.	Fully compliant	No manually operated recovery electronics.	Simple check	N
EuRoC-LV-RQT-0280	Recovery electronics access	All electronics switches or connectors that need to be manually operated shall be mounted on the vehicle side opposite to the launch rail.	Fully compliant	No manually operated recovery electronics.	Simple check	N
EuRoC-LV-RQT-0290	Recovery system energetic devices	All stored-energy devices (i.e., energetics) used in recovery systems shall comply with the energetic device requirements defined in Section 6.1 of this document.	N/A	No energetic devices		N
EuRoC-LV-RQT-030	Onboard power systems	All onboard systems shall be free of batteries with either lithium-polymer or lithium (non-rechargeable) chemistry.	Fully compliant	Li-ion batteries only.	Simple confirmation, inspection	N
EuRoC-LV-RQT-0310	Onboard power systems access	Onboard batteries shall be readily accessible from the ground, when the rocket is in vertical launch position.	Partially compliant	Ground power helps maintain battery charge.	Simple checl	N
EuRoC-LV-RQT-0320	Launch rail standby time	Onboard power systems shall have at least six hours of battery lifetime on the launch rail.	Partially compliant	Theoretically infinite lifetime but not on battery power alone	Simple confirmation	N
EuRoC-LV-RQT-0330	Non-parachute/parafoil recovery systems	Teams exploring other recovery methods (i.e., non-parachute or parafoil based) shall mention it in the dedicated field of the Technical Questionnaire [RD04].	N/A			N
EuRoC-LV-RQT-0340	Dual deployment recovery	Each independently recovered launch vehicle body, anticipated to reach an apogee above 450 m above ground level (AGL), shall follow a dual deployment recovery operations concept.	Fully compliant	The launch vehicle will feature a reefed parachute opening at apogee which will then disreef at 450m AGL.	Reasoned argumentation, calculations	N
EuRoC-LV-RQT-0350	Initial deployment event altitude	The initial deployment event shall occur at or near apogee.	Fully compliant	Command sent once apogee is detected.	Reasoned argumentation, calculations	N
EuRoC-LV-RQT-0360	Initial deployment event descent velocity	The initial deployment event shall result in a descent velocity between 23 and 46 m/s.	Fully compliant	The parachute is sized to reduce the launch vehicle's descent velocity to between 30 and 35 m/s after deployment.	Reasoned argumentation, calculations	N
EuRoC-LV-RQT-0370	Main deployment event altitude	The main deployment event shall occur at an altitude no higher than 450 m AGL.	Fully compliant	The main deployment event will happen at 450m AGL.	Reasoned argumentation, calculations	N
EuRoC-LV-RQT-0380	Main deployment event descent velocity	The main deployment event shall result in a descent velocity of less than 9 m/s.	Fully compliant	The parachute is sized to reduce the launch vehicle's descent velocity to 5.6 m/s after main deployment.	Reasoned argumentation, calculations	N
EuRoC-LV-RQT-0390	Ejection gas protection	The recovery system shall implement adequate protection (e.g., fire-resistant material, pistons, baffles etc.) to prevent hot ejection gases (if implemented) from causing burn damage to retaining chords, parachutes, and other vital components as the specific design demands.	N/A	The recovery system does not include any hot ejection gases.		N
EuRoC-LV-RQT-040	Parachute swivel links	The recovery system rigging (e.g., parachute lines, risers, shock chords, etc.) shall implement swivel links at any connections including single-threaded anchors.	Fully compliant	The recovery system includes swivel links.	Simple confirmation, inspection	N
EuRoC-LV-RQT-0410	Dual deployment parachute coloration	Dual deployment parachutes shall be visually highly dissimilar from one another.	N/A	The launch vehicle features a reefed parachute.		N
EuRoC-LV-RQT-0420	Parachute coloration	Utilised parachutes shall use colours providing a clear contrast to a blue sky, a grey/white cloud cover and ground vegetation (i.e. avoiding certain shades of green and brown, as well as black).	Fully compliant	The parachute is made from bright fabric and can easily be seen from the ground.	Simple check	N
EuRoC-LV-RQT-0430	Mandatory system	Launch vehicle stages and deployable payloads shall feature a mandatory operational CATS Vega Flight Computer for official altitude logging and landing site tracking purposes.	Fully compliant		Simple check	N
EuRoC-LV-RQT-0440	CATS transmitter call-sign	Teams shall assign to each transmitter a “call-sign” (referred to in the CATS User Manual as the tele_link_phrase telecommand) respecting a specific string format to be found in Appendix D.	Fully compliant		Simple check	N
EuRoC-LV-RQT-0450	CATS Vega firmware update	Teams will be required to fly a specific firmware version in each mandatory CATS flight computer, mandated by the EuRoC organization.	Fully compliant		Simple check	N
EuRoC-LV-RQT-0460	CATS receiver	The CATS Ground Station shall be used for telemetry and tracking in conjunction with the mandatory system.	Fully compliant		Simple check	N
EuRoC-LV-RQT-0470	CATS electronics	CATS devices shall comply with the electronics general electronics requirements EuRoC-LV-RQT-0260, EuRoC-LV-RQT-0270 and EuRoC-LV-RQT-0280.	Fully compliant		Simple check	N
EuRoC-LV-RQT-0480	Cable management	All safety critical wiring shall implement a cable management solution (e.g., wire ties, wiring, harnesses, cable raceways).	Fully compliant		Simple check, inspection	N
EuRoC-LV-RQT-0490	Secure connections	All safety critical wiring/cable connections shall be sufficiently secure as to prevent de-mating due to expected launch loads.	Fully compliant		Inspection	N

EuRoC-LV-RQT-050	Cryo-compatible wire insulation	In case of propellants with a boiling point of less than -50°C any wiring or harness passing within close proximity of a cryogenic device (e.g., valve, piping, etc.) or a cryogenic tank (e.g., a cable tunnel next to a LOX tank) shall utilize safety critical wiring with cryo-compatible insulation (i.e., Teflon, PTFE-variants, etc.).	N/A			N
EuRoC-LV-RQT-0510	Electronics thermal testing	Teams shall thermally test the electronics to know the reliable operational temperature range, implement cooling or venting provisions and monitor at least one temperature sensor representative of the electronics temperature.	Fully compliant		Test	Y
EuRoC-LV-RQT-0520	Recovery system ground test demonstration	All recovery system mechanisms shall be successfully (without significant anomalies) tested prior to EuRoC, either by flight testing, or through one or more ground tests of key subsystems.	Partially compliant	Will be fully compliant after we do testing	Test	Y
EuRoC-LV-RQT-0530	Energetic device safing and arming	All energetics shall be “safed” until the rocket is in the launch position, at which point they may be "armed".	Fully compliant		Simple check	N
EuRoC-LV-RQT-0540	Arming device access	All energetic device arming features shall comply with the requirements EuRoC-LV-RQT-0260, EuRoC-LV-RQT-0270 and EuRoC-LV-RQT-0280.	Fully compliant		Simple check	N
EuRoC-LV-RQT-0550	Arming device location	All energetic device arming features shall be located on the airframe.	Fully compliant		Simple confirmation	N
EuRoC-LV-RQT-0560	Burst discs	Each SRAD pressure vessel and every propellant tank shall implement an over-pressure safety measure, in the form of a (replaceable) burst disc, with a diaphragm orifice diameter of no less than 6 millimetres. The burst (or rupture) disc solution can be either COTS or SRAD.	Fully compliant	COTS Certificate required	Reasoned argumentation, inspection	N
EuRoC-LV-RQT-0570	Burst disc pressure	Burst discs (COTS or SRAD) shall be selected or calibrated to rupture at a pressure no higher than 1,25 times the nominal tank pressure.	Fully compliant	70 bar	Reasoned argumentation, inspection, calculations	N
EuRoC-LV-RQT-0580	Burst disc marking	Burst disc orifices (the body which determines the rupture pressure) shall be clearly and permanently marked with the average rupture pressure determined by testing, along with a unique identifier, tracing each burst disc orifice to an associated test report.	Fully compliant	COTS Certificate required	Inspection	N
EuRoC-LV-RQT-0590	Burst discs material	All SRAD burst discs shall come from the same stock material sheet, both for flight, testing and rupture pressure characterization.	N/A			N
EuRoC-LV-RQT-0600	Relief device	SRAD pressure vessels shall implement an additional relief device, set to open in the range of 1,10 to 1,20 times the nominal operating pressure.	Fully compliant	SPRVs on SRAD Tanks	Reasoned argumentation, test	Y
EuRoC-LV-RQT-0610	Designed burst pressure for metallic pressure vessels	SRAD and modified COTS pressure vessels constructed entirely from isotropic materials (e.g., metals) shall be designed to a burst pressure no less than 2 times the maximum expected operating pressure.	Fully compliant	120 bar	Reasoned argumentation, in depth proofing (theoretical)	N
EuRoC-LV-RQT-0620	Designed burst pressure for composite pressure vessels	All SRAD and modified COTS pressure vessels either constructed entirely from non-isotropic materials (e.g., fibre reinforced plastics (FRP), composites) or implementing composite overwrap of a metallic vessel (i.e., composite overwrapped pressure vessels (COPV)), shall be designed to a burst pressure no less than 3 times the maximum expected operating pressure.	N/A	1000 bar		N
EuRoC-LV-RQT-0630	Burst discs testing	Individual test reports are required for each SRAD burst disc orifice, tied to its unique identifier or serial number. Each burst disc orifice test report must contain a minimum of five consecutive rupture tests, preferably using a data logging system and a pressure transducer for optimum rupture pressure documentation. The burst disc sheet metal must also be specified in detail.	N/A			N
EuRoC-LV-RQT-0640	Proof pressure testing	SRAD and modified COTS pressure vessels shall be proof pressure tested successfully (without significant anomalies) to 1,5 times the maximum expected operating pressure for no less than twice the maximum expected system working time, using the intended flight article(s) (e.g., the pressure vessel(s) used in proof testing must be the same one(s) flown at EuRoC).	Fully compliant	90 bar 1.5*MEOP	Test to proof pressure	Y
EuRoC-LV-RQT-0650	Restricted control functionality	Launch vehicle active flight control systems, if implemented, can only be implemented for pitch and/or roll stability augmentation, for aerodynamic "braking", guided recovery systems, precision landing or guided deployable loads.	N/A	The vehicle does not have any active flight control system		N
EuRoC-LV-RQT-0660	Unnecessary for stable flight	Flight vehicles implementing active flight controls shall be naturally stable without these controls being implemented.	N/A			N
EuRoC-LV-RQT-0670	Designed to fail safe	Control Actuator Systems shall be designed to Fail Safe in any abnormal condition or during an active flight abort (if such functionality is implemented).	N/A			N

F Checklists

Team 18 - PLUTO			Imperial College Rocketry London		
C - Pyro Tent					
Location: Pyro Tent			**Summary: Upon completion, the rocket will have passed final flight integration and ready to move to the pad.**		
Lead: Andrei					
Members: Rudra					
Step	**Time To Launch**	**Responsible**	**Task**	**Comment**	**Check**
C-1		**Andrei**	**Pre-pyro tent checks**		
C-1-1		Andrei	B-Final Assembly sign-off		
C-1-2		Andrei	Rocket LRR sign-off		
C-1-3		Andrei	EuRoC go for pyro sign-off		
C-2		**Andrei**	**Transport rocket to pyro tent**		
C-2-1		Andrei	Move rocket stands to pyro tent		
C-2-2		Andrei	Move rocket to pyro tent		
C-2-2		Andrei	Move fin can to pyro tent		
C-3		**Andrei**	**Ignitor Assembly**		
C-3-1		Rudra	Check the igniton tube assembly		
C-3-2		Rudra	Feed the e-match cable through the engine		
C-3-3		Rudra	Attach the e-match cable to the outside of the engine with masking tape		
C-3-4		Rudra	Thread the ignition tube onto the engine and tighten		
C-3-5		Rudra	Assemble fin can		
C-4		**Andrei**	**Prepare launch rail toolkit**		
C-5		**Andrei**	**Move rocket to final flight qualification**		
C-5-1		Andrei	Collect all members of the launch rail team		
C-5-2		Andrei	Collect launch rail toolkit		
C-5-3		Andrei	Lift the rocket with 4 members of the launch team		
C-5-4		Andrei	Walk the rocket to the range safety tent		
Pyro tent assembly complete, move to D-Launch Rail					
				Approved by:	

Team 18 - PLUTO		Imperial College Rocketry London			
D - Launch Rail					
Location:	Pad	**Summary: The rocket is at the pad, upon completion, all personnel will be ready to evacuate the pad.**			
Lead:	Andrei				
Members:	Raghav, Soham, Andrei, Rudra				
Step	**Time To Launch**	**Responsible**	**Task**	**Comment**	**Check**
D-1		**Andrei**	**Before Moving Rocket to Launch Rail**		
D-1-1			Has the team received clearance to move to the launch rail?		
D-1-2			Has the launch rail tool kit been collected and checked?		
D-1-3			Is MC set up and ready to go?		
D-1-4			Has MC/LC established radio communication?	Ensure the team has three or more fully charged radios	
D-1-5			Has the launch rail been prepped for arrival?		
D-1-6			Has the team got the relevant safety equipment		
D-1-7			Has the launch rail team taken a bio break?		
D-2		**Andrei**	**Transport the Rocket to The Launch Rail**		
D-3		**Andrei**	**Load Rocket onto the Launch Rail**		
D-4	**START**	**Andrei**	**Insert PDU0 PDU1 Remove Before Flight Pins**		
D-5		**Andrei**	**Attach PDU0 and PDU1 Power Xt60 Keys**		
D-6		**Andrei**	**Check Avionics System**		
D-6-2			Connect **EQD** and A**QD**	Make sure the GSS is turned on	
D-6-3		Soham	**DTRH** Check	Check data task request handler is not behind, DTRH might need to be reset for accurate stats	
D-7	00:59:00	**Andrei**	**Systems Check**		
D-7-1			Remove PDU0 RBF pin		
D-7-2			PDU0 transition to LIVE state		
D-7-3			Bus voltage checks	Logic Power: 3.2v - 3.4v, Deploy Power: 14.8v >	
D-8	00:57:00	**Soham**	**Valve Check**	Listen for nominal valve operation. In the case of GSS valves, a visual check can also be performed. Verify that all valves return to a closed state after checkout. Confirm Readout of valve position	
D-8-1			Close **GSS-OX-NEEDLE**	Close the GSS needle valves	

D-8-2			Close **GSS-N2-NEEDLE**	Close the GSS needle valves	
D-8-3			ARM, OPEN, CLOSE, OPEN, DISARM **ROC-SOL-N2**	audible click	
D-8-4			ARM, OPEN, CLOSE, OPEN, DISARM **ROC-SOL-OX**	audible click	
D-8-5			ARM, OPEN, CLOSE, OPEN, DISARM **ROC-SOL-FUEL**	audible click	
D-8-6			ARM, PRESS, DISARM **ROC-EREG**	Pressurize default angle is 40-45	
D-8-7			ARM, OPEN, CLOSE, DISARM **ROC-OX-VENT**		
D-8-8			ARM, OPEN, CLOSE, DISARM **ROC-OX-MAIN**		
D-8-9			ARM, OPEN, CLOSE, DISARM **ROC-FUEL-MAIN**		
D-8-10			ARM, OPEN, CLOSE, DISARM GSS-**N2-FILL**		
D-8-11			ARM, OPEN, CLOSE, DISARM GSS-**N2-HOSE-VENT**		
D-8-12			ARM, OPEN, CLOSE, DISARM GSS-**OX-FILL** 0		
D-8-13			ARM, OPEN, CLOSE, DISARM GSS-**OX-HOSE-VENT**		
D-9-1			Disarm all actuators		
D-9-2		Andrei	Insert PDU0 RBF pin to safe deployment power		
D-9-3		Soham	Check **PICKLE, PDU0, PDU1, GREG, GOOFY** flight ready	Check states in IDLE / Flight ready	
D-9-4		Andrei	Turn on cameras		
D-11	00:51:00	**Baboucarr**	**Attach fluid quick disconnects**		
D-11-1			Remove kapton tape and attach **OX** quick disconnect at the base of the rocket. Pull down on hose to check fully seated		
D-11-2			Remove kapton tape and attach **N2** quick disconnect at the base of the rocket. Pull down on hose to check fully seated		
D-12	00:49:00	**Baboucarr**	**Begin IPA Filling**		
D-12-1		Baboucarr	Check IPA plumbing line is assembled correctly and that the equipment is clean	IPA FILLING TEAM	
D-12-2		IPA Filling team (IFT)	**Ensure IPA FILLING TEAM (IFT) wearing fuel fill PPE**	Safety glasses / faceshield, latex gloves	

D-12-3		IFT	Attach fuel filling hose to the fuel fill port		
D-12-5		IFT	Begin IPA Filling	Begin filling the rocket with IPA by slowly opening the fill valve until IPA starts to drip from the vent line	
		Soham	Wait for rocket mass to increase by **6kg**		
D-12-6		IFT	Close **FUEL-FILL**	close ball valve on the rocket and reopen the push fit filling valve.	
D-12-7		IFT	Depressurize **FUEL-TRANSFER-TANK**, remove **FUEL-HOSE,** add **FUEL-DRAIN-CAP**		
D-12-8		IFT	Move and store the fuel filling equipment		
D-13	00:36:00	**Baboucarr**	**Prepare Remote Propellant Filling**		
D-13-1			Check nitrous plumbing is assembled correctly, including hoses to engine	Check hose fittings are tightened and bottle adapter is tight on the bottle. Ensure the needle valve is fully closed (turn clockwise to close)	
D-13-2			**Verify OX-MAIN, OX-VENT, OX-HOSE-VENT, OX-FILL** are **CLOSED**		
D-13-3			Check correct PPE is being worn	Nitrous safe gloves and a face shield	
D-13-4			All Unnecessary Personel Evacuate	**Andrei, Baboucarr** only	
D-13-6		Andrei	Switch on Pad Cameras		
D-13-8			Rudra connects igniter QD		
D-13-9		Andrei	Pull **PDU0, PDU1** RBF Pins Out		
D-13-10		Soham	**Confirm PDU0, PDU1 in Ready state**		
D-13-11		Andrei	**Verfiy OX-MAIN, OX-VENT, OX-HOSE-VENT, OX-FILL** are **CLOSED** with a **VISUAL CHECK**		
D-14	00:34:00	**Baboucarr**	**Visualy Check GSS Valves are Closed**		
D-15	00:34:00	**Baboucarr**	**Open the nitrous bottle**		
D-15-1			Check that the pressure of the bottle is in a suitable range using the gauge on the GSS	Between 30 - 65 bar	
D-16		**Baboucarr**	**Open the nitrogen cylinder**		
D-16-1			Check that the pressure of the N2 bottle is in a suitable range using the gauge on the GSS	Above 250 bar	
D-17		**Baboucarr**	**All Personnel Evacuate the Pad**		
Launch Rail Checklist complete, move to E-PreLaunch					
Approved by:					

Team 18 - PLUTO			Imperial College London Rocketry		
E - Prelaunch					
Location:	MCC		**Summary: Upon completion the rocket is ready for go/no-go and launch.**		
Lead:	Soham				
Members:	Raghav				
Step	**Time To Launch**	**Responsible**	**Task**	**Comment**	**Check**
E-1	00:32:00	**Soham**	**Before Moving to Prelaunch**		
E-1-1			Have all items on previous checklists been completed?		
E-1-2			Is the team prepared to launch in the next 15 - 60 minutes?		
E-1-4			Does the weather look good for the upcoming launch window?		
E-1-5			Are all systems running nominally?		
E-1-6			Are all nessecary members of the team in mission control?		
E-1-7		**Soham**	Has the launch site been cleared of debris and non critcal equipment?		
			Test Engine Ignitier Continuity		
E-1-8			ARM and CLOSE **SOL-N2**		
E-2	00:29:00	**Soham**	**N2 COPV Filling**		
E-2-1		Soham	Check **N2-HOSE-VENT** valve is **CLOSED**		
E-2-2			Check **OX-HOSE-VENT** valve is **CLOSED**		
E-2-3			Check **EREG** is **CLOSED** and **DISARMED**		
E-2-4			ARM and SLOW FILL with **N2-FILL** valve		
E-2-5			Wait for **N2 PRESSURE** to reach slow rate of increase		
E-2-6			Wait until **N2 PRESSURE** has reached approximately bar		
E-2-7			CLOSE **N2-FILL** valve and DISARM		
E-2-8			**SOL-OX SOL-FUEL** Closed		
E-2-9			Check **N2 PRESSURE** is **STABLE (~250bar)**		
E-2-10			Check **OX TANK PRESSURE** and **FUEL PRESSURE** are at **ATMOSPHERIC**		
E-3	00:25:00	**Soham**	**OX Tank Filling**		

E-3-1			ARM and CLOSE **OX SOLENOID VENT** valve		
E-3-2			ARM and **OPEN OX VENT** valve to **SLOW VENT** position		
E-3-3			Check that **OX TANK PRESSURE** is still at atmospheric		
E-3-4			ARM and OPEN OX FILL valve		
E-3-5			Zero ROCKET MASS load cell		
E-3-6			Check that OX TANK PRESSURE is increasing to between 30-50 bar		
E-3-7			If OX TANK PRESSURE is above 40 bar, open OX VENT valve to FAST VENT position		
E-3-8			Watch for plume from vent outlet. CLOSE OX FILL valve when this occurs		
E-3-9			Continue blipping OX VENT valve to FAST VENT from SLOW VENT until OX TANK PRESSURE reaches 25-30 bar. Do not fully close the vent valve		
E-3-10			OPEN OX FILL valve until plume is visible from vent again		
E-3-11			CLOSE OX FILL valve and DISARM		
E-3-12			CLOSE OX VENT valve and DISARM		
E-3-13			Verify that OX TANK PRESSURE is below 25 bar (if it is, repeat steps E-11-9 to E-11-13)		
E-3-14			ARM and OPEN OX HOSE VENT valve		
E-3-15			Wait until OX HOSE PRESSURE drops to atmospheric		
E-3-16			CLOSE OX HOSE VENT and DISARM		
E-4	00:19:00	**Raghav**	**Propulsion Systems Check (Go/No Go #1)**		
E-4-1			Are all pressures and temperatures nominal?		

E-4-2			Has sufficient propellant been loaded?	Ox: 15.7, Fuel: 5.2, Total: **~21kg**	
E-4-3			Do the propellants seem stable		
E-5		**Soham**	**Hold Until Hotfire**		
E-6	00:06:00	**Soham**	**Pressurise Propellants**		
E-6-1			ARM and CLOSE FUEL SOLENOID valve		
E-6-2			Check that FUEL TANK PRESSURE is still at atmospheric		
E-6-3			ARM EREG valve		
E-6-4			Run the PRESSURISE command for the EREG		
E-6-5			Monitor FUEL TANK PRESSURE to check that they are increasing steadily		
E-6-6			When FUEL TANK PRESSURE reaches the OX TANK PRESSURE, check that both pressure values keep increasing to 40 bar		
E-6-7			Check that the EREG closes once the FUEL pressures reach 40 bar. If it doesn't, close it manually.		
E-6-8			Check that both tank pressures are stable and not increasing or decreasing		
E-7	00:02:00	**Soham**	**N2 COPV Repress**		
E-7-1			ARM and SLOW FILL with N2 FILL valve		
E-7-2			Wait for N2 PRESSURE to reach slow rate of increase		
E-7-3			Move to FAST FILL with N2 FILL valve		
E-7-4			Wait until either N2 PRESSURE has reached approximately 250 bar		
E-7-5			CLOSE N2 FILL valve and DISARM		
E-7-6			Check N2 PRESSURE is stable and OX TANK PRESSURE and FUEL PRESSURE still at 40 bar		
E-7-7			ARM and OPEN N2 HOSE VENT valve		

E-7-8			Wait until N2 HOSE PRESSURE drops to atmospheric		
E-7-9			CLOSE N2 HOSE VENT and DISARM		
E-8	00:01:00	**Soham**	**Avionics Systems Check**		
E-8-1			Rocket: ARM Goofy, Check and Disarm		
E-8-2			Rocket: ARM E-Reg, Check and Disarm		
E-17	00:00:30	**Raghav**	**Propulsion Systems Check (Go/No Go #2)**		
E-17-1			Are all pressures and temperatures nominal?		
E-17-2			Do the propellants seem stable?		
Prelaunch checklist complete, move to F - Launch					
				Approved by:	

Team 18 - PLUTO			Imperial College Rocketry London		
F - Launch					
Location: MCC **Lead:** Soham			**Summary: Upon completion the rocket has been launched**		
Members:					
Step	**Time To Launch**	**Responsible**	**Task**	**Comment**	**Check**
F-1		**Soham**	**Start Subsystems Go/No Go**		
F1-1			Recovery go/no go	Verify continuity on recovery igniters	
F1-2			Avionics go/no go		
F1-3			Propulsion go/no go		
F-2		**Soham**	**Flight go/no go**		
F-3		**Soham**	**Arm Rocket for Launch**	ARM launch button	
F-4		**Soham**	**Launch Control go/no go**		
F-5		**Soham**	**Inform RSO vehicle ready**		
F-6	**HOLD**	**Soham**	**Countdown Starts**		
F-7	00:00	**Soham**	**Launch**	PRESS Launch Button to initiate launch autosequence	
			Rocket has successfully launched		
				Approved by:	

G Detailed calculations

G.1 SRAD Common Bulkhead Tank Calculations

G.1.1 Material Properties

The tank tubes are made from stock 6082-T6 extruded aluminium. They have an outer diameter of 190.7 mm and a wall thickness of 6.4 mm. AL 6082-T6 is chosen for its high strength-to-weight ratio and is easy to source in the desired size. UTS and YTS of aluminium tubes in table 26 are obtained from supplier data sheet [3]. Shear strength of aluminium tubes is calculated using an industry standard approximation of $0.6 \times UTS$. This estimate is carried out because the tubes have lower UTS compared to an industry standard UTS of 330 MPa for AL 6082-T6 [4]. The industry standard approximation for BYS is $1.5 \times YTS$ [5]. Due to the scarcity of BYS data for aluminium alloys, a more conservative approximation of $BYS = 1.25 \times YTS$ is used in table 26.

The tank bulkheads are machined in-house from a round bar of 7075 aluminium alloy. This material is chosen for its high strength-to-weight ratio. To verify material properties, a tensile test was performed on dog bone samples machined from the same stock. The UTS and YTS of the bulkhead material in table 26 were obtained from this test. For bulkhead material, the shear strength and BYS are estimated using the same approximation applied to the aluminium tubes.

Table 26: Material properties of components of tank. All values are in MPa.

Property	Tubes (AL 6082-T6)	Bulkheads (AL 7075)
Ultimate Tensile Strength (UTS)	310	430
Yield Tensile Strength (YTS)	260	320
Shear Strength	186	258
Bearing Yield Strength (BYS) (e/d = 2)	325	400

G.1.2 Stresses in thin-walled pressure vessels

For a cylinder to be categorised as thin walled-pressure vessel, the following expression has to be true [6]:

$$\frac{R}{t} > 10$$

The thin-walled pressure vessel anaylsis is valid on the AL-6082-T6 tubes with outer diameter 190.7 mm and wall thickness of 6.4 mm, as they have a $\frac{R}{t} = 14.90$. Hoop stress and Axial stress formulas can be used to calculate the two dimensional Von Mises stress [7].

$$\sigma_h = \frac{P \times D}{2t}$$

$$\sigma_a = \frac{P \times D}{4t}$$

$$\sigma_v = \sqrt{\sigma_h^2 + \sigma_a^2 - \sigma_h \sigma_a}$$

A tank with 177.9 mm inner diameter and 6.4 mm wall thickness, an internal pressure of 60 bar (MEOP) gives an overall safety factor of 3.60. This safety factor is for the two dimensional Von Mises stresses against tensile yield of the tank wall.

G.1.3 Bolt shear failure

Each bulkhead is constrained to a tube with a set of $24\times$ 6 mm shoulder bolts. The bolts are made of 12.9 high tensile steel with a shear strength of 517 MPa [8].

The axial force on the bulkhead resulting from internal pressure is calculated by multiplying the MEOP by the internal diameter of the tube. Divide this force by the total cross-sectional area of all the shoulder bolts to find the shear stress in each bolt [9].

$$F_{ax} = \frac{\pi}{4} D_{i,tube}^2 \times MEOP$$

$$\sigma_{\text{bolt shear}} = \frac{F_{ax}}{N \times \frac{\pi}{4} d_{bolt,shoulder}^2}$$

For a tank with inner diameter of 177.9 mm and 60 bar MEOP, the axial force on each bulkhead is 149 kN. Dividing this by the total cross-sectional area of the 24 shoulder bolts gives an overall safety factor of 2.35 against the shear yield of the bolts.

G.1.4 Bolt Tear-Out Failure

Bolt tear-out failure occurs when the bolts are close to the edge of the tube or the tube is relatively thin [9]. The most conservative shear area is the rectangular area just after the edge of the bolts to the edge of the tube. This failure mode is also present in the bulkhead where the bolts apply force against a small area of material between the bolt and the O-ring groove. The following equations from Half Cat [9] can be used to calculate the bolt tear out shear stress.

$$F_{\text{bolt}} = \frac{F_{ax}}{N}$$

$$E_{\min} \equiv E - \frac{d_{\text{bolt,shoulder}}}{2}$$

$$\sigma_{\text{tear-out}} = \frac{F_{\text{bolt}}}{E_{\min} \times 2t}$$

Where $E \geq 2d_{\text{bolt,shoulder}}$ needs to be satisfied to meet the requirements to use a higher bearing yield strength. For both the tubes and the bulkheads, the edge distance is $E = 12$ mm, twice the shoulder diameter of the bolt. For a tube with a wall thickness of 6.4 mm, the bolt tear-out safety factor is 3.45. For simplification, the interaction between the bolt shoulder and the bulkhead is used as the wall thickness to calculate the bolt tear-out failure for the bulkhead. For a bulkhead with wall thickness of 5.9 mm, the bolt tear-out safety factor is 4.41.

G.1.5 Tube Tensile failure between bolts

Tube tensile failure occurs when the internal pressure causes the material between the bolt holes to stretch beyond its braking point [9]. This failure is most likely to occur in designs with a large number of relatively large bolts or when the tube is relatively thin. The common bulkhead wall is subjected to radially outwards force from the internal pressure. This can cause the material between the bolt holes in the common bulkhead to stretch beyond its breaking point. Tube tensile failure can be calculated by dividing the axial force, F_{ax} by the minimum cross-sectional area of the tube between the bolt holes [9].

$$\sigma_{\text{tensile}} = \frac{F_{ax}}{\left[(D_{o,tube} - t)\pi - N \times d_{\text{bolt,shoulder}}\right] \times t}$$

For the AL 6082-T6 tubes with 190.7 mm outer diameter, 6.4 mm wall thickness and 60 bar MEOP, the overall safety factor against tensile yield of the tube between bolts is 4.85. For the common bulkhead with 177.5 mm outer diameter, 5.9 mm wall thickness and 60 bar MEOP, the overall safety factor against the tensile yield of the material between the bolts is 5.00.

G.1.6 Hole Bearing Failure

Bearing stress is due to the force of the bolts pushing against the bolt holes. If the stress is too high, plastic deformation can occur, eventually leading to material failure. Bearing stress can be calculated by the dividing force on each bolt, F_{bolt} by the interaction area between the bolt and the bolt hole. This area can be found by multiplying half the bolt circumference by the wall thickness of the tube. This gives the following formula for bearing stress:

$$\sigma_{\text{bearing}} = \frac{F_{\text{bolt}}}{0.5 \times \pi \times d_{bolt,shoulder} \times t}$$

For a more conservative approach the interaction area can be assumed to be the product of bolt diameter and the wall thickness [9].

$$\sigma_{\text{bearing,conservative}} = \frac{F_{\text{bolt}}}{d_{bolt,shoulder} \times t}$$

The AL 6082-T6 tubes with 6.4 mm wall thickness and 60 bar MEOP, have an overall safety factor against bearing yield failure of 3.15 and of 2.01 for the conservative approach. The 7075 aluminium alloy bulkheads with 5.9 mm wall thickness and 60 bar MEOP, have an overall safety factor against bearing yield failure of 3.58 and of 2.28 for the conservative approach.

G.1.7 Bulkhead stresses

The bulkhead stresses can be modelled as a uniformly loaded circular disc with the outer edge fixed [9]. The following formula from Half Cat rocketry [9] is used to calculate the stresses in the bulkhead.

$$\sigma_{\text{bulkhead}} = \frac{3 \times MEOP \times r_{\text{disk}}^2}{4t^2}$$

The top bulkhead with 63.9 mm disk radius, 12.2 mm thickness and 60 bar MEOP, has an overall safety factor of 2.59 against tensile yield of the top bulkhead disk. The bottom bulkhead with 65.4 mm disk radius, 12 mm thickness and 60 bar MEOP, has an overall safety factor of 2.39 against tensile yield of the bottom bulkhead disk. The common bulkhead with 64.9 mm disk radius, 13 mm thickness and 60 bar MEOP, has an overall safety factor of 2.85 against tensile yield of the bottom bulkhead disk. The common bulkhead has the highest safety factor to avoid a scenario in which the two propellants mix in the tank.

G.1.8 Uniform longitudinal compression in thin walled circular tube

The critical yield force due to the longitudinal compressive load is the tensile yield strength of the AL 6082-T6 tubes multiplied by the cross-sectional area of the circular tube.

$$F' = \frac{1}{4} \times YTS \times \pi \times (D_{o,tube}^2 - D_{i,tube}^2)$$

The AL 6082-T6 tubes with outer diameter 190.7 mm, inner diameter 177.9 mm, have a longitudinal critical yield force of 963 kN. This calculation assumes their is no internal pressure in the tank to resist the longitudinal compressive forces.

Due to the compressive nature of the force, buckling analysis for a thin-walled circular tube is conducted. The following experientially derived formula, from Roark's [6] can be used to calculate the value of critical yield stress in a thin walled circular tube under uniform longitudinal compression.

$$\sigma' = \frac{0.3Et}{r}$$

The length of the tube needs to be several times more than $1.72\sqrt{rt}$ to achieve the most accurate results [6]. The length of the fuel tube is 8.19 times as great as $1.72\sqrt{rt}$. The length of the oxidiser tube is 19.65 times as great as $1.72\sqrt{rt}$. The critical buckling force can be calculated by multiplying the critical buckling stress by the cross-sectional area of the circular tube.

$$F' = \frac{1}{4} \times \pi \times \sigma' \times (D_{o,tube}^2 - D_{i,tube}^2)$$

The AL 6082-T6 tubes with 190.7 mm outer diameter and 6.4 mm thickness have a critical buckling force of 5141 kN. Both the critical yield force and the critical buckling force are much larger than the maximum compressive longitudinal force of 6 kN.

G.1.9 O-Ring seal

Nitrile 70 Shore rubber O-rings are used to seal the tank. Nitrile O-rings are selected for their wide temperature range and excellent chemical resistance. The Ceetak online O-ring calculator is used to determine the size of the O-ring. Figure 57 shows the calculated results for the O-ring and groove size in Figure 56.

Input	Size (mm)	Tolerance	Lower	Upper	Min. Dim	Max. Dim
Inside Diameter A	167	ISO	-1.27	1.27	165.73	168.27
Cross Section B	5	Custom	-0.10	0.10	4.90	5.10
Bore Diameter C	177.9	Custom	-0.300	0.300	177.600	178.200
Piston Diameter D	177.5	Custom	-0.100	0.100	177.400	177.600
Groove Diameter E	170.6	Custom	-0.100	0.100	170.500	170.700
Groove Width F	7.5	Typ	0	0.2	7.500	7.700
Groove Radius G	0.5	Typ	-0.2	0	0.300	0.500

Figure 56: O-Ring and Groove dimensions

Calculated Results	Min.	Max.
Squeeze (%)	19.588	31.505
Compression (mm)	0.938	1.587
Gap (mm)	0.000	0.400
Housing Fill (%)	62.410	78.920
Elongation on Installation (%)	1.323	3.001
Installed Cross Section with Elongation (mm)	4.788	5.037
Compression Outside	0.000	0.490
Eccentric Squeeze (%)	9.145	33.491
Eccentric Squeeze Compression (mm)	0.438	1.687
Extrusion Gap		0.800

Figure 57: O-ring calculated results

G.2 Recovery Calculations

G.2.1 OSCALC Software

The OSCALC software is based on this equation:

$$F_{max} = \left(\frac{1}{2}\rho V_{stretch}^2\right)(S_a C_d)_{sd} C_k \tag{2}$$

Where ρ is air density,V_{strech} is the fall rate at line stretch, S_a is the nominal surface area, C_d is the steady descent coefficient of drag, C_k is the opening shock factor.

The opening shock factors are based off empirical data as seen in Figure 58, in order to use this you need the mass ratio and read the minimum and maximum values for the specified mass ratio.

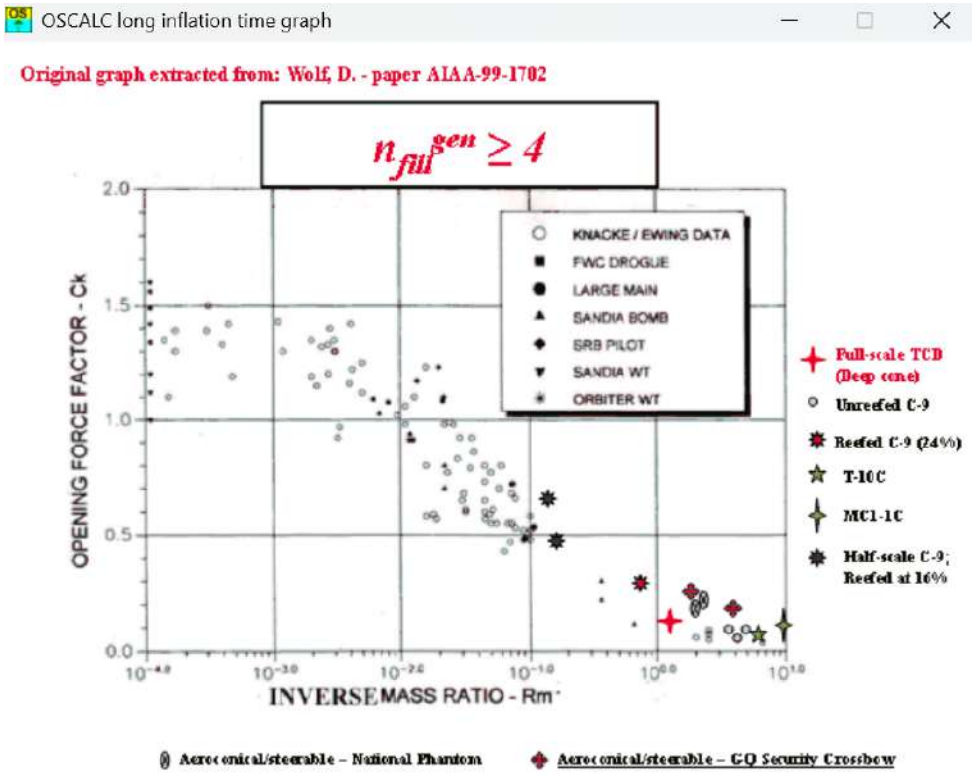

Figure 58: Long inflation time graph

G.2.2 Shock Load calculations

The shock load for Pluto were based mostly off of Nimbus 24 IMU data. This was translated into a vertical force taking in account for heavy swinging motions to standardise the shock force with programs the team was using. The Swinging motion was calculated as a pendulum from video, the length pendulum was from the recovery bulkhead to the IMU. this gave a vertical force of $\sim$ 6500 N and a horizontal force of $\sim$ 3000 N.

The OSCALC Nimbus 24 shock load is seen in Figure 59. The estimated fall rate at line stretch of 85 was chosen to line up with vertical force data. As the Nimbus 24 and Pluto uses the same parachute. The drag from steady descent data section was used.

This was translated into the Pluto shock load calculations as seen in Figure 60. The fall rate of the line stretch is dependent on the atmospheric pressure, hence different between the two.

The minimum shock load of $\sim$ 4200 N and the maximum shock load of $\sim$ 8400 N was found. A shock load value of $\sim$ 8000 N was chosen to be designed against.

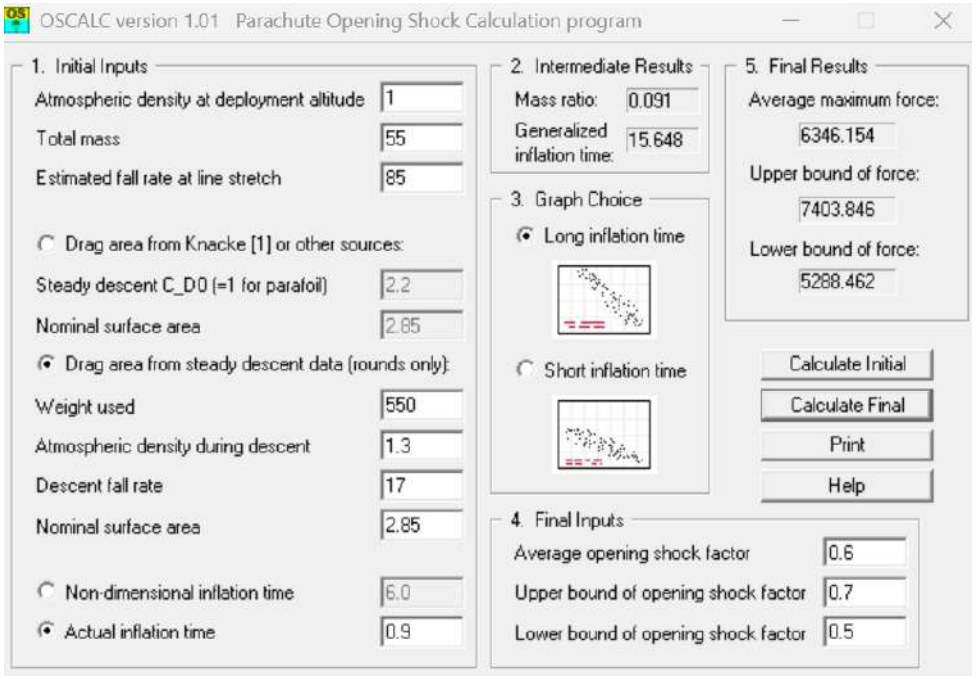

Figure 59: OSCALC Nimbus 24 Shock Loads Calculations

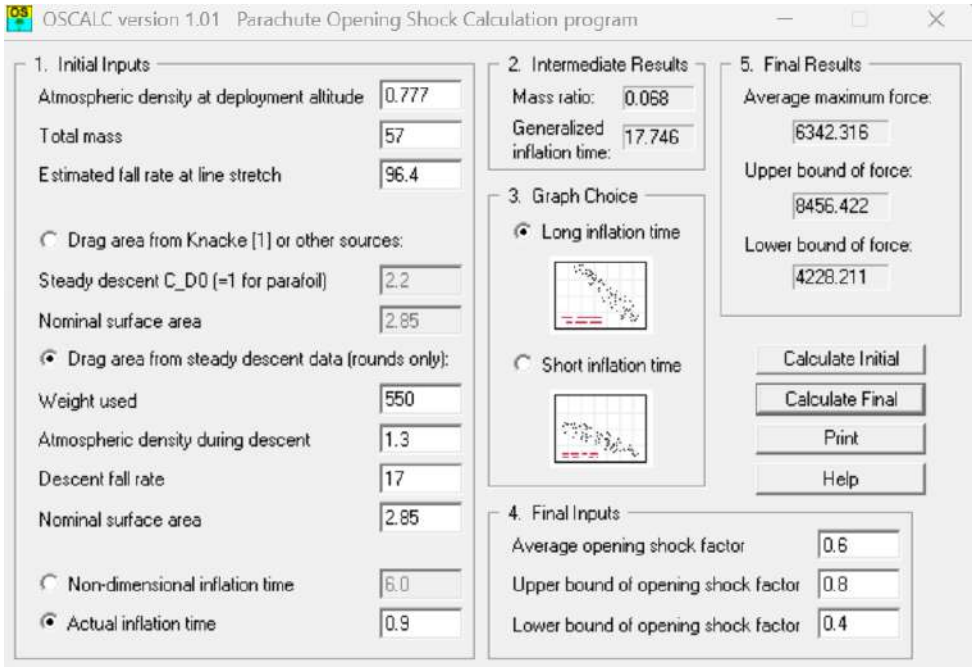

Figure 60: OSCALC Pluto Shock Loads Calculations

H Project FEA Reports

H.1 Recovery Bulkheads

H.1.1 Upper Recovery Bulkhead

Simulation Name	Upper Recovery Bulkhead Static Simulation
Description	Applying static recovery shock load to determine if the upper bulkhead fails due to rocket separation
Responsible Engineers	Ahmed Gilani
Software	Abaqus CAE
Objectives	To determine whether the upper bulkhead will fail during separation and recovery
Expected Outcome	The bulkhead should not fail with the calculated recovery shock loads. Higher stresses should be found at geometries with severe discontinuities such as hole edges. The safety factor should remain above the ICLR standard of 1.5, and deflections should remain minimal as to not disrupt the performance of the shock cord connecting eyebolt.
Data Location	Abaqus CAE
Summary	The upper recovery bulkhead is bonded onto the inside recovery tube that is separated from the main rocket body. It transfers the shock load from the parachute to the structure of the recovery tube and nose cone. Despite the extra holes visible on the central portion of the upper bulkhead, only the central hole is used for the shock cord eyebolt. A conservative shock load value of 10kN was applied to ensure a safety factor of greater than 1.5, and 1.72 was achieved with a maximum stress of 157MPa.

Background

This simulation was carried out to ensure that the bulkhead does not fail and result in failed recovery of the recovery tube, and thus preventing damage of this section of *Pluto*. It should be noted that a washer is used as part of the bulkhead assembly to distribute the force from the nut of the eyebolt.

Simulation Set Up

The STEP bulkhead part was imported into Abaqus, as well as a washer. The two were put into an assembly and positioned as they would be in the real assembly. Aluminim 6061 T6 material properties and allowables were inputted and applied to the bulkhead part and those of steel were inputted and applied to the washer part. The application of the load was required to be as close to real life as possible, with a single force applied to the internal surface to the eyebolt hold not acceptible. Given that the eyebolt hole is not threaded, the load will be delivered through the nut, and subsequently the washer. Thus the conservative 10kN force was transferred to a uniform pressure by dividing by the surface area of the washer. Only normal pressure was considered as this was identified as the most severe load case, as any oblique loading would result in compression of some spokes, meaning the safety factor would decrease in comparison. Thus a pressure of 58.7MPa was uniformly applied to the underneath of the washer.

In order for the load to be transferred to the bulkhead, an "interaction" needed to be set up, with "rough" tangential behaviour and "hard contact" normal behaviour, adequately capturing the

interaction of the real life assembly. Given that the bulkheaad's outer ring surface will be bonded using epoxy to the inside of the recovery tube, an encastre boundary condition was applied to the outer surface.

Results

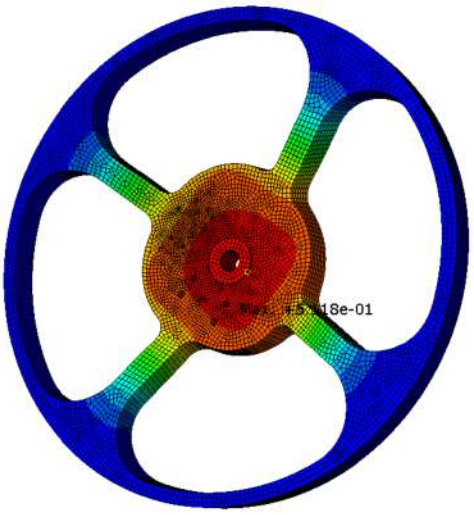

Figure 61: Upper Recovery Bulkhead FEA Simulation Overall Displacement Distribution

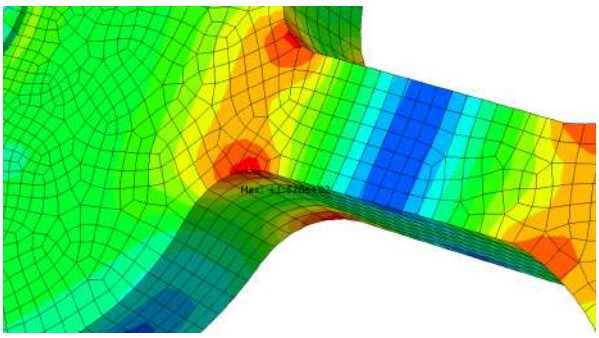

Figure 62: Upper Recovery Bulkhead Maximum Stress Location

Figure 20 shows the resulting stress distribution. It follows the prediction made with the stress concentrations being found in locations with tight corners. Figure 62 shows where the maximum stress is located on the part, again in an expected location. The maximum stress of 157MPa resulted in a safety factor of 1.72, an acceptable value. Thus it can be determined that the Upper Recovery Bulkhead will not fail under the maximum possible shock load. The displcement distribution shown in figure 61 shows that the maximum displacement occurs at the centre, where the load is applied. The magnitude of this maximum displacement is 0.511mm, sufficiently small to conclude that the functionality of the component will not be affected. Thus this design for the Upper Recovery Bulkhead can be qualified for flight.

Simulation Number	1 - Tensile Upper Recovery Bulkhead Shock Loading
Simulation Date	24/05/2025
Inputs	
10kN static load	Applied Load as Pressure
Outputs	
157 MPa	Maximum Von Mises stress
0.511 mm	Maximum deflection
Location of maximum stress	Max stress concentration is at the corner where a spoke connects to the central mounting section.

H.1.2 Lower Recovery Bulkhead

Simulation Name	Lower Recovery Bulkhead Static Simulation
Description	Applying static recovery shock load to determine if the lower bulkhead fails due to rocket separation
Responsible Engineers	Ahmed Gilani
Software	Abaqus CAE
Objectives	To determine whether the lower bulkhead will fail during separation and recovery
Expected Outcome	The bulkhead should not fail with the calculated recovery shock loads. Higher stresses should be found at geometries with severe discontinuities such as hole edges. The safety factor should remain above the ICLR standard of 1.5, and deflections should remain minimal as to not disrupt the performance of the shock cord connecting eyebolt and the recovery mechanism hardware fastened to it
Data Location	Abaqus CAE
Summary	The loweer recovery bulkhead is bonded onto the inside of the body tube of the main rocket body. It transfers the shock load from the parachute to the structure of the main rocket airframe. The extra holes visible on the central portion of the lower bulkhead, are used to mount the spool assembly and solenoid of the recovery mechanism. A conservative shock load value of 10kN was applied to ensure a safety factor of greater than 1.5, and 1.53 was achieved with a maximum stress of 176MPa.

Background

This simulation was carried out to ensure that the bulkhead does not fail and result in failed recovery of the recovery tube, and thus preventing damage of this section of *Pluto*. It should be noted that a washer is used as part of the bulkhead assembly to distribute the force from the nut of the eyebolt.

Simulation Set Up

The STEP bulkhead part was imported into Abaqus, as well as a washer. The two were put into an assembly and positioned as they would be in the real assembly. Aluminim 6061 T6 material properties and allowables were inputted and applied to the bulkhead part and those of steel were inputted and applied to the washer part. The application of the load was required to be as close to real life as possible, with a single force applied to the internal surface to the eyebolt hold not acceptible. Given that the eyebolt hole is not threaded, the load will be delivered through the nut, and subsequently the washer. Thus the conservative 10kN force was transferred to a uniform pressure by dividing by the surface area of the washer. Only normal pressure was considered as this was identified as the most severe load case, as any oblique loading would result in compression of some spokes, meaning the safety factor would decrease in comparison. Thus a pressure of 58.7MPa was uniformly applied to the underneath of the washer.

In order for the load to be transferred to the bulkhead, an "interaction" needed to be set up, with "rough" tangential behaviour and "hard contact" normal behaviour, adequately capturing the interaction of the real life assembly. Given that the bulkheaad's outer ring surface will be bonded using epoxy to the inside of the recovery tube, an encastre boundary condition was applied to the outer surface.

Results

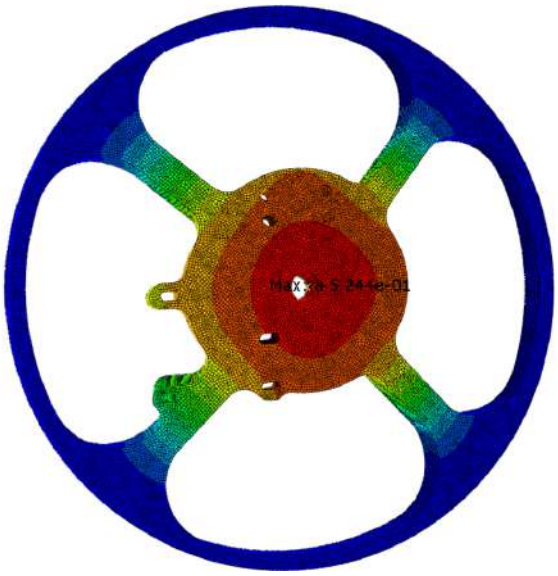

Figure 63: Lower Recovery Bulkhead FEA Simulation Overall Displacement Distribution

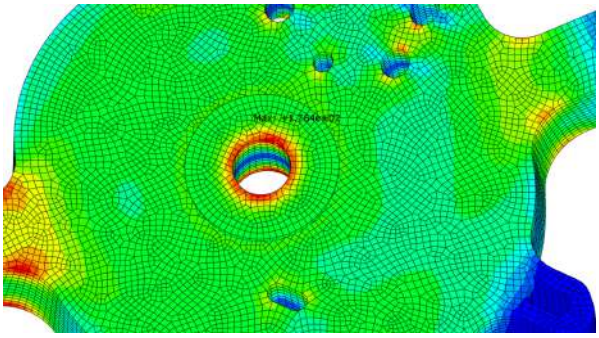

Figure 64: Lower Recovery Bulkhead Maximum Stress Location

Figure 21 shows the resulting stress distribution. It follows the prediction made with the stress concentrations being found in locations with tight corners, in this case the corner of the eyebolt hole. Figure 64 shows where the maximum stress is located on the part, again in an expected location. The maximum stress of 176MPa resulted in a safety factor of 1.53, an acceptable value. Thus it can be determined that the Upper Recovery Bulkhead will not fail under the maximum possible shock load. The displcement distribution shown in figure 63 shows that the maximum displacement occurs at the centre, where the load is applied. The magnitude of this maximum displacement is 0.524mm, sufficiently small to conclude that the functionality of the component will not be affected. Thus this design for the Upper Recovery Bulkhead can be qualified for flight.

Simulation Number	1 - Tensile Lower Recovery Bulkhead Shock Loading
Simulation Date	05/09/2025
Inputs	
10kN static load	Applied Load as Pressure
Outputs	
176 MPa	Maximum Von Mises stress
0.524 mm	Maximum deflection
Location of maximum stress	Max stress concentration is at the corner of the eyebolt mounting hole.

H.2 Stringers

Simulation Name	Stringer Buckling Simulation
Description	Applying 6kN engine loads to stringers to determine buckling safety factor
Responsible Engineers	Erica Keung, Rohan Woodcock
Software	Abaqus CAE
Objectives	To determine whether stringer will fail during liftoff and thrust phase
Expected Outcome	The 3 stringers should not fail by buckling with the nominal engine thrust of 6kN. The safety factor should remain above the ICLR standard of 1.5.
Data Location	Abaqus CAE
Summary	The stringers transmit loads from the engine to the rest of the rocket. Buckling simulations were performed with a compressive load of 2kN per stringer to ensure that a safety factor of greater than 1.5 was achieved.

Background

The stringers are made of Aluminium 6082 T6 with a Young's Modulus of 69GPa and Poisson's Ratio of 0.33.

Simulation Set Up

The STEP file for a stringer was imported into Abaqus. A solid section was created and material properties assigned. A quadratic tet mesh (C3D10) was applied to the part, with 240,000 nodes. The bolt holes that interface with the bottom bulkhead of the tank were given encastre boundary conditions. The bolt holes that the engine truss connect to were constrained in all but the Y (vertical) direction. A compressive load of 2kN was distributed between both bolt holes.

Results

Table 27: Key Results - Buckling of Stringer

Applied Load (kN)	Buckle mode	Eigen Value (MPa)	Buckle Safety Factor
2	1	3.6046	3.6046
2	2	7.3377	7.3377
2	3	14.294	14.294

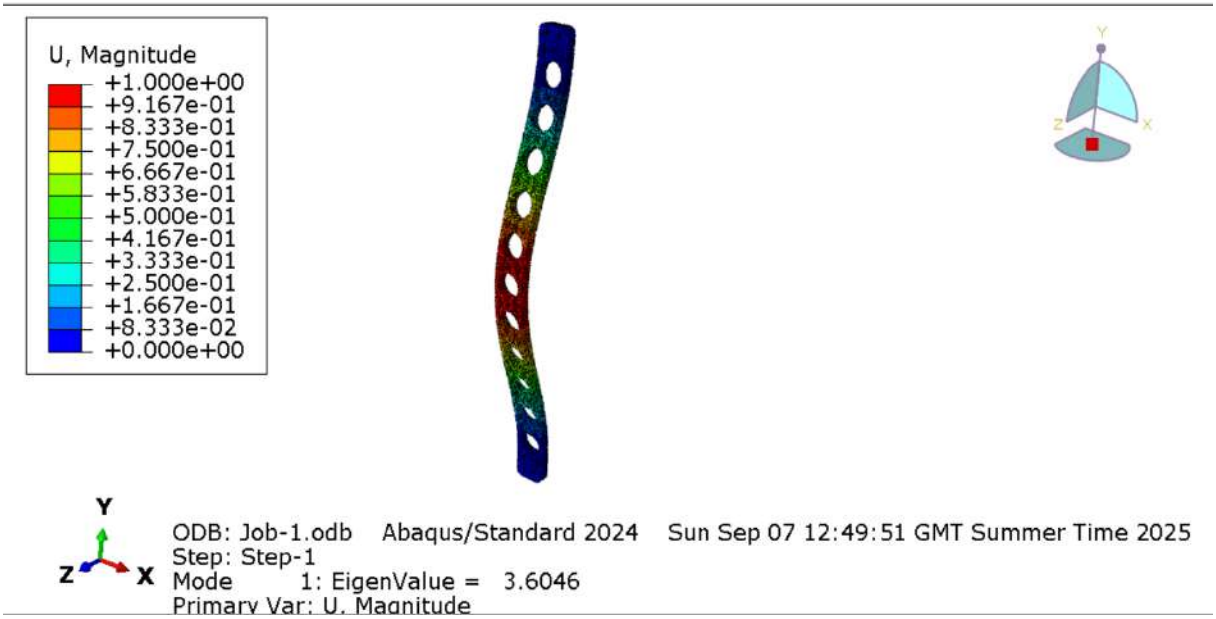

Figure 65: Stringer Mode 1 Buckling Simulation

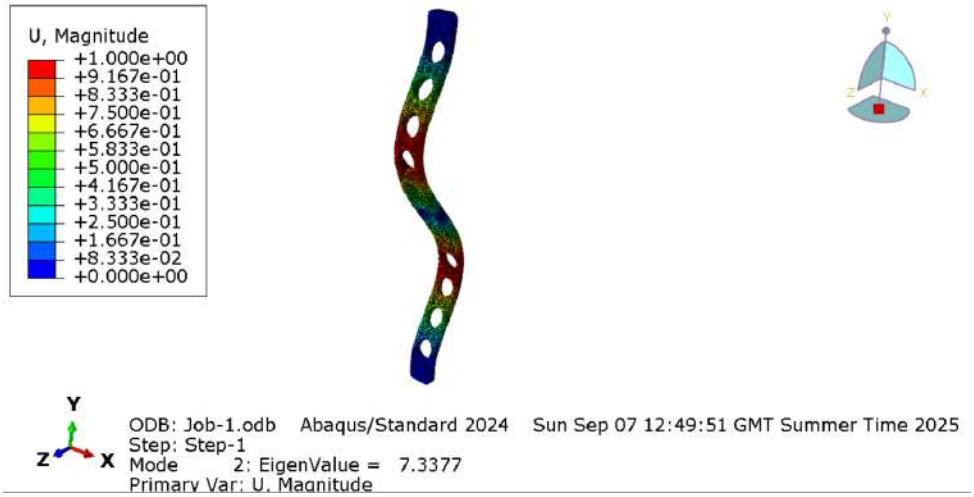

Figure 66: Stringer Mode 2 Buckling Simulation

As shown on Table 27, the safety factor for buckling modes 1-3 is larger than the required 1.5.

H.3 Body Tubes

Simulation Name	Body Tubes Buckling and Compression Simulation
Description	Applying 12kN loads to the body tubes to determine compressive failure, buckling modes and safety factors
Responsible Engineers	Ruchika Musa
Software	Abaqus CAE
Objectives	To determine the likely failure modes of the body tubes and see if they will fail during ascent.
Expected Outcome	The body tubes should not fail in buckling or compression at the launch force of 6kN. The safety factors should be unreasonably high (over 100) to account for likely defects and inconsistencies in hand-manufacturing composites.
Data Location	Abaqus CAE
Summary	The body tubes take the compressive load between the tanks and the payload during launch, an expected 6kN. They house plumbing, electronics and recovery systems. A simulated load of 12kN is used to give a larger safety factor, and because transverse loads, not simulated, may exist during launch.

Background

The propulsion and recovery tubes are made from a Kevlar-reinforced, epoxy-matrix composite. They are 185mm in diameter; a wall thickness of 2mm; and are 120cm and 60cm long respectively. They also have holes for accessing electronics

Simulation Set Up

The STEP file for a stringer was imported into Abaqus. A solid section was created and material properties assigned. A quadratic tet mesh (C3D10) was applied to the part, with 240,000 nodes. The bolt holes that interface with the bottom bulkhead of the tank were given encastre boundary conditions. The bolt holes that the engine truss connect to were constrained in all but the Y (vertical) direction. A compressive load of 2kN was distributed between both bolt holes.

The ube was extruded as a 3D deformable in Abaqus, with three holes, 33x33mm, 33x33mm and 60x90mm, cut 15mm from the end edges. Partitions were made at 110mm, 500mm, 507.5mm, 780mm and 902.5mm to simulate different forces at different areas (due to bulkheads and mountain points etc). The composite is Aramid and Epoxy, both contributing to the average material properties, described in Table 28.

Results

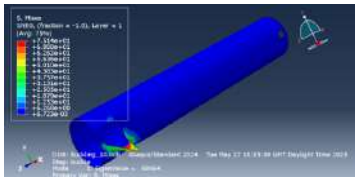

Figure 67: Body tube buckling mode 1

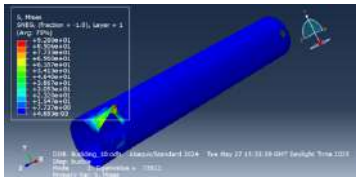

Figure 68: Body tube buckling mode 2

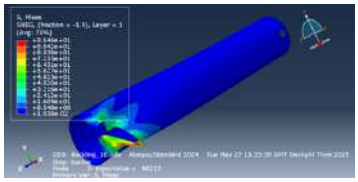

Figure 69: Body tube buckling mode 3

As shown on Table 29, the safety factors are incredibly high. This means that when the tubes are made by hand and inevitably weaker, they should still hold up. We do not yet have an empirical

Young's Modulus (longitudinal)	Young's Modulus (transverse)	Poisson ratio	
69640 MPa	6733 MPa	0.3443	
Sheer Modulus (12)	**Sheer Modulus (13)**	**Sheer Modulus (23)**	**Density**
25903 MPa	25903 MPa	2404.6 MPa	1350.5 kg/mm3
Tensile Strength (Longitudinal)	**Compressive Strength (Longitudinal)**	**Tensile Strength (Transverse)**	
1800 MPa	230 MPa	18 MPa	
Compressive Strength (Transverse)	**Shear Strength (Longitudinal)**	**Shear Strength (Transverse)**	
142 MPa	75 MPa	75 MPa	

Table 28: Combined properties for Aramid-Epoxy Composite

Table 29: Key Results - Buckling of Body Tubes

Applied Load (N)	Buckle mode	Eigen Value (MPa)	Buckling Safety Factor
1	1	68664	68664
1	2	72922	72922
1	3	80217	80217

Table 30: Key Results - Compression of Body Tubes

Applied Load (N)	Max Stress (MPa)	Max Displacement (mm)	Stress Safety Factor
12	35.23	0.2967	68664

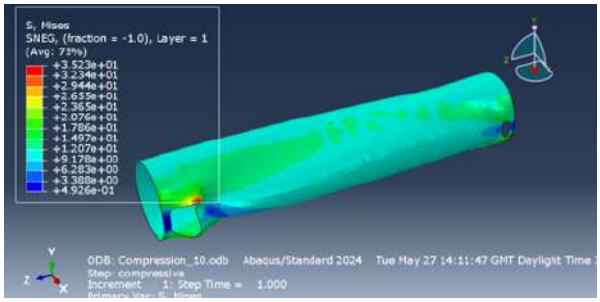

Figure 70: Stress distribution in compressive failure mode

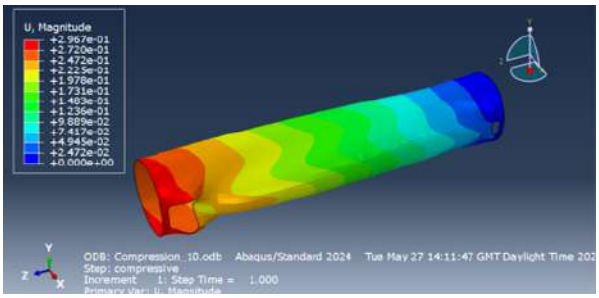

Figure 71: Displacement distribution in compressive failure mode

measure of the decrease in safety factor usually caused by our hand-moulding process, but our destructive tests previously have suggested that we require a safety factor around 1000 time greater. The lowest buckling safety factor at 12kN (the 1kN SF divided by 12) is 5700, which is more than sufficient.

H.4 Engine Truss

Simulation Name	Engine Truss Static Simulation
Description	Applying maximum static engine load to determine if the engine truss fails
Responsible Engineers	Ahmed Gilani, Rohan Woodcock
Software	Autodesk Fusion
Objectives	To determine whether the engine truss will fail during flight and to analyse maximum stress, minimum safety factor and maximum displacement
Expected Outcome	The engine truss should not fail with the calculated maximum engine thrust load. Higher stresses should be found at geometries with severe discontinuities such as hole edges or corners. The safety factor should remain above the ICLR standard of 1.5. As this is an additively manufactured part, a safety factor of 2 was chosen due to possible manufacturing inconsistencies. Deflections should remain minimal as to not disrupt the airframe in a very sensitive area.
Data Location	Autodesk Fusion
Summary	The engine truss is fastened to 3 stringers, which is attached to the bottom tank bulkhead in the main rocket body. It transfers the engine thrust load from engine to the structure of the rocket body. A maximum thrust load of 6kN was calculated and divided by 3 to simulate the load received by each connection point. A safety factor of 2.4 was achieved with a maximum stress of 100MPa.

H.4.1 Background

This simulation was carried out to ensure that the engine truss does not fail and result in failure during flight and consequently severe damage to *Pluto*.

H.4.2 Simulation Set Up

The engine truss CAD was loaded in Fusion. It was put into a simulation and AlSi10Mg material properties and allowables were inputted and applied to the component. The application of the load was required to be as close to real life as possible, with a single bolt force applied to the internal surface of the fastener. The maximum 6kN force was divided by 3 and applied to the inside of the bolt hole. Given the truss would be attached to the stringers via the mounting holes, an encastre boundary condition was applied to the inside of the fastener holes.

H.4.3 Results

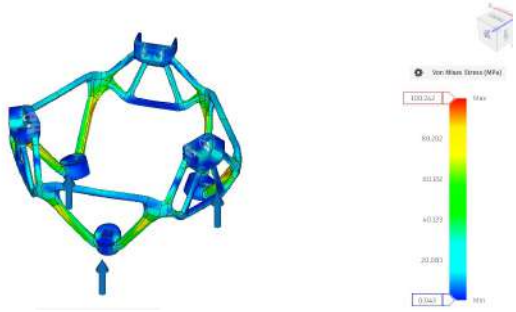

Figure 72: Engine Truss FEA simulation showing stress distribution

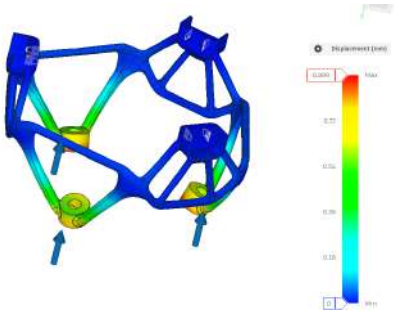

Figure 73: Engine Truss FEA simulation showing displacement distribution

Figure 73 shows the resulting stress distribution. It follows the prediction made with the stress concentrations being found in locations with tight corners. The maximum stress of 100MPa results in a minimum safety factor of 2.394. Thus it can be determined that the Engine Truss will not fail under the maximum possible engine thrust load. The displcement distribution shown in figure 73 shows that the maximum displacement occurs at the bolt holes, where the load is applied. The magnitude of this maximum displacement is 0.899mm, sufficiently small to conclude that the functionality of the component will not be affected. Thus this design for the Engine Truss can be qualified for flight.

Simulation Number	1 - Static Engine Truss Simulation
Simulation Date	25/06/25
Inputs	
6kN static load split into three 2kN loads	Applied Load inside fastener holes
Outputs	
100 MPa	Maximum Von Mises stress
0.899mm	Maximum deflection
Location of maximum stress	Max stress concentration on the bottom members near the corners.

H.5 SRAD Pressure Vessel Bulkheads

Simulation Name	SRAD Pressure Vessel Bulkhead Simulation
Description	Applying 60 bar pressure load to bulkheads o determine safety factor
Responsible Engineers	Rohan Woodcock, Hardik Modi
Software	Abaqus CAE
Objectives	To determine whether the bulkheads will fail during pressurisation
Expected Outcome	The bulkheads should not fail at the MEOP of 60 bar. The safety factor in yield should be at minimum 2, in line with EuRoC requirements for metal SRAD pressure vessels.
Data Location	Abaqus CAE
Summary	Each bulkhead is retained to the tank tubes through a set of 24 threaded holes, where shoulder bolts are inserted. A pressure load of 60 bar was applied to the bulkhead to ensure that a safety factor in yield was greater than 2.

Background

This simulation was carried out to ensure that all bulkheads, and therefore the tank does not fail. Yield strength for the Al 7075 alloy used in the bulkheads was taken as 330MPa. This was verified experimentally through tensile testing of ATSM E8m Subsize samples.

Simulation Set Up

The STEP file for each bulkhead was imported into Abaqus CAE. A solid section was assigned to the part with the material properties of the Al 7075 alloy. A quadratic tet mesh (C3D10) with at least 200k nodes was applied to the part (250k is the Abaqus 2024 Teaching License limit). A pressure load of 60 bar (6MPa) was applied to all interior surfaces, including the O-ring grooves. Pinned constraints were applied to the shoulder of all bolt holes. The threaded section was not constrained, as bolt sizing was based on the unthreaded shoulder.

The common bulkhead was simulated with pressure loads on either side separately, to consider the worst case scenario.

Results

Table 31: Key Results - Bulkhead Simulations

Bulkhead Name	Max Stress (MPa)	Safety Factor
Top Bulkhead	153	2.09
Bottom Bulkhead	150	2.13
Common Bulkhead (Top Pressurised)	124	2.58
Common Bulkhead (Bottom Pressurised)	93	3.44

As seen in Table 31, all bulkheads had a greater than 2 safety factor, therefore meeting the objectives of the simulation.

All Abaqus CAE models are shown with the bottom limit at 165MPa, as $\sigma_y = 320$MPa

Top (Fuel) Bulkhead

Figure 74: Top Bulkhead Simulation

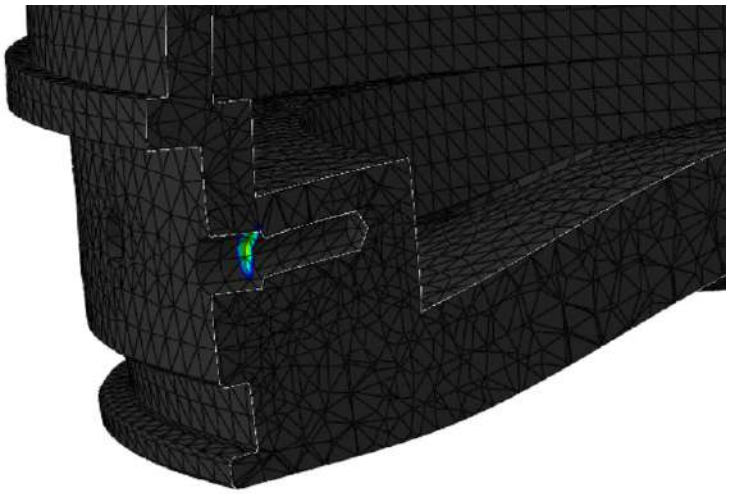

Figure 75: Hole Edge Stress Concentration

Table 32: Mesh Convergence Study on Bolt Holes

Local Seed Element Size (mm)	Stress (MPa)
3.3	310
1.5	371
0.6	519

Figure 75 shows stress concentrations that were observed at the bolt hole to thread edge. Local seeding was used to perform a mesh convergence study. As seen in Table 32, there is clear evidence of a discontinuity at the edge. Therefore, the stresses at the hole edge are not considered.

Bottom (Oxidiser) Bulkhead

Figure 76: Bottom Bulkhead Simulation

Common Bulkhead

Figure 77: Common Bulkhead with Top Pressurized

Figure 78: Common Bulkhead with Bottom Pressurized

I Engineering Drawings

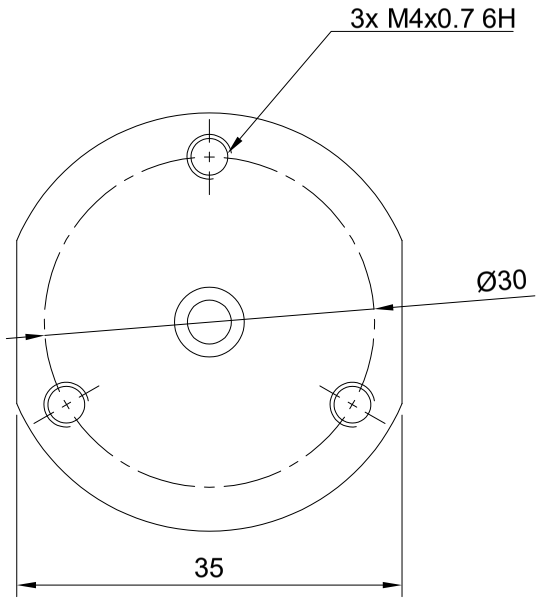

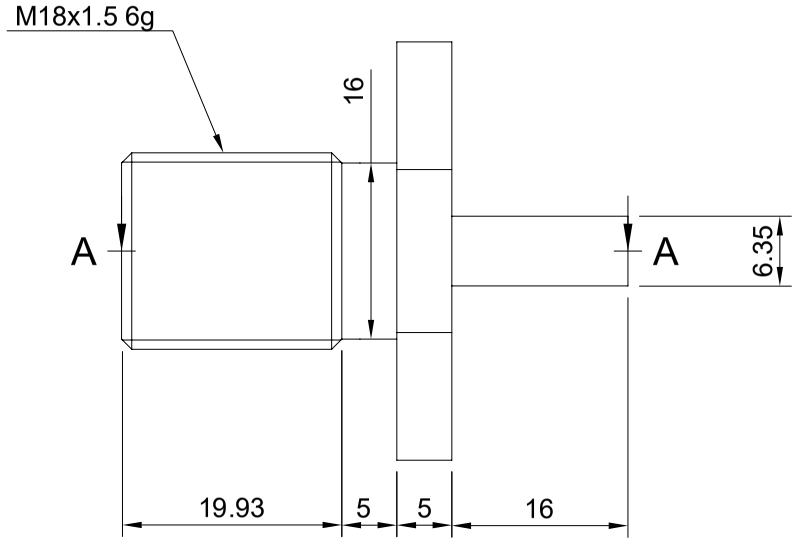

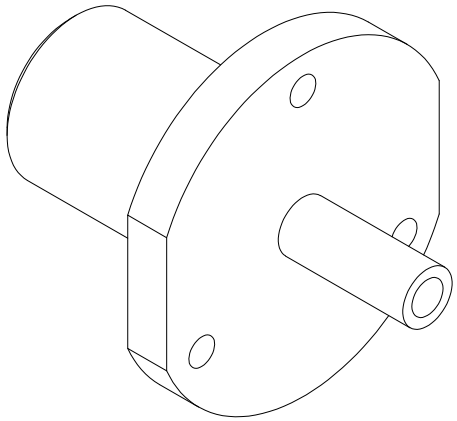

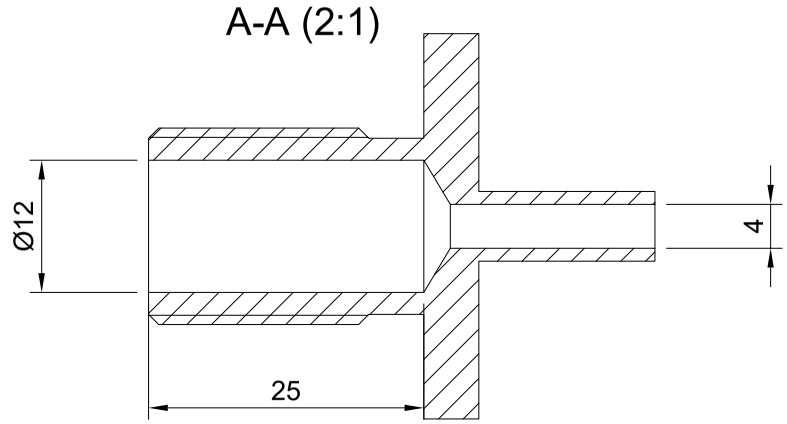

TOLERANCES		THIRD ANGLE PROJECTION
X = ± 0.5 X.X = ± 0.1 X.XX = ± 0.02	ANGULAR ± 1° SURFACE FINISH MACHINED FACES Ra 6.3	

	NAME	DATE
DRAWN	Rudra Nakade	06/09/2025
CHECKED		
APPROVED		

MATERIAL: Stainless Steel

ALL DIMENSIONS ARE IN MILLIMETRES

DO NOT SCALE DRAWING

A3 SCALE 2:1

TITLE: 1/4" COPV Adapter

DWG NO. 1/4 Tank Adapter

SHEET 1/1

REVISION:

A-A (1:2)

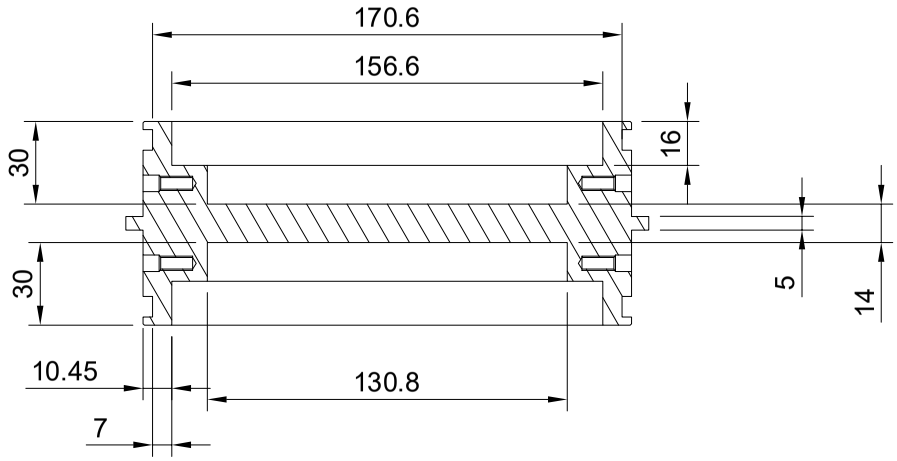

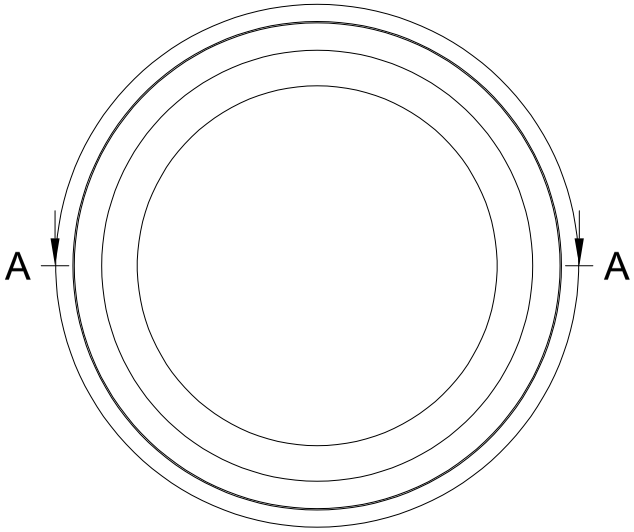

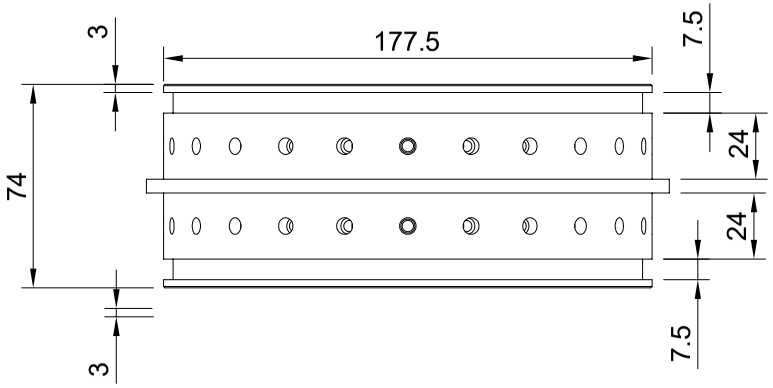

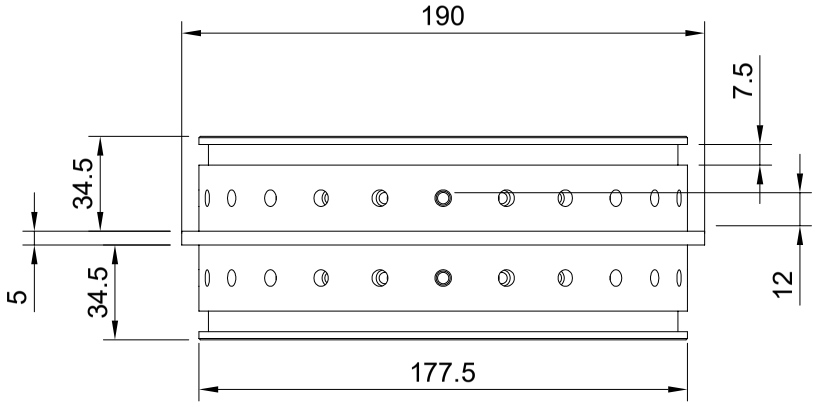

TOLERANCES		FIRST ANGLE PROJECTION	MATERIAL: 7075-T6 Endcap
X = ± 0.5 X.X = ± 0.1 X.XX = ± 0.02	ANGULAR ± 1° SURFACE FINISH MACHINED FACES Ra 6.3		ALL DIMENSIONS ARE IN MILLIMETRES
	NAME	DATE	DO NOT SCALE DRAWING
DRAWN	Rohan Woodcock	03/08/2025	
CHECKED			
UNDIMENSIONED SURFACES MACHINE FROM CAD			A3 SCALE 1:2

TITLE: Common Endcap 2 v39

FINISH/TREAT:

MASS (g): 2280.1165 g

IF IN DOUBT ASK

BREAK ALL SHARP EDGES WITH MIN RAD OR CHF UOS

SHEET 1/1

REVISION:

IMPERIAL COLLEGE LONDON, EXHIBITION ROAD, LONDON, SW7 2AZ

C-C (1:2)

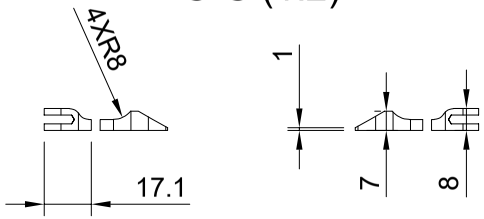

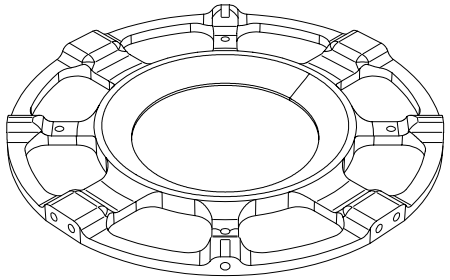

ISO VIEW
NOT TO SCALE

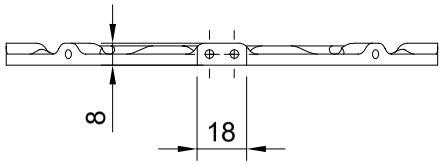

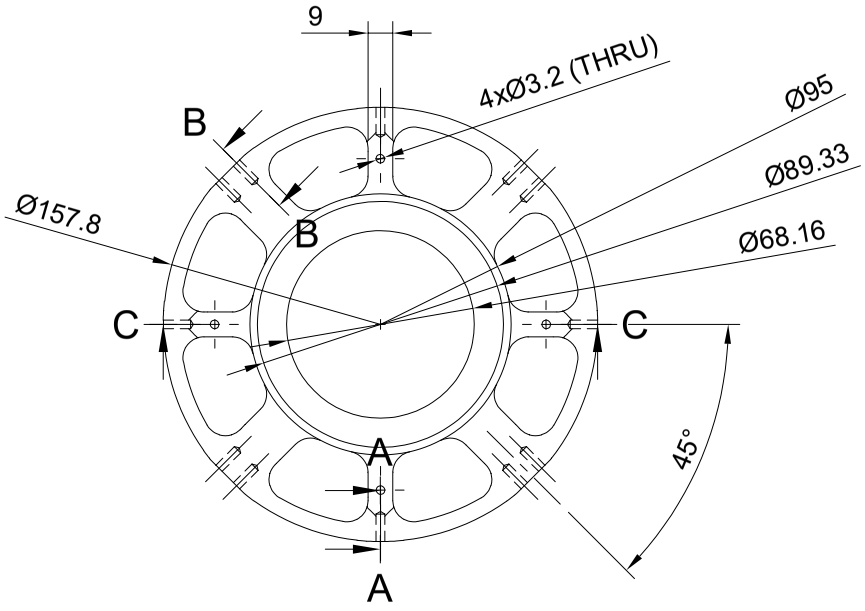

B-B (1:2)

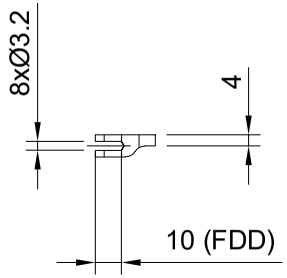

A-A (1:2)

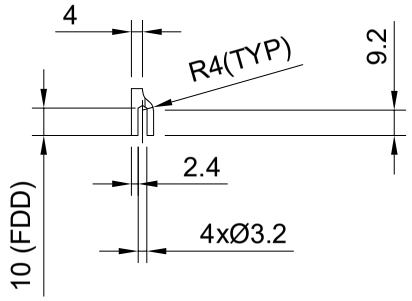

TOLERANCES		THIRD ANGLE PROJECTION
X = ± 0.5 X.X = ± 0.1 X.XX = ± 0.02	ANGULAR ± 1° SURFACE FINISH MACHINED FACES Ra 6.3	
	NAME	DATE
DRAWN	Marks Parmalis	31/05/2025
CHECKED		
UNDIMENSIONED SURFACES MACHINE FROM CAD		

MATERIAL: 6082T6-Al	TITLE: N2 BOT BULKHEAD-PLUTO
ALL DIMENSIONS ARE IN MILLIMETRES	FINISH/TREAT: CLEAN AND DEBURR SHARP EDGES
DO NOT SCALE DRAWING	MASS (g): 140 g
A3 SCALE 1:2	IF IN DOUBT ASK BREAK ALL SHARP EDGES WITH MIN RAD OR CHF UOS

IMPERIAL COLLEGE LONDON ROCKETRY ESTD. 2018

SHEET 1/1 | REVISION: A

IMPERIAL COLLEGE LONDON, EXHIBITION ROAD, LONDON, SW7 2AZ

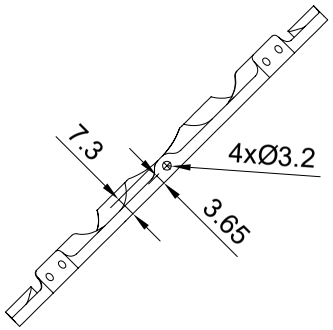

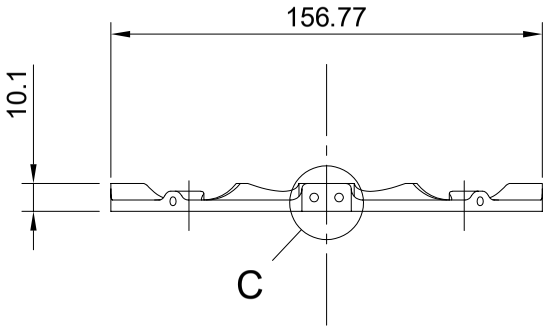

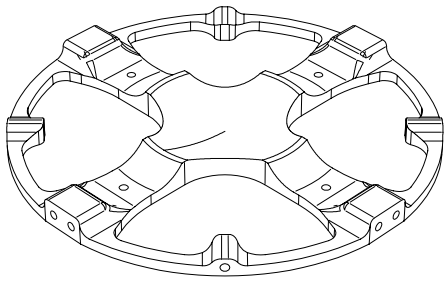

ISO VIEW
NOT TO SCALE

C (2:1)

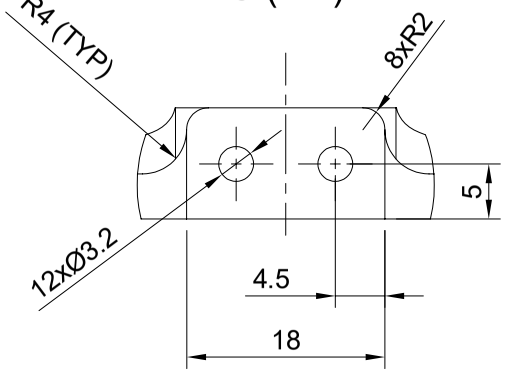

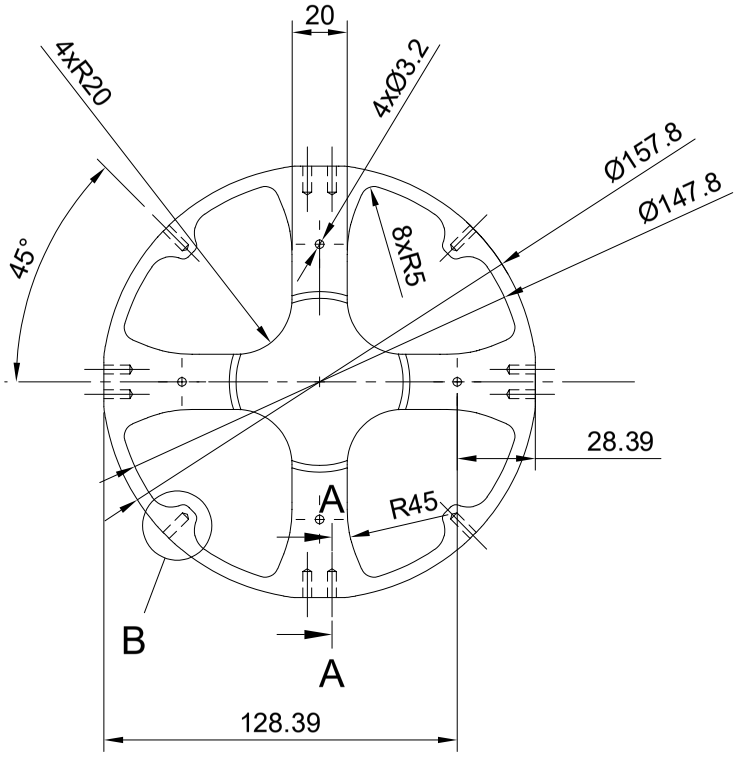

A-A (1:2)

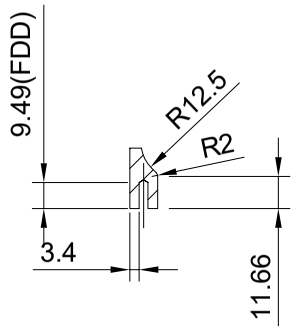

B (1:1)

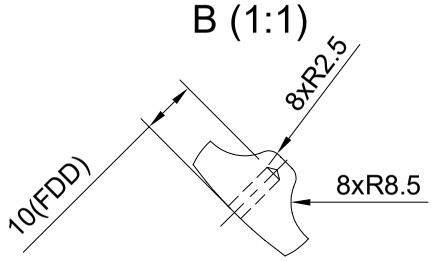

TOLERANCES		THIRD ANGLE PROJECTION
X = ± 0.5 X.X = ± 0.1 X.XX = ± 0.02	ANGULAR ± 1° SURFACE FINISH MACHINED FACES Ra 6.3	

	NAME	DATE
DRAWN	Marks Parmalis	18/03/2025
CHECKED		

UNDIMENSIONED SURFACES MACHINE FROM CAD

MATERIAL: 6082T6-Al

ALL DIMENSIONS ARE IN MILLIMETRES

DO NOT SCALE DRAWING

A3 SCALE 1:2

TITLE: N2 TOP BULKHEAD-PLUTO v64

FINISH/TREAT: CLEAN & DEBURR SHARP EDGES

MASS (g): 150g

IF IN DOUBT ASK

BREAK ALL SHARP EDGES WITH MIN RAD OR CHF UOS

SHEET 1/1

REVISION: A

IMPERIAL COLLEGE LONDON, EXHIBITION ROAD, LONDON, SW7 2AZ

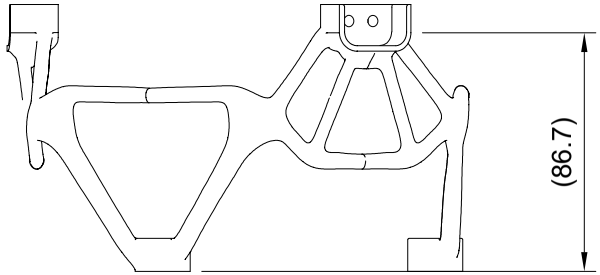

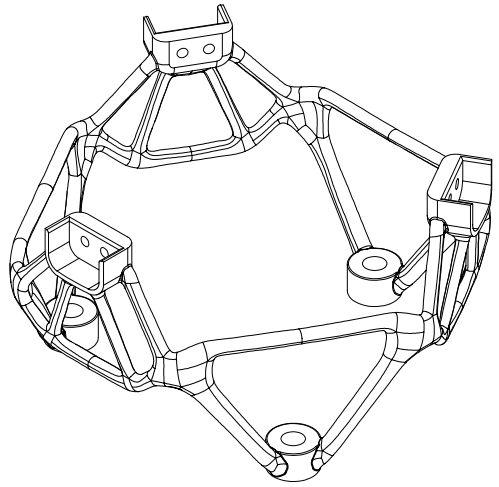

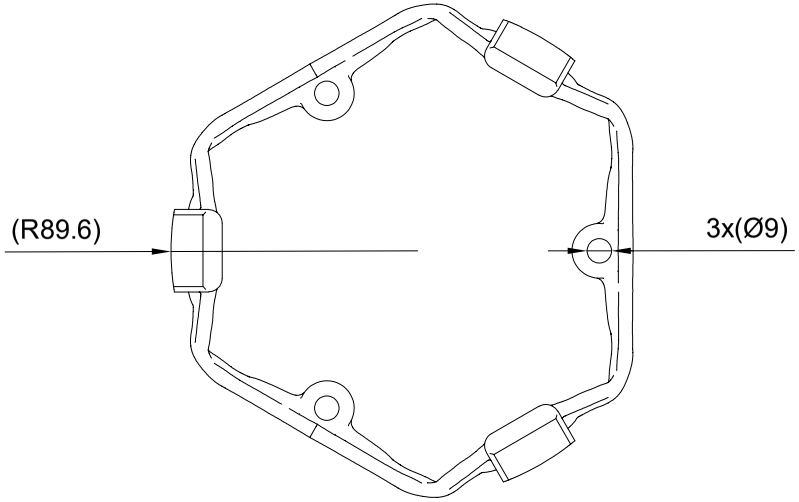

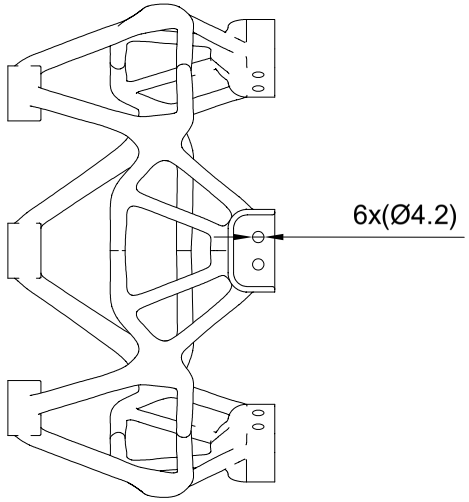

TOLERANCES		THIRD ANGLE PROJECTION	
X = ± 0.5 X.X = ± 0.1 X.XX = ± 0.02	ANGULAR ± 1° SURFACE FINISH MACHINED FACES Ra 6.3		
	NAME	DATE	
DRAWN	Lothaire Valex	22/03/2025	
CHECKED			
UNDIMENSIONED SURFACES MACHINE FROM CAD			

MATERIAL: Aluminum AlSi10Mg	TITLE: ENGINE TRUSS-PLUTO v7
ALL DIMENSIONS ARE IN MILLIMETRES	FINISH/TREAT:
DO NOT SCALE DRAWING	MASS (g): 168.1 g
A3 SCALE 1:2	IF IN DOUBT ASK BREAK ALL SHARP EDGES WITH MIN RAD OR CHF UOS
	SHEET 1/1 REVISION:

IMPERIAL COLLEGE LONDON, EXHIBITION ROAD, LONDON, SW7 2AZ

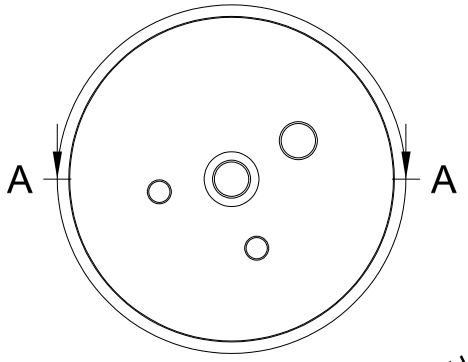

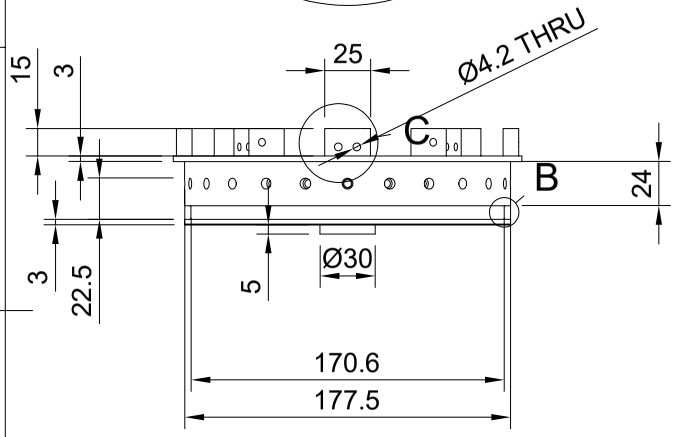

A-A (1:3)

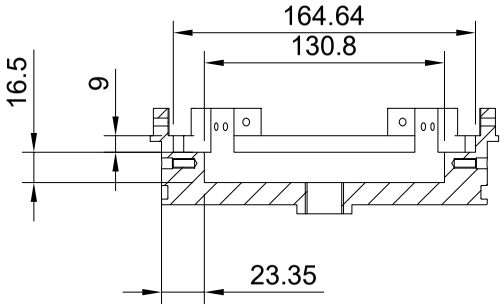

C (1:1)

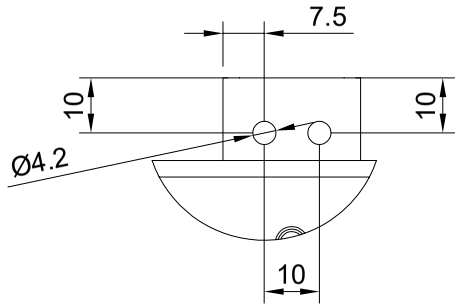

B (1:1)

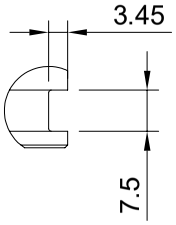

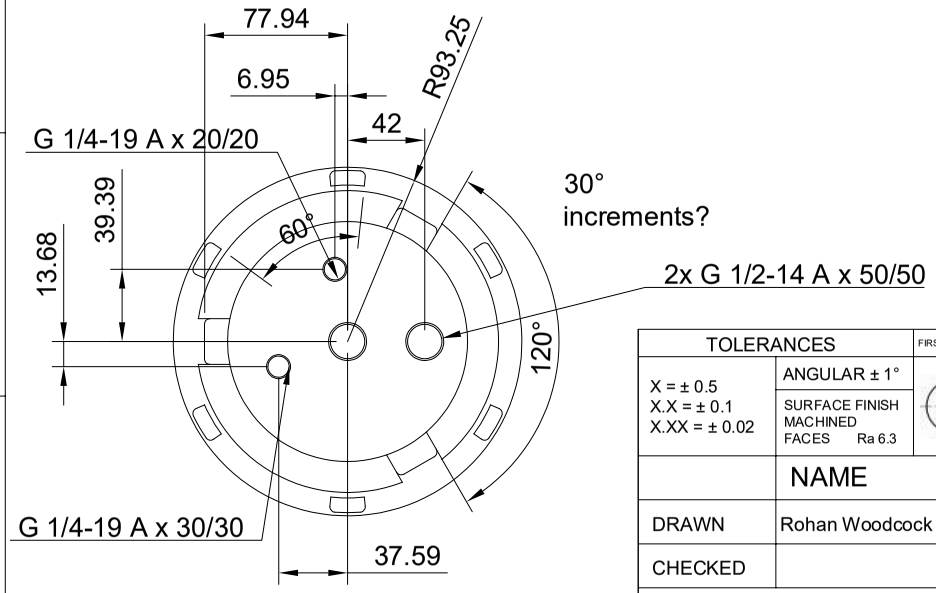

All holes will be drilled after CNC

TOLERANCES		FIRST ANGLE PROJECTION
X = ± 0.5 X.X = ± 0.1 X.XX = ± 0.02	ANGULAR ± 1° SURFACE FINISH MACHINED FACES Ra 6.3	
	NAME	DATE
DRAWN	Rohan Woodcock	12/08/2025
CHECKED		
UNDIMENSIONED SURFACES MACHINE FROM CAD		

MATERIAL: 7075-T6 Endcap	TITLE: OX BOTTOM SLOTTED ENDCAP-STRINGER-PLUTO v17	
ALL DIMENSIONS ARE IN MILLIMETRES	FINISH/TREAT:	
DO NOT SCALE DRAWING	MASS (g): 1498.6257 g	
A3 SCALE 1:2	IF IN DOUBT ASK BREAK ALL SHARP EDGES WITH MIN RAD OR CHF UOS	SHEET 1/1 REVISION:

IMPERIAL COLLEGE LONDON, EXHIBITION ROAD, LONDON, SW7 2AZ

Ensure this surface is the flat and oriented like this relative to the drilled holes

Face off and get part thickness to 54.2mm, then use front face as reference for future operations

Mount in 4 jaw chuck and adjust based on runout using machined outer surface

A-A (1:1)

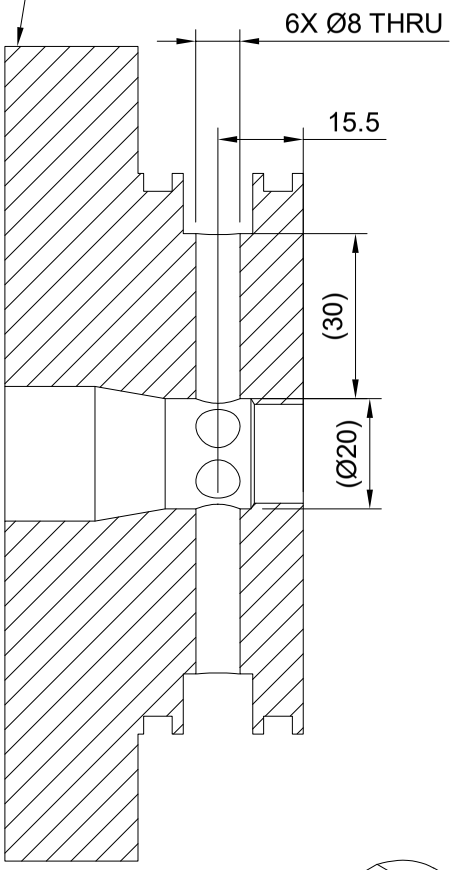

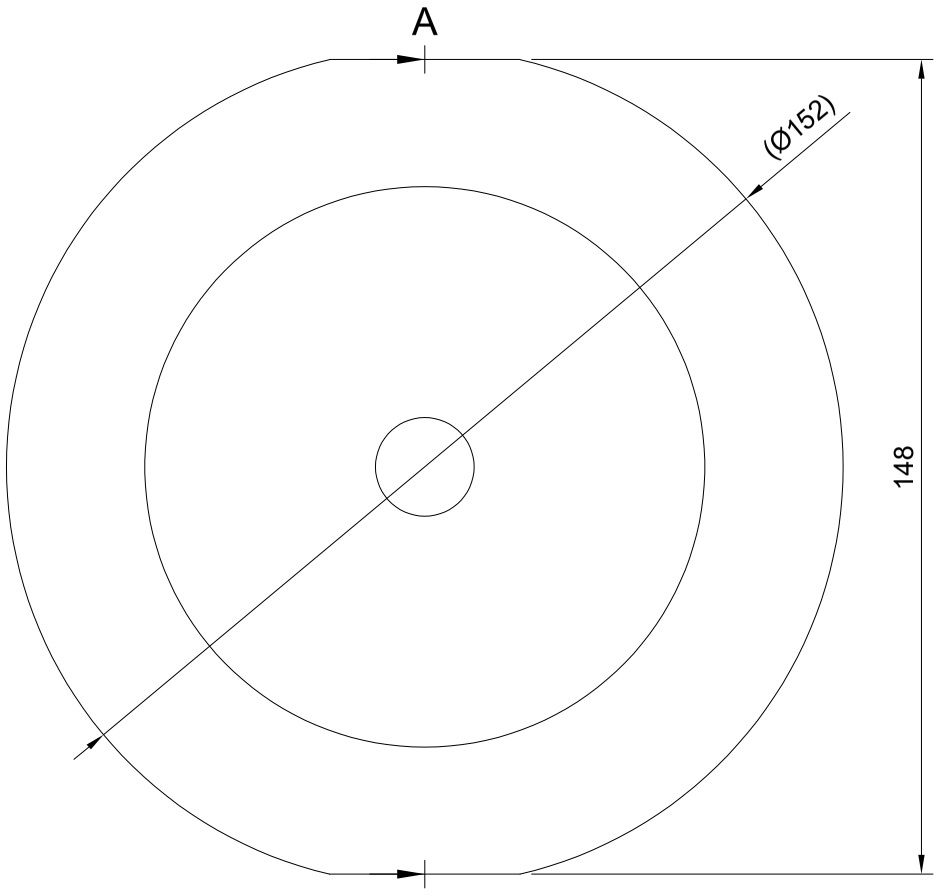

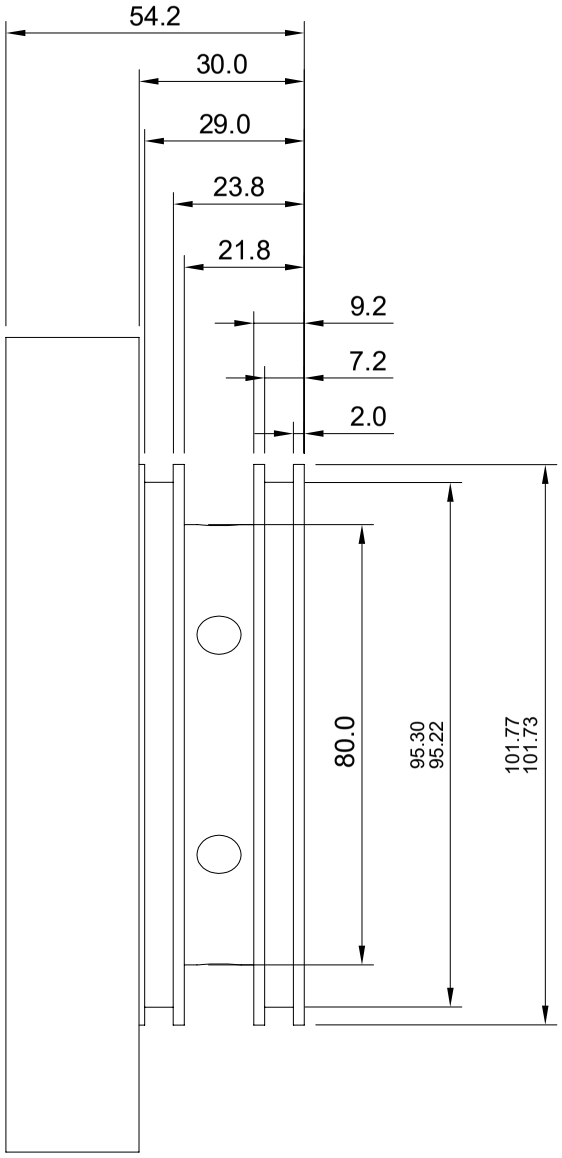

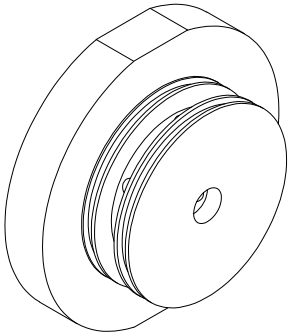

TOLERANCES		THIRD ANGLE PROJECTION
X = ± 0.5 X.X = ± 0.1 X.XX = ± 0.02	ANGULAR ± 1° SURFACE FINISH MACHINED FACES Ra 6.3	

	NAME	DATE
DRAWN	Rudra Nakade	16/06/2025
CHECKED		
APPROVED		

MATERIAL: Aluminum 6061

ALL DIMENSIONS ARE IN MILLIMETRES

DO NOT SCALE DRAWING

A3 SCALE 1:1

TITLE: Injector Head Stock

DWG NO. Injector Head Stock

SHEET 1/1 REVISION: 1

A (1:1)

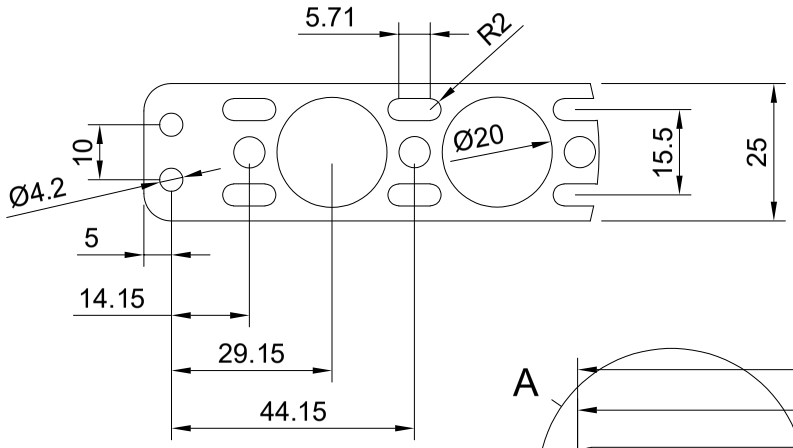

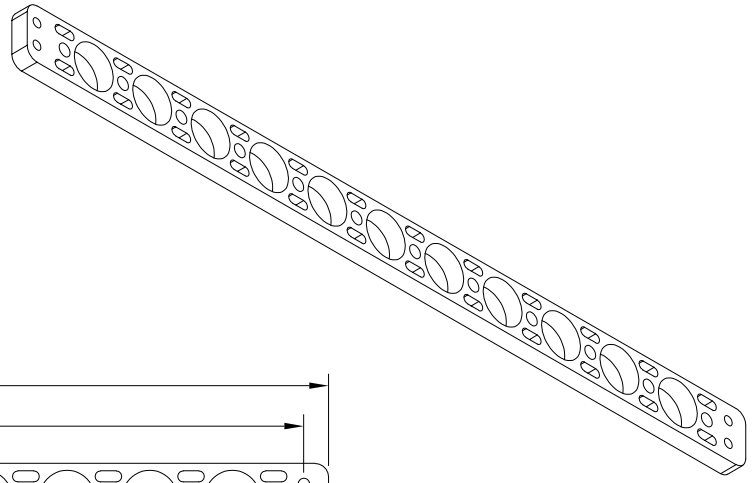

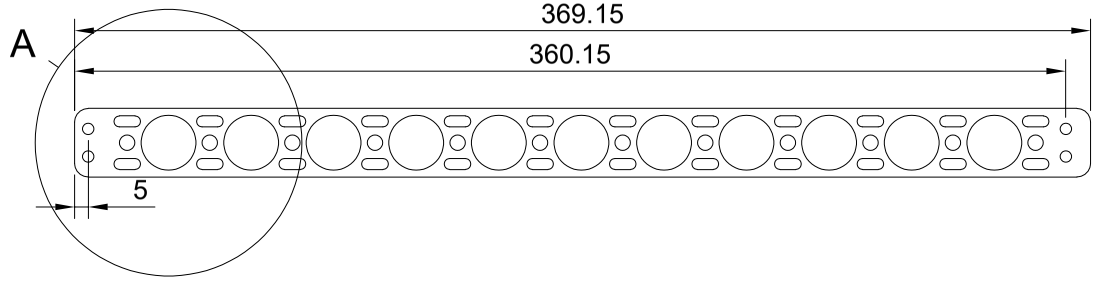

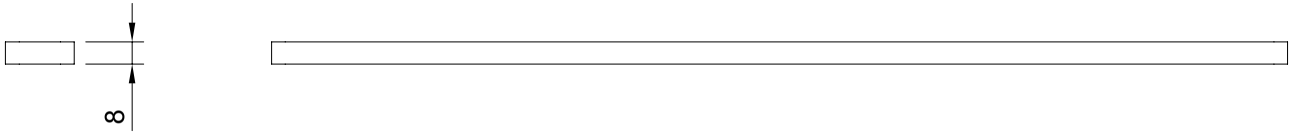

TOLERANCES		THIRD ANGLE PROJECTION
X = ± 0.5 X.X = ± 0.1 X.XX = ± 0.02	ANGULAR ± 1° SURFACE FINISH MACHINED FACES Ra 6.3	

	NAME	DATE
DRAWN	Louis Brouwer	18/03/2025
CHECKED		

UNDIMENSIONED SURFACES MACHINE FROM CAD

MATERIAL: Aluminum 6061

ALL DIMENSIONS ARE IN MILLIMETRES

DO NOT SCALE DRAWING

A3 SCALE 1:2

TITLE: STRINGER-I CHANNEL-PLUTO v14

FINISH/TREAT:

MASS (g): 98.0275 g

IF IN DOUBT ASK

BREAK ALL SHARP EDGES WITH MIN RAD OR CHF UOS

SHEET 1/1

REVISION:

IMPERIAL COLLEGE LONDON, EXHIBITION ROAD, LONDON, SW7 2AZ

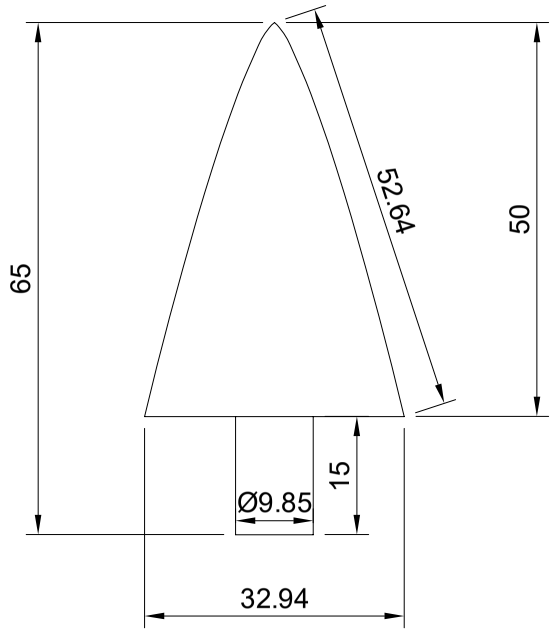

Dept.	Technical reference	Created by gauhiit gupta 7/9/2025	Approved by
		Document type	Document status
		Title TIP1-FULL-PLUTO v1	DWG No.
			Rev. / Date of issue / Sheet 1/1

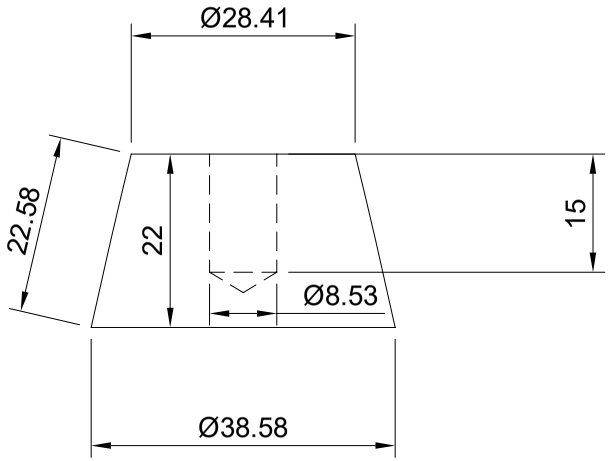

Dept.	Technical reference	Created by gauhiit gupta 7/9/2025	Approved by	
		Document type	Document status	
		Title TIP2-FULL-PLUTO v8	DWG No.	
			Rev. / Date of issue	Sheet 1/1

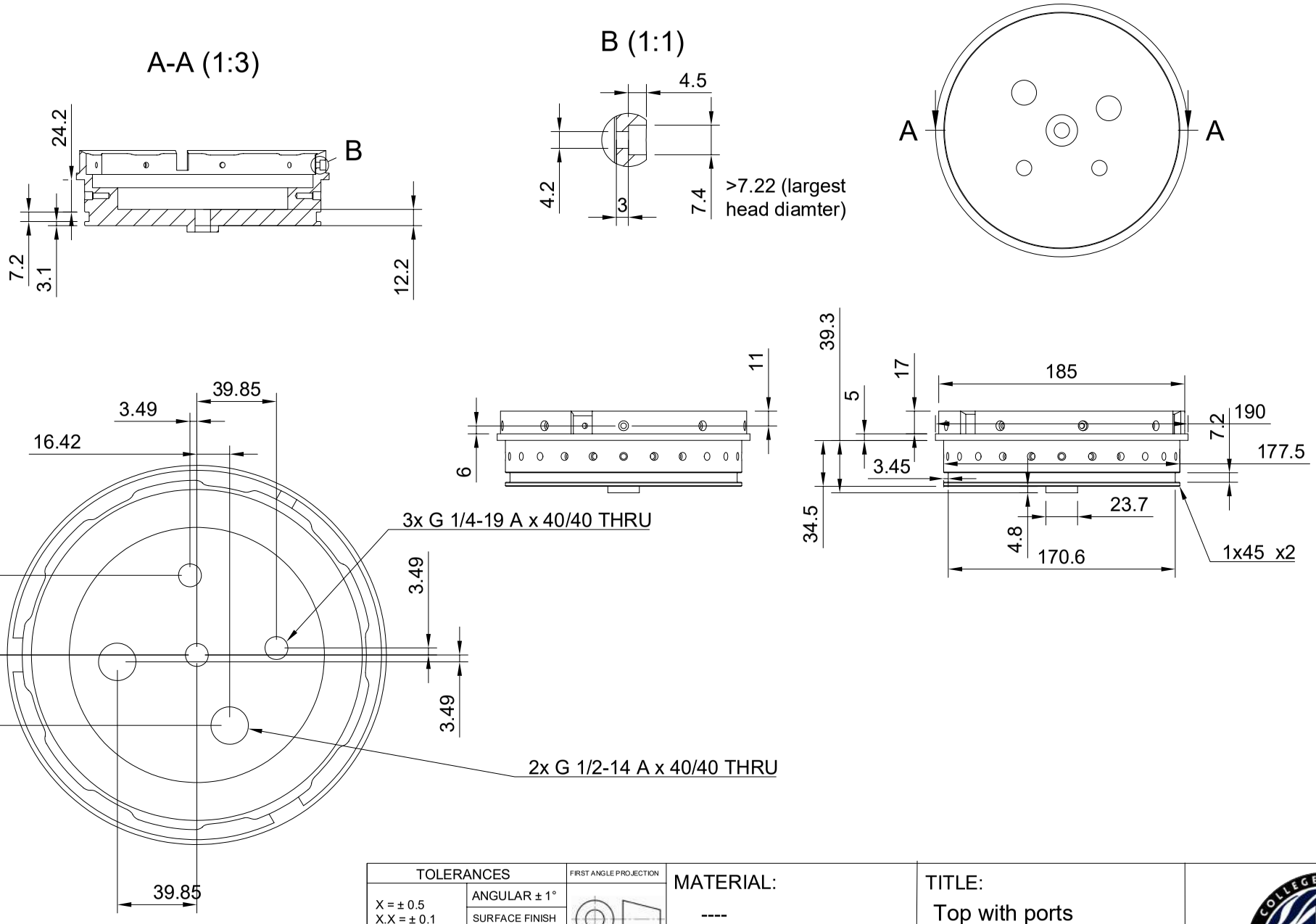

TOLERANCES		FIRST ANGLE PROJECTION	MATERIAL: ----
X = ± 0.5 X.X = ± 0.1 X.XX = ± 0.02	ANGULAR ± 1° SURFACE FINISH MACHINED FACES Ra 6.3		TITLE: Top with ports
	NAME	DATE	ALL DIMENSIONS ARE IN MILLIMETRES
DRAWN	Rohan Woodcock	06/08/2025	FINISH/TREAT:
CHECKED			DO NOT SCALE DRAWING
UNDIMENSIONED SURFACES MACHINE FROM CAD			MASS (g): 0.00 g
A3	SCALE 1:2		IF IN DOUBT ASK BREAK ALL SHARP EDGES WITH MIN RAD OR CHF UOS
SHEET 1/1	REVISION:		

IMPERIAL COLLEGE LONDON, EXHIBITION ROAD, LONDON, SW7 2AZ

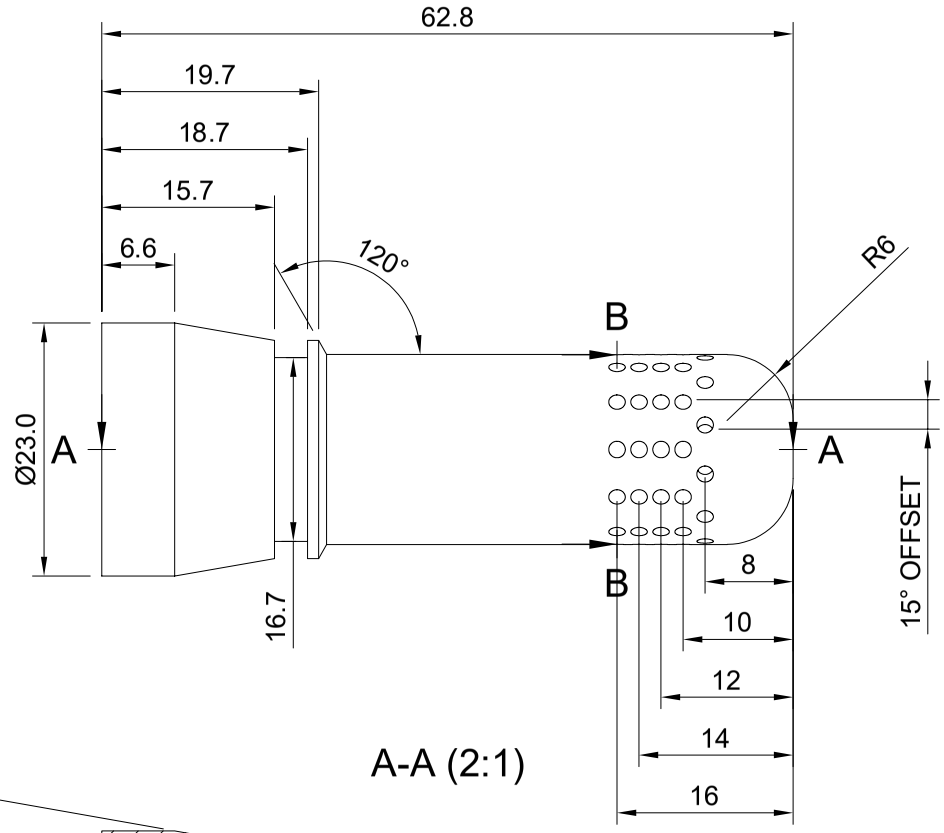

B-B (2:1)

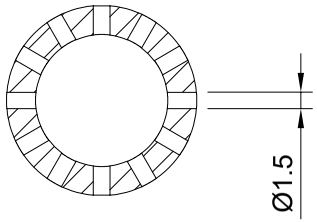

12 HOLES / ROW
5 ROWS

A-A (2:1)

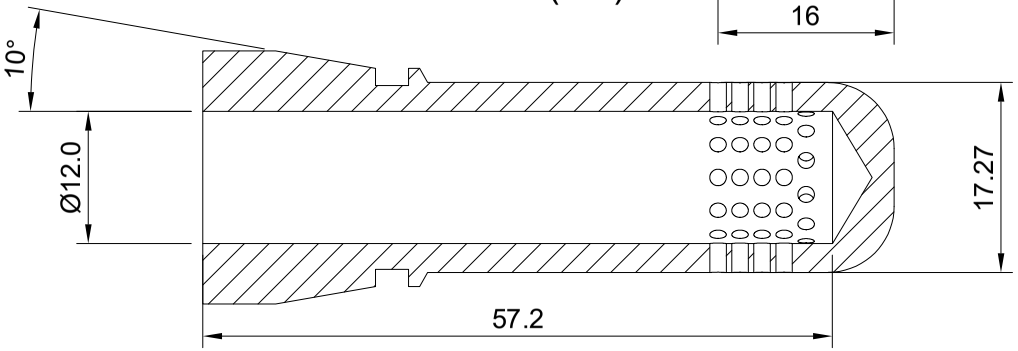

TOLERANCES		THIRD ANGLE PROJECTION
X = ± 0.5 X.X = ± 0.1 X.XX = ± 0.02	ANGULAR ± 1° SURFACE FINISH MACHINED FACES Ra 6.3	

	NAME	DATE
DRAWN	Rudra Nakade	06/09/2025
CHECKED		
APPROVED		

MATERIAL: Stainless Steel

ALL DIMENSIONS ARE IN MILLIMETRES

DO NOT SCALE DRAWING

A3 SCALE 2:1

TITLE: Pintle Insert

DWG NO. Pintle Insert

SHEET 1/1 REVISION:

A-A (2:3)

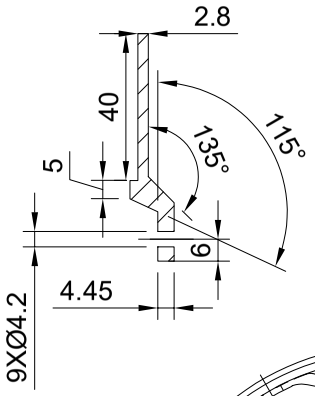

B-B (2:3)

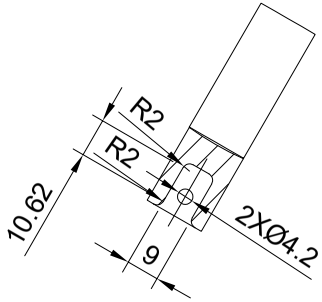

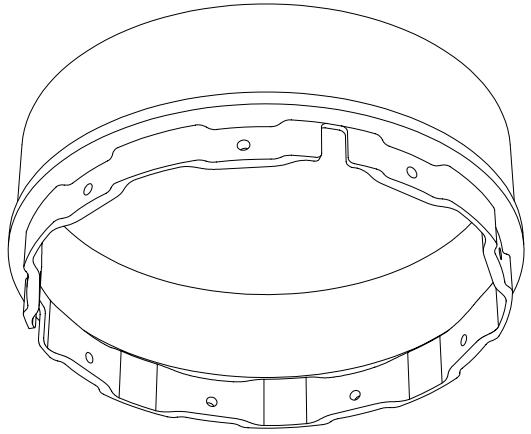

ISOMETRIC VIEW
NOT TO SCALE

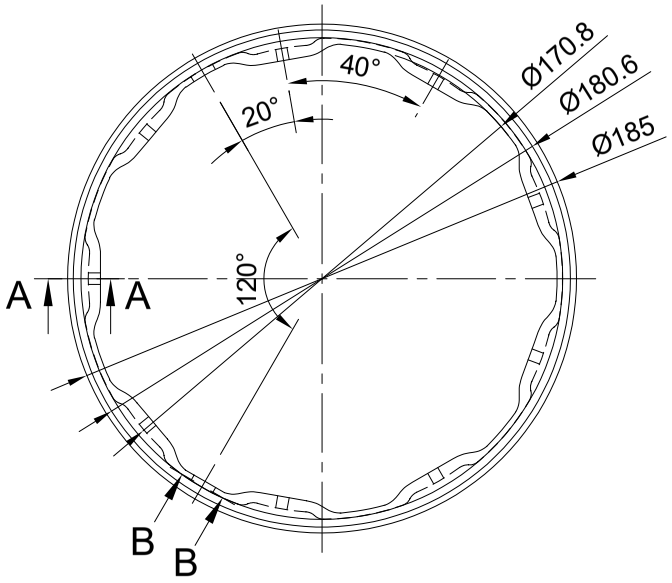

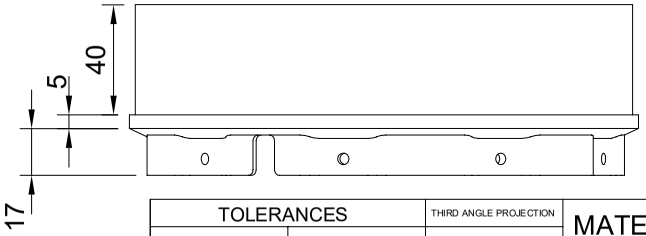

TOLERANCES		THIRD ANGLE PROJECTION
X = ± 0.5 X.X = ± 0.1 X.XX = ± 0.02	ANGULAR ± 1° SURFACE FINISH MACHINED FACES Ra 6.3	
	NAME	DATE
DRAWN	John Drace-Francis	03/06/2025
CHECKED		
UNDIMENSIONED SURFACES MACHINE FROM CAD		

MATERIAL: Aluminium 6082T6	TITLE: TOP COUPLER-UPR PROP TUBE-PLUTO v3
ALL DIMENSIONS ARE IN MILLIMETRES	FINISH/TREAT:
DO NOT SCALE DRAWING	MASS (g): 321.9262 g
A3 SCALE 1:2	IF IN DOUBT ASK BREAK ALL SHARP EDGES WITH MIN RAD OR CHF UOS
SHEET 1/1	REVISION: B

IMPERIAL COLLEGE LONDON, EXHIBITION ROAD, LONDON, SW7 2AZ

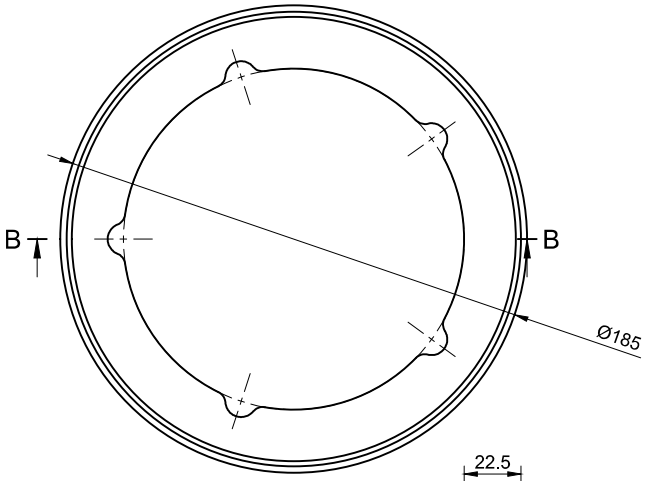

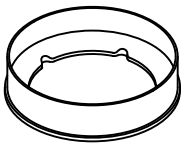

ISO VIEW NOT TO SCALE

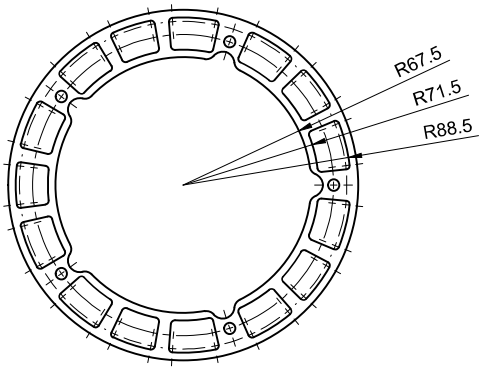

BOTTOM VIEW

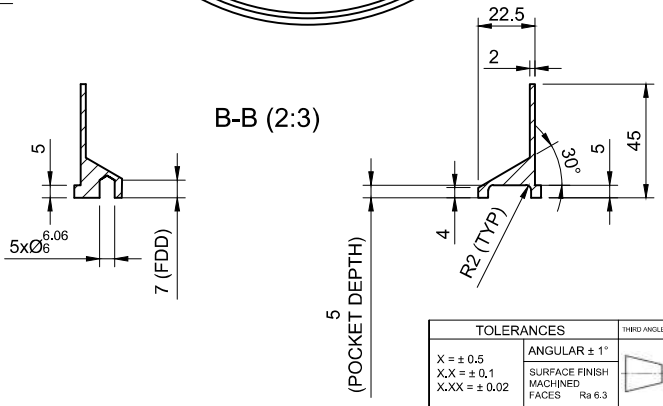

TOLERANCES		THIRD ANGLE PROJECTION
X = ± 0.5 X.X = ± 0.1 X.XX = ± 0.02	ANGULAR ± 1° SURFACE FINISH MACHINED FACES Ra 6.3	
	NAME	DATE
DRAWN	Clement Liu	21/05/2025
CHECKED	Ahmed Gilani	24/05/2025
UNDIMENSIONED SURFACES MACHINE FROM CAD		

MATERIAL: Aluminum 6061	TITLE: TOP COUPLER-RECOVERY-PLUTO	
ALL DIMENSIONS ARE IN MILLIMETRES	FINISH/TREAT: CLEAN & DEBURR SHARP EDGES	
DO NOT SCALE DRAWING	MASS (g): 344 g	
	IF IN DOUBT ASK	
A3 SCALE 1:1	BREAK ALL SHARP EDGES WITH MIN RAD OR CHF UOS	SHEET 1/1 REVISION: A

IMPERIAL COLLEGE LONDON, EXHIBITION ROAD, LONDON, SW7 2AZ

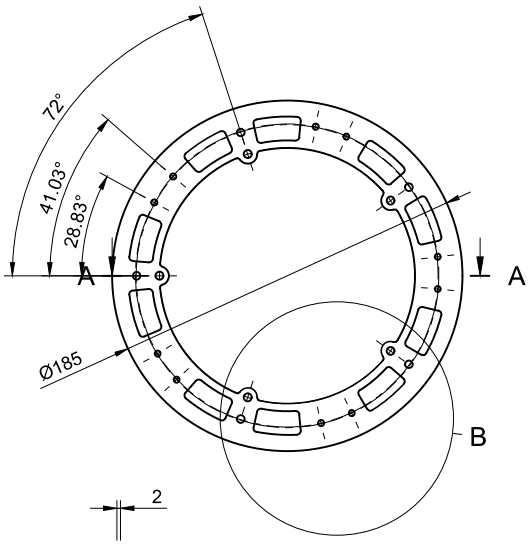

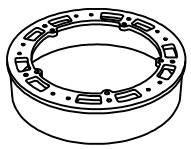

ISO VIEW NOT TO SCALE

B (1:1)

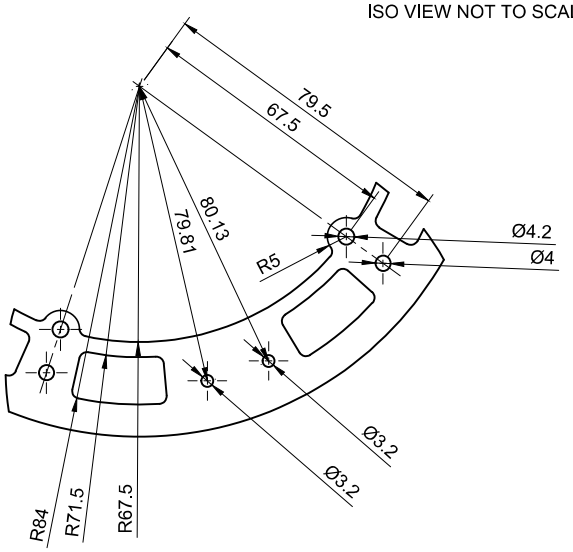

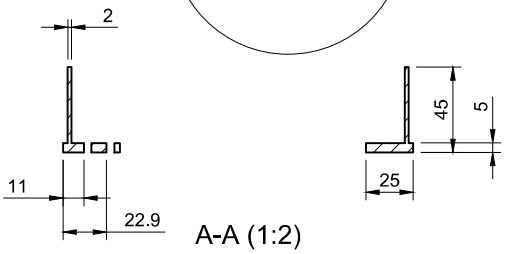

A-A (1:2)

TOLERANCES	THIRD ANGLE PROJECTION	MATERIAL: Aluminum 6061	TITLE: BOTTOM COUPLER-RECOVERY-PLUTO v5	
X = ± 0.5 X.X = ± 0.1 X.XX = ± 0.02	ANGULAR ± 1° SURFACE FINISH MACHINED FACES Ra 6.3	ALL DIMENSIONS ARE IN MILLIMETRES	FINISH/TREAT: CLEAN AND DEBURN SHARP EDGES	
	NAME / DATE	DO NOT SCALE DRAWING	MASS (g): 251 g	
DRAWN: Clement Liu 27/05/2025			IF IN DOUBT ASK	
CHECKED: Ahmad Shaeel 10/08/2025		A3 SCALE 1:2	BREAK ALL SHARP EDGES WITH MIN RAD OR CHF UOS	SHEET 1/1 REVISION: A
UNDIMENSIONED SURFACES MACHINE FROM CAD				

IMPERIAL COLLEGE LONDON, EXHIBITION ROAD, LONDON, SW7 2AZ

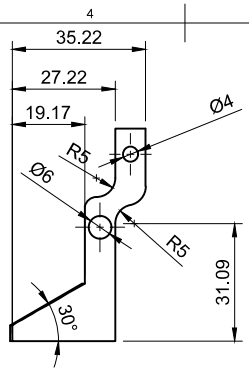

SIDE VIEW

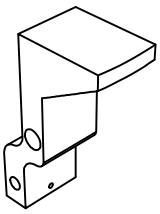

ISO VIEW

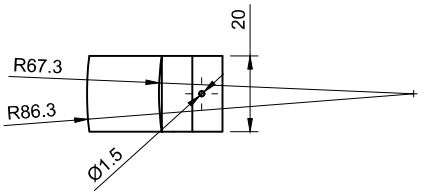

TOP VIEW

TOLERANCES X = ± 0.5 X.X = ± 0.1 X.XX = ± 0.02	THIRD ANGLE PROJECTION ANGULAR ± 1° SURFACE FINISH MACHINED FACES Ra 6.3		MATERIAL: Aluminum	TITLE: CLAMP V5-RECOVERY-PRINT v5	
	NAME	DATE	ALL DIMENSIONS ARE IN MILLIMETRES	FINISH/TREAT: CLEAN AND DEBURR EDGES	
DRAWN	Justin Ku	03/06/2025	DO NOT SCALE DRAWING	MASS (g): 34 g	
CHECKED	Ahmad Shaeel	10/08/2025		IF IN DOUBT ASK	
UNDIMENSIONED SURFACES MACHINE FROM CAD			A3 SCALE 1:1	BREAK ALL SHARP EDGES WITH MIN RAD OR CHF UOS	SHEET 1/1 REVISION: A

IMPERIAL COLLEGE LONDON, EXHIBITION ROAD, LONDON, SW7 2AZ